

**ASSESSING THE CUMULATIVE IMPACT OF WILDLAND FIRES AND  
SEISMIC LINE DISTURBANCE ON PEATLANDS IN NORTHERN ALBERTA**

**HUMAIRA ENAYETULLAH**  
**Bachelor of Science, University of Lethbridge, 2020**

A thesis/project submitted  
in partial fulfilment of the requirements for the degree of

**MASTER OF SCIENCE**

in

**ENVIRONMENTAL SCIENCE**

Department of Geography  
University of Lethbridge  
LETHBRIDGE, ALBERTA, CANADA

© Humaira Enayetullah, 2021

ASSESSING THE CUMULATIVE IMPACT OF WILDLAND FIRES AND SEISMIC  
LINE DISTURBANCE ON PEATLANDS IN NORTHERN ALBERTA

HUMAIRA ENAYETULLAH

Date of Defence: December 2, 2021

Dr. L. Chasmer Supervisor	Associate Professor	Ph.D.
------------------------------	---------------------	-------

Dr. C. Hopkinson Thesis Examination Committee Member	Professor	Ph.D.
---	-----------	-------

Dr. D. Cobbaert Thesis Examination Committee Member	Wetland Scientist	Ph.D.
--	-------------------	-------

Dr. S. Kienzle Chair, Thesis Examination Committee	Professor	Ph.D.
---	-----------	-------

## **DEDICATION**

This thesis is dedicated to my grandfather, Imamuddin Enayetullah, who always encouraged and supported me in all my endeavours.

## ABSTRACT

This thesis examined the impact of wildland fires and seismic line fragmentation on peatlands in northern Alberta. The objectives were to determine if wildland fires alter regeneration trajectories of conifer vs deciduous species and lead towards the regeneration of woody vegetation adjacent to seismic lines. Multi-spectral lidar data were collected for a boreal peatland chronosequence of 5, 18, 30, and 38 years since fire (YSF) and were compared with areas that had not burned to quantify changes in the post-fire distribution of shrubs and trees.

The results illustrated that there was high shrub regeneration in peatlands up to and including 38 YSF and trees tended to grow above shrubs by 18 YSF. Wildland fires promoted woody vegetation regeneration adjacent to seismic lines with taller deciduous trees and conifers found in more mature post-fire peatlands (30 to 38 YSF). However, fens were more vulnerable to seismic line fragmentation and had less post-fire regeneration compared to bogs.

## ACKNOWLEDGEMENTS

I would like to express my sincere gratitude to a lot of people who have guided, supported, and encouraged me throughout my masters degree and made my experience at the University of Lethbridge very memorable.

Firstly, I would like to extend my most sincere thanks to my supervisor Dr. Laura Chasmer for her constant support, patience, and guidance throughout this thesis. I feel very fortunate to have the chance to work with her and learn so much. Thanks for all the hours you spent editing, reviewing, and discussing various aspects of my thesis. I would also like to thank you for providing me the opportunity to present my research at conferences and providing career and networking opportunities. Our fieldwork in Fort McMurray would always be my most adventurous trip.

Secondly, I would like to thank Dr. Chris Hopkinson, Dr. Dan Thompson, and Dr. Danielle Cobbaert for being a part of my supervisory committee and providing invaluable feedback. I really appreciate all the excellent ideas you provided to make this thesis better.

I would also like to thank my field work partners and members of the ARTeMiS / Peaters lab. Thanks to Chinyere Ottah and Nick Cuthbertson for their assistance in the field and for making wetland sampling fun. To all the members of the ARTeMiS / Peaters lab, thanks for all the technical help, suggestions, and motivating Zoom conversations during stressful times: Celeste Barnes, Maxim Okhrimenko, Emily Jones, Jesse Aspinall, Kailyn Nelson, Linda Flade, Farnoosh Aslami, Sam Gerrand, Chinyere Ottah, Danika King, and Travis Grant.

Lastly, I would like to thank my family and friends for their continuous support throughout this degree. To my mom, who always encouraged me and provided late night coffees. To my dad, who always supported my education. To my fiancé and his family for listening to my thesis talks and comforting me. To my sisters, who made me laugh during stressful times and to my family in Bangladesh for all their prayers and good wishes. A special thanks to my uncle, who has been my role model in pursuing environmental science.

## TABLE OF CONTENTS

<b>DEDICATION</b> .....	<b>iii</b>
<b>ABSTRACT</b> .....	<b>iv</b>
<b>ACKNOWLEDGEMENTS</b> .....	<b>v</b>
<b>LIST OF TABLES</b> .....	<b>x</b>
<b>LIST OF FIGURES</b> .....	<b>xi</b>
<b>LIST OF SYMBOLS AND ABBREVIATIONS</b> .....	<b>xiv</b>
<b>CHAPTER 1: INTRODUCTION</b> .....	<b>1</b>
1.1 BACKGROUND.....	1
1.2 KEY DEFINITIONS.....	5
1.2.1 Peatlands (bogs vs. fens) .....	5
1.2.2 Seismic lines.....	7
1.2.3 Fire chronosequence.....	9
1.3 STUDY REGION - BOREAL PLAINS ECOZONE .....	10
1.4 STUDY OBJECTIVES.....	12
1.5 THESIS ORGANIZATION.....	13
<b>CHAPTER 2. LITERATURE REVIEW: IMPACTS OF CLIMATE CHANGE AND ANTHROPOGENIC DISTURBANCES ON PEATLANDS</b> .....	<b>15</b>
2.1. INTRODUCTION.....	15
2.2. CLIMATE MEDIATED IMPACTS TO PEATLANDS .....	18
2.2.1 Changes in fire regimes .....	18
2.2.2 Changes in peatland hydrology .....	21
2.3. ANTHROPOGENIC DISTURBANCES TO PEATLANDS .....	23
2.3.1 Peatland fragmentation by seismic lines .....	23
2.3.2 Proximal effects of seismic lines .....	26
2.4. HOW PEATLANDS RESPOND TO COMBINED DISTURBANCES.....	28
2.5. USE OF REMOTE SENSING TO STUDY PEATLANDS.....	30
2.5.1 Passive remote sensing (optical sensors).....	31
2.5.2 Active remote sensing (Lidar and SAR).....	34
2.6. INTEGRATION OF FIELD AND REMOTE SENSING MEASUREMENTS.....	36

**CHAPTER 3: IDENTIFYING CONIFER TREE VS. DECIDUOUS SHRUB AND TREE REGENERATION TRAJECTORIES IN A SPACE-FOR-TIME BOREAL PEATLAND FIRE CHRONOSEQUENCE USING MULTISPECTRAL LIDAR . 38**

ABSTRACT .....	38
3.1 INTRODUCTION.....	39
3.2 MATERIAL AND METHODS .....	45
3.2.1 Study area .....	45
3.2.2 Field data collection.....	47
3.2.3 Lidar data collection .....	48
3.2.4 Supplementary geospatial data .....	49
3.2.5 Data analysis.....	50
3.3 RESULTS.....	56
3.3.2 Classification of conifer vs deciduous shrub/ tree in post-fire peatlands using lidar .....	59
3.3.3 Proportional of conifer and deciduous shrubs and/or trees in post-fire peatlands .....	64
3.3.4 Cumulative growth of conifers vs deciduous tree and shrubs in the years since fire.....	66
3.4 DISCUSSION .....	67
3.4.1 Use of lidar to identify conifers and deciduous trees and shrubs .....	67
3.4.2 Changes in proportional coverage of conifers and deciduous tree/shrubs .....	69
3.4.3 Spatial variation in vegetation height in bogs and fens .....	71
3.4.4 Use of remote sensing and possible limitations.....	72
3.5 CONCLUSION .....	74
ACKNOWLEDGEMENTS .....	75

**CHAPTER 4. IMPACTS OF SEISMIC LINE DISTURBANCE ON POST-FIRE REGENERATION IN A SPACE-FOR-TIME BOREAL PEATLAND FIRE CHRONOSEQUENCE USING MULTISPECTRAL LIDAR ..... 76**

ABSTRACT .....	76
4.1 INTRODUCTION.....	77
4.2. MATERIAL AND METHODS .....	82
4.2.1 Study area .....	82
4.2.2 Lidar data collection and processing .....	85
4.2.3 Supplementary geospatial data .....	86



4.2.4 Data Analysis.....	89
4.3. RESULTS.....	95
4.3.1 Influence of seismic lines on conifer and deciduous shrub and/or trees heights .....	95
4.3.2 Anthropogenic/environmental correlates of vegetation succession in peatlands .....	100
4.4 DISCUSSION .....	106
4.4.1. Interaction between seismic lines and vegetation response.....	106
4.4.2 Interaction between the primary drivers of vegetation growth.....	109
4.4.3 Limitations.....	111
4.5 CONCLUSION .....	112
<b>Chapter 5: CONCLUSIONS.....</b>	<b>113</b>
5.1 Summary of research.....	113
5.2 Recommendations and future directions .....	114
<b>REFERENCES.....</b>	<b>116</b>
<b>APPENDIX 1: GLOSSARY .....</b>	<b>135</b>

## LIST OF TABLES

<b>Table 3. 1</b> Lidar metrics derived for identifying shrubs and trees using return height above ground greater than 0.5 m. Lidar metrics in bold were used in the final model based on their importance. Other metrics were also generated but were not included in the forest-based classification (described below) because they were highly auto-correlated (Pearson’s correlation $\geq 0.60$ ). All metrics generated had a cell resolution of $2 \times 2$ m, except for slope and aspect, which had a resolution of $5 \times 5$ m, resampled to $2 \times 2$ m for the random forest classification. C1 = 1550 nm (shortwave infrared, SWIR); C2 = 1064 nm (near infrared, NIR); C3 = 532 nm (green).....	51
<b>Table 3. 2</b> Variable importance for each fire chronosequence and unburned area generated using forest-based classification, where YSF refers to years since fire. ....	60
<b>Table 3. 3</b> Model performance for the study area. Sensitivity is the percentage of time each observed category was correctly predicted, while accuracy takes into consideration how well each category is predicted and how often it is miscategorised .....	61
<b>Table 3. 4</b> Confusion matrix of forest-based regression between deciduous shrubs, deciduous trees, conifers within burned and recently unburned peatlands.....	62
<b>Table 4. 1</b> Explanatory variables used in PCA analysis.....	92
<b>Table 4. 2</b> Average vegetation descriptive characteristics determined for peatland classes/ fire age for burned chronosequence and unburned peatlands.....	96
<b>Table 4. 3</b> Correlation matrix of the explanatory variables used.....	101
<b>Table 4. 4</b> Total variance explained by each component.....	102
<b>Table 4. 5</b> Rotated component matrix for the PCA.....	103

## LIST OF FIGURES

<b>Figure 1. 1</b> Conventional seismic line through an unburned peatland near Wandering River, Alberta surveyed on August 1, 2020.....	9
<b>Figure 1. 2</b> Map outlining the study area in the Boreal Plains Ecozone of Canada. Current oilsands project boundaries (active as of 2015) and wildland fires from 1931-2019 are included.....	11
<b>Figure 2. 1</b> Peatland feedback response to climatic and anthropogenic disturbances based on known literature (Kettridge et al., 2015; Dabros et al., 2018; Filicetti and Nielsen, 2020; Stevenson et al 2019; Nelson et al., 2021).....	30
<b>Figure 2. 2</b> Lidar point cloud distribution indicating (a) ground normalised returns, where brown is the classified ground surface and green represents all returns above the ground surface; and (b) returns from individual lidar wavelengths/channels (SWIR, NIR, Green). .....	35
<b>Figure 3. 1</b> Location of 5 year, 18 years, 30 years and 38 years since fire chronosequence near Fort McMurray, Alberta surveyed using multi-spectral lidar. The region is within the Boreal Plains ecozone. Areas that have not been burned in the recent history of scientific observation (since ~1930) are found in between the fire scars, predominantly between 1982 and 2002 fires in the western lidar polygon.....	46
<b>Figure 3. 2</b> Examples of seismic line transects for shrub and tree height validation through (a) burned peatland and (b) forest looking into an unburned treed peatland.....	48
<b>Figure 3. 3</b> Box plot of the top four variables a) IQR of height, (b) NDIR, and (c) percent cover used to separate between species. The values are derived from lidar data for deciduous and conifer species identified in unmixed plots in the field ( $n = 44$ ). .....	58
<b>Figure 3. 4</b> Average SWIR (shortwave infrared, 1550 nm) and NIR (near infrared, 1064 nm) intensities for field-identified, unmixed pixels with deciduous and conifer species using all returns of SWIR and NIR > 0.5 m ( $n = 44$ ). .....	59
<b>Figure 3. 5</b> Prediction raster generated for (a) western lidar polygon including vegetation regeneration 18 YSF, 38 YSF, and recently unburned peatlands and (b) eastern lidar polygon including vegetation regeneration 5 YSF and 30 YSF. No data areas shaded in grey represent vegetation height less than 0.5 m. These low vegetation areas are typically representing ground cover, Labrador tea, and herbaceous species. ....	63

**Figure 3. 6.** Proportional cover of wetland conifer vs. deciduous species per fire chronosequence, in (a) bogs and (b) fens..... 65

**Figure 3. 7** Average vegetation height (at 99<sup>th</sup> percentile of lidar returns) with stand age for boreal peatland fire chronosequence ( $R^2 = 0.96$  for bogs,  $R^2 = 0.98$  for fens). Unburned peatlands are plotted with an arbitrary stand age of  $90 \pm 10$  years, though there may be many more years since the last fire, but not determined in the field and not included in the recent history of scientific observation (since ~1930). ..... 67

**Figure 4. 1** Location of lidar survey polygons near Fort McMurray, Alberta that have been temporarily or permanently disturbed by industrial land use activities. Areas that have not been burned in the recent history of scientific observation (since ~1930) are found in between the fire scars, predominantly between 1982 and 2002 fires in the western lidar polygon, while the eastern lidar polygon was burned by fires in 1990 and 2015..... 84

**Figure 4. 2** Example for a single peatland of near (0 – 30 m), intermediate (30 – 60 m), and far (60 – 90 m) buffers along manually delineated seismic lines within peatlands used to quantify the proximal effects of seismic lines on vegetation regeneration..... 90

**Figure 4. 3** Canopy height model for example peatlands found in the study area. Upland and transitional areas have taller vegetation while peatlands fragmented by seismic lines have vegetation height less than 6 m. .... 96

**Figure 4.4** Variation in vegetation height in bogs for deciduous shrubs, deciduous trees, and conifers trees across burn chronosequence and with distance from seismic lines. Whiskers represent the standard deviation of height within each period/buffer, whereas the symbols represent the average height. Here Cont. ae reference peatlands that are unburned with no seismic lines..... 98

**Figure 4. 5** Variation in vegetation height in fens for deciduous shrubs, deciduous trees, and conifers trees across burn chronosequence and with distance from seismic lines. Whiskers represent the standard deviation of height within each period/buffer, whereas the symbols represent the average height. Here Cont. ae reference peatlands that are unburned with no seismic lines..... 100

**Figure 4. 6** Plots of scaled peatland explanatory attribute score and arrows of loadings for the first two principal components (PC1 34% and PC2 20% of variance) of PCA for both bogs and fens. The length of their respective arrows illustrates the component loadings of the indices, while individual bogs and fens found in the study area are also

included ( $n = 155$ ). Circles represent strong clustering of bogs and fens that cluster with years since fire. .... 104

**Figure 4. 7** PCA loading plots for (a) fen only ( $n = 79$ ) (b) bogs only ( $n = 76$ ) based on peatland type: open, shrubby, and treed. Circles represent strong clustering of some bog and fen forms (open, shrubby, treed). .... 105

## LIST OF SYMBOLS AND ABBREVIATIONS

YSF	Year Since Fire
BPE	Boreal Plains Ecozone
Lidar	Light Detection and Ranging
DEM	Digital Elevation Model
DSM	Digital Surface Model
CHM	Canopy Height Model
TPI	Topographic Position Index
IQR	Interquartile Range of height
NDIR	Normalized Difference Infrared Index
GPS	Global Positioning System
GNSS	Global Navigation Satellite System
UAV	Unmanned Aerial Vehicles
ABMI	Alberta Biodiversity Monitoring Institute
LIS	Low Impact Seismic line
PCA	Principal component Analysis
PC	Principal Component

## CHAPTER 1: INTRODUCTION

### 1.1 BACKGROUND

Peatlands are a type of wetland primarily categorized as bogs and fens due to their waterlogged conditions and slow decomposition of organic material (i.e., peat), resulting in the accumulation of peat > 0.4 m in depth (Gorham, 1991). The characteristics of peatlands allow for the storage of large amounts of carbon due to their high soil moisture and high water table position (Vitt et al., 1994). It is estimated that peatlands in Canada store more than 147 Gt of soil organic carbon (Tarnocai and Stolbovoy, 2006).

Moreover, peatlands can also serve as climate refugia due to their water conserving feedback mechanisms (Stralberg et al., 2020). However, they constitute only 12% of the land area in Canada. About 97% of Canadian peatlands are found in the boreal and subarctic biomes (Tarnocai, 2009). Additionally, peatlands provide a range of ecosystem services including provisioning services (food, fresh water, other), regulating services (water purification, climate regulation), cultural services (recreational, spiritual, and educational opportunities) along with supporting services (nutrient cycling, habitat for species) (Kimmel and Mander, 2010).

Despite the various ecosystem services they provide, peatlands are undergoing significant cumulative stress due to climate mediated drying and anthropogenic disturbances (Flannigan et al., 2000; Dabros et al., 2018). As a result, the carbon balance of peatlands is changing such that there is a decline in carbon sequestration capacity, and increased occurrences of wildland fires releasing more carbon into the atmosphere (Flannigan et al., 2000). Moreover, peatland sensitivity models predict that 50% of the

total organic carbon mass in peatlands will be severely to extremely severely affected due to changing climate (Tarnocai, 2009).

Peatlands in the Boreal Plains Ecozone exist within a moisture deficit sub-humid region with high variability in precipitation patterns (Mwale et al, 2009; Waddington et al., 2015). Moreover, with climate change, there is a net decrease in moisture and water availability due to increased evaporative demand, thereby increasing the carbon available for fuels, making peatlands more sensitive to wildland fires (Flannigan et al., 2015; Thompson et al., 2019). Enhanced drying has caused relatively high intensity smoldering fires in boreal peatlands, often with greater than 20 cm depth of burn, releasing 10–85 kg C per m<sup>2</sup> (Wilkinson et al., 2018). The deep burns occurring within peatlands in recent years may cause shifts in peatland ecosystem structure and function. Moreover, high intensity fires may push forest species beyond their adaptive limits (Whitman et al., 2019), causing shifts in northern latitude vegetation species, (Kasischke and Turetsky, 2006).

In addition to impacts from fire, boreal forests and peatlands are fragmented by linear anthropogenic disturbances including seismic lines used by the oil and gas industries for accessing oil reserves (Dabros et al., 2018). Seismic lines are constructed often in dense grids with seismic line density greater than 10 km/km<sup>2</sup>. Seismic lines can impact vegetation regeneration and species composition along these lines (Lee and Boutin, 2006; Lovitt et al., 2018) by altering abiotic factors associated with line construction including changes to hydrology (Dabros et al., 2018), soil properties (Davidson et al., 2020), enhanced incoming solar radiation and energy receipt due to openings along lines, and changes in local wind and turbulence (Stern et al., 2018).



Moreover, these linear disturbances can affect biodiversity by allowing disturbance tolerant invasive species to establish (Finnegan et al. 2018) and alter habitat for woodland caribou (Dabros et al., 2021).

Peatlands are sensitive to climate drying and seismic line disturbances. For example, Chasmer et al. (2021) found that peatlands with higher proportions of seismic lines tended to have more shrubs. Also, Treed peatlands are less likely to recover from seismic line construction due to changes in microtopography (hummocks vs. hollows) and wetter site conditions (van Rensen et al., 2015; Filicetti and Nielson, 2020). Despite the combined stressors from climatic drying and seismic lines, wildland fires may be able to reduce the impacts of seismic lines by acting as a passive restoration mechanism by initiating secondary succession. However, there is limited evidence supporting this claim (Filicetti and Nielsen, 2020). Fire reinforces hollow elevations and microhabitat conditions in peatlands, which can increase the availability of water for *Sphagnum* moss development (Benscoter et al., 2015). Additionally, wildland fires can accelerate vegetation regeneration by stimulating germination via belowground vegetative parts and serotinous cones (Brown et al., 2000). However, opposite to this, lowering of the water table and climate drying can cause extensive peat loss via burning and aerobic decomposition (Stralberg et al., 2020). Therefore, the combination of seismic lines and wildland fire impacts on peatlands should be examined as these might hinder or exacerbate future wildland fire regimes.

In addition to the above, ecosystem response to stressors can take many years to accumulate and become evident, but it is difficult to characterize these additive effects due to lack of baseline data. Hence, it is challenging to quantify the cumulative effects of

these disturbances within a short period of time due to remoteness and density of seismic lines. The range of variability or response that might exist within and between peatlands may also vary over time due to alterations in environmental conditions. Field measurements are critically important for understanding the impacts that seismic lines and climate change have on peatlands because they can be used to measure changes in processes that impact ecosystem dynamics (Tiner et al., 2015). However, it is difficult to measure these changes across a large number of peatlands or over a long temporal period. Therefore, this requires a combination of remote sensing and field approaches. Remotely sensed data provides information about the object without touching, thus allowing sampling beyond field plots (Tiner et al., 2015). It can be used to separate sites spatially based on environmental gradients that can be used as proxy for quantifying ecosystem recovery over time.

The research in this thesis is conducted in the Boreal Plains Ecozone south of Fort McMurray, Alberta using airborne lidar data in combination with field plots to identify the combined effects of natural (fire) and anthropogenic (seismic line) disturbances on peatlands. Specifically, it aims to understand which peatland ecosystems (class and form) are more or less resilient to seismic line disturbances and quantifies post-fire regeneration in these ecosystems. The outcomes of this research are of interest to Alberta Environment and Parks, and Canadian Forest Services in terms of future management of these disturbed areas.

## 1.2 KEY DEFINITIONS

This thesis will examine processes related to key terms, described below:

### 1.2.1 Peatlands (bogs vs. fens)

Peatlands are wetlands that have greater than 40 cm accumulation of peat and organic matter (National Wetland Working Group, 1997; Ducks Unlimited Canada, 2015). Peat is defined as partially decomposed plant matter, primarily mosses and sedges with a von Post humification value of  $\leq 5$ , which indicates undecomposed to partially decomposed organic matter (Government of Alberta, 2015). Moss and sedge biomass accumulate under water saturated conditions when the rate of decomposition is less than primary production by plants (Vitt, 1994). Peat columns are further separated into upper, partially saturated “acrotelm” where peat accumulates first due to high rates of decomposition (Ingram, 1978), followed by a lower, fully saturated, and anaerobic layer, the “catotelm”, where decomposition is slow (Clymo, 1984; Vitt 2019). The two main classes of peatlands are bogs and fens, which constitute 67% and 32% of peatland area found in Canada respectively (Tarnocai, 2009). These are differentiated based on water source, nutrition levels, and vegetation species (Kuhry et al., 1993; Government of Alberta, 2015).

Fens are largely minerogenous receiving water inputs from a variety of sources including groundwater, surface runoff, and precipitation (Government of Alberta, 2015). Moreover, along with hydrological inputs, fens are nutrient rich, receiving inputs from surface and subsurface layers as they are lower in elevation than the surrounding landscape (Vitt, 1994; Vitt 2019). The organic layer of fens consists of decomposing

sedges, reeds, cattails, and mosses making them typically more saturated, and younger in peatland successional stage than bogs with a poorly developed acrotelms (Gorham, 1991; Vitt, 2019). Also, fens are more alkaline having a higher range of pH from 4.0 to 7.5 (Warner and Asada, 2006; Government of Alberta, 2015). Hence, fens are more hydrologically complex and can be separated into rich and poor fens depending on water chemistry and vegetation structure. The water flow from sub-surface layers supports water-adapted vegetation (Stevenson et al., 2019). Rich fens have higher alkalinity due to abundance of base cations, such as calcium, and are dominated by brown mosses (Vitt, 2019). In contrast, poor fens are older in terms of peatland successional stages and are similar to bogs in terms of hydrology, with typically lower pH and more *Sphagnum* dominated groundcover (Ducks Unlimited Canada, 2015). Based on vegetation, fens can be classified into treed, shrubby, and graminoid forms, which provides a more detailed description. Treed fens have more than 25% stunted coniferous species consisting of *Picea mariana* and less flammable *Larix laricina* along with shrub and moss species. Shrubby fens are characterized by a variety of deciduous species including *Betula glandulosa*, *Betula pumila* and *Salix* spp., which are typically less than 2 m in height, while graminoid fens have less than 25% tree and shrub cover dominated by sedges such as *Carex lasiocarpa* or *Carex limosa*. (Government of Alberta, 2015). Hence, fens have a higher diversity of species with bryophytes, graminoids, and low shrubs being the primary indicator species of the type of fen.

Unlike fens, bogs are ombrogenous wetlands that receive their nutrient and water inputs solely (or for most part) from precipitation because their surface is raised above the surrounding terrain (Vitt 1994). Hence, bogs are typically isolated from groundwater

inputs due to elevation as their ground surfaces are often  $\geq 40$  cm above the water table (Government of Alberta, 2015). Moreover, ombrogenous bogs have well developed acrotelms that are composed of variably decomposed *Sphagnum* moss, which maintains water table close to the surface (Vitt 2019; Ducks Unlimited Canada, 2015). Chemically, bogs are acidic with pH < 4.0 to 5.0, cation poor, and have poor nutrient availability of nitrogen, phosphorus, and other minerals limiting the diversity of plant species that can establish (Vitt et al., 1994; Government of Alberta, 2015). Similar to fens, bogs may be classified as treed, shrubby, and open forms based on vegetation. However, they are less diverse with treed bogs dominated by *Picea mariana*. Shrubby bogs consist of *Ledum groenlandicum*, *Vaccinium vitis-idaea*, and *Oxycoccus microcarpu* while open bogs are *Sphagnum* dominated (Government of Alberta, 2015). Hence, bogs are more homogenous with more flammable black spruce constituting the tree canopy making them more susceptible to wildland fires and climate mediated drying (Thompson et al., 2019).

### **1.2.2. Seismic lines**

In the boreal region, seismic lines are a dominant form of anthropogenic disturbance of forests and peatlands (Lee and Boutin, 2006). With over 168 billion barrels of recoverable oil found in the Alberta's oilsands (Dabros et al., 2018), the industrial exploitation of these boreal ecosystems has increased since the early 1960's when oil sands development first began. Mapping sub-terranean petroleum reserves require the use of seismic surveys, which identify the presence and depth of oil and gas reserves (Government of Alberta, 2021). Seismic lines are the remnants or legacy of these seismic surveys and are defined as narrow, linear forest clearings used in

exploration to access oil reserves and transport seismic survey equipment (Sheriff and Geldart, 1995; Government of Alberta, 2021). It is estimated that seismic lines in Alberta extent over 1.5 to 1.8 million kilometers in length with high density in northeastern Alberta (Dabros et al., 2018)

Historical seismic lines installed through the 1970's to 1990's were 5 to 10 m wide, and about 300 - 500 m apart, defined as "conventional seismic lines" (Figure 1.1). These were constructed in straight lines using bull dozers, clearing the surrounding trees and ground vegetation (Dabros et al., 2018). Also, these seismic lines were constructed in winters when it was easier to remove the vegetation. Oil and gas resources were then determined by using surface vibrators or drilling shot holes with explosives along seismic lines (Sheriff and Geldart, 1995; Dabros et al., 2018). From the early 2000's improvement in Global Positioning System (GPS) technology accuracy and smaller equipment size lead to the creation of "low-impact seismic lines" (LIS) which were 1.5 to 3 m wide. These were constructed using low ground pressure mulchers in a meandering path design to keep the soil intact and reduce ecosystem impacts (Government of Alberta, 2021). In Alberta, seismic lines cover over 1,900 km<sup>2</sup> of total area of peatlands and leave a visible human footprint due to slow regeneration within seismic lines that cross forests and peatlands (Stracks et al., 2019; Dabros et al., 2021). Current regulations across Canadian provinces and territories (Alberta, British Columbia, and Yukon) encourage the use of LIS, while reclamation focuses on cleanup and limiting further disturbances with little emphasis on re-vegetation (Dabros et al., 2018). However, the environmental regulatory framework for Alberta's oilsands require that the energy sector restores the post-mining landscape to equivalent land capabilities prior to disturbance, so that it can



be functionally productive, but will not be identical to pre-disturbance level (Nwaishi et al., 2016).



**Figure 1. 1** Conventional seismic line through an unburned peatland near Wandering River, Alberta surveyed on August 1, 2020.

### **1.2.3. Fire chronosequence**

Wildland fires are defined as any nonstructured fire other than prescribed burns (Brown et al, 2000) and are a major form of natural disturbance in the Boreal Plains (Flannigan et al., 2009). Increasingly severe fires often cause significant pollution emissions associated with burning of biomass, while post-fire regeneration is slow, resulting in altered ecosystems in the years following fire (Flannigan et al., 2000; van der Werf et al., 2010). Peatlands usually have a fire return interval of about 100-120 years (Turetsky et al., 2004), but with climate change, Whitman et al. (2019) found a decrease in fire return interval, making it difficult for boreal ecosystems to recover during the early to intermediate period, post-fire. Chronosequence-based approaches are an indirect

approach for measuring temporal dynamics of plant communities in an area that has similar soil characteristics and climate (Walker et al., 2010). Measurements of vegetation within a fire chronosequence is one approach that may be useful for quantifying and understanding changes in ecosystem productivity over time, without the need for long-term study over years to decades at a single site. Here fire acts as natural disturbance regime that creates a mosaic of ecosystems with different ages since fire influenced by local and regional factors (Bolton et al., 2017).

### **1.3 STUDY REGION - BOREAL PLAINS ECOZONE**

The study is conducted approximately 230 km south of Fort McMurray near Wandering River, Alberta (112° 12' 31" W, 55° 37' 46" N) in the Boreal Plains Ecozone (herein 'BPE'). The BPE is the third largest ecozone of Canada covering 58% of Alberta (Alberta Parks, 2015), and parts of Saskatchewan, and Manitoba with some extension into northeastern British Columbia and parts of the Northwest Territories (Figure 1.2). The BPE is Canada's driest boreal ecozone with extreme annual variations in temperature and total annual precipitation between 300-500 mm (Canadian Councils of Resource Ministers, 2014). The closest weather station (Lac La Biche) had a total annual precipitation of 482 mm with mean annual temperature of 2°C for the year 2020 (Government of Canada, 2021). Summers are moderately warm with daily average temperatures greater than 15°C (Alberta Parks, 2015). The surficial geology is characterized by deposits of glacial till and fine-grained glaciolacustrine deposits (San-Miguel, 2020). Over 60% of the ecozone consists of coniferous, broadleaf deciduous, and



mixed forests while wetlands are found in the poorly drained flat areas (Ireson et al., 2015).

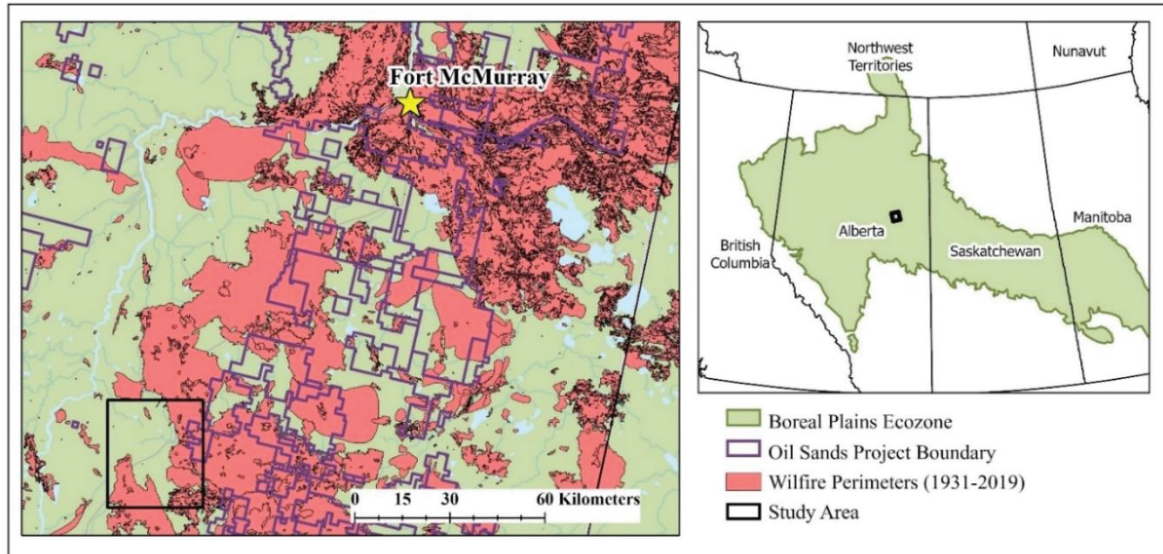


**Figure 1. 2** Map outlining the study area in the Boreal Plains Ecozone of Canada. Current oilsands project boundaries (active as of 2015) and wildland fires from 1931-2019 are included.

The BPE is highly sensitive to climate change and the warming climate is predicted to convert Alberta's boreal zone into parkland (Ireson et al., 2015; San-Miguel, 2020). Moreover, the BPE has a high percentage of area burned by wildland fires and is fragmented by oilsands exploration and agricultural clearing causing a decline in forest cover by 3% from 1985 to 2005 (Canadian Councils of Resource Ministers, 2014). Wetlands constitute 45% of the boreal Oil Sands Region in Alberta (~ 64,000 km<sup>2</sup>), and these wetlands are at risk due to degradation from resource extraction and other human disturbances (Ficken et al., 2019). These human activities have also impacted wildlife populations, plant species composition, and ecosystem services of the BPE and needs to be monitored to maintain the ecological integrity of this region.

## 1.4 STUDY OBJECTIVES

The overall goal of this research is to determine the cumulative impacts of natural (wildfire) and anthropogenic disturbances (seismic lines) on peatlands (particularly bogs and fens) and how these influence post-disturbance deciduous shrub and conifer regeneration trajectories within a region that is undergoing climate change. To understand these gaps in research, a chronosequence of 5 year, 18 years, 30 years, 38 years since fire, and unburned in the recent recorded history since about 1930 near Fort McMurray, Alberta was used to understand the impact of time since fire and seismic line disturbances on peatland regeneration and recovery.

This overall goal will be addressed through two primary objectives that are subdivided into sub-objectives.

1. Using a space-for-time-chronosequence of 5 years, 18 years, 30 years, 38 years, since fire (and ‘mature’), determine how wildland fire affects the regeneration trajectory of conifer trees vs. deciduous shrub and tree communities in seismic line-disturbed and natural (undisturbed) boreal peatlands.
  - (a) Determine the utility of multi-spectral lidar for identifying deciduous vs. conifer trees, and shrubs species.
  - (b) Quantify proportional coverage of post-fire shrub vs. tree regeneration within peatlands.
  - (c) Determine the approximate timing of dominance of shrub vs. tree species determined from growth rate within the fire chronosequence.

2. Do wildland fires that burn over seismic lines in peatlands result in regeneration of woody vegetation situated adjacent to seismic lines, relative to peatlands fragmented by seismic lines only?
  - (a) Assess how the spatial distribution of deciduous and conifer vegetation varies within and with distances from seismic lines in a peatland post-fire burn chronosequence, compared with recently unburned and undisturbed 'mature' reference peatlands.
  - (b) Determine the primary environmental and anthropogenic drivers (as correlates) of post-fire and post-seismic line vegetation regeneration within and adjacent to seismic lines in boreal peatlands with time since fire.

Based on literature we hypothesize, more shrubification in peatlands during the early years post-fire, and as regenerating forests age, the fuel content shifts from deciduous to conifer, providing more fuels for wildland fire. In terms of seismic lines, we hypothesize that there will be higher deciduous regeneration proximal to seismic lines as a proxy indicator of changes in resource availability and abiotic factors compared with undisturbed parts of peatlands. Furthermore, seismic line attributes combined with incoming solar radiation and soil moisture availability will influence vegetation regeneration trajectories

## **1.5 THESIS ORGANIZATION**

This thesis is divided into five chapters. Chapter 2 provides a literature review of climate mediated and anthropogenic disturbances to peatlands in the Boreal Plains

Ecozone and how peatlands recover from these disturbances. It also addresses the use of remote sensing and field methods to quantify and monitor these disturbances over time. The next two chapters are written as standalone journal articles addressing each of the main objectives.

Chapter 3 addresses objective 1 and uses multispectral lidar data collected from a fire chronosequence boreal peatland to identify conifer vs. deciduous shrub and tree regeneration trajectories. It also identifies the important variables used for species classification and the limitations of using a remote sensing-based approach.

Chapter 4 addresses objective 2 and uses manually delineated seismic line buffers to quantify spatial distribution of deciduous shrubs, deciduous trees, and conifers within peatlands. It also determines what general peatland attributes and seismic line characteristics explain the variability in average vegetation height within peatlands.

Chapter 5 concludes this thesis by summarizing the key findings of the research and the limitations. It also provides recommendations for future study.

## **CHAPTER 2. LITERATURE REVIEW: IMPACTS OF CLIMATE CHANGE AND ANTHROPOGENIC DISTURBANCES ON PEATLANDS**

### **2.1. INTRODUCTION**

Warming of Canada's climate has caused severe impacts on natural ecosystems, including peatlands. Human activities have exacerbated increases in surface air temperatures (Hawkins et al., 2017), extreme weather events (Cheng et al., 2012), and have altered precipitation patterns (Zhang et al., 2013) causing changes in species distribution and climatic zones (van der Werf et al., 2010; Nunez et al., 2019). The average annual air temperature in Canada has increased by 1.7 °C between 1948 to 2016, which is approximately double the increase in the global average (Bush and Lemmen, 2019). Moreover, at higher latitudes in northern Canada, air temperature has increased by 2.3 °C on average from 1948 to 2016, causing ecosystems to be vulnerable to additional natural and anthropogenic disturbances (e.g., Chasmer and Hopkinson, 2017). Peatlands are important ecosystem that have large carbon stocks, allowing them to accumulate high moisture conditions, thereby creating broad areas of ecological refugia due to their moist conditions (Waddington et al., 2015; Thompson et al., 2019). About  $1142 \times 10^3$  km<sup>2</sup> of land surface of Canada consists of peatlands, which is 87% of all peatlands found in North America (Tarnocai and Stolbovoy, 2006). However, with increased drying of peatlands, climate models predict that anthropogenic climate change will cause a positive climate feedback response in carbon emissions from these peatlands (Gorham, 1991; Weltzin et al., 2003). With enhanced warming, peatlands release more carbon into the atmosphere as CO<sub>2</sub> due to enhanced decomposition and changes in soil moisture (Waddington et al., 2015). In peatlands with high water table and high vascular

plants (primarily sedges), these are expected to enhance methane (CH<sub>4</sub>) production, especially as deep roots can transport carbon rich substrate to methanogens for anaerobic decomposition (Vitt, 2019).

Apart from climate change, wildland fire also has a significant impact on the structure and function of ecosystems. Fires are natural disturbances that are important because they initiate secondary succession, maintain diversity, and change ecosystem equilibrium (Flannigan et al., 2000). However, land use and land cover change associated with converting forests and peatlands to agriculture and other uses, often requires the use of fires, especially prevalent in tropical peatlands. While this method is not widely applied to northern boreal peatlands, the burning of tropical peatlands has added 0.5 Pg of carbon per year to the atmosphere (van der Werf et al., 2010).

Also, boreal peatlands that exist in a sub-humid zone, climate change is likely to have a profound impact on fire activity, causing peatlands to become more susceptible to climate mediated drying, providing more fuel for intense fires (Gorham 1991; Vitt et al., 1994). Warmer air temperatures earlier in the spring and later in the fall are also expected to lengthen the fire season by 22% (Flannigan et al., 2015). Hence, future climate models predict that there will be more fires in a warmer world, and especially in boreal peatlands if there is not significant increase in precipitation that is required to offset the overall effect of warming (Flannigan et al., 2015). Based on Canadian Fire Weather Index (FWI), Flannigan et al. (2015) predict that for every degree of warming, precipitation needs to increase by 15% for fine surface fuel, 10% for upper forest fuel layers, and 5% for deep organic soils to compensate for the drying of peatlands. Despite these requirements, the amount of precipitation has not increased over the last couple of

decades, making peatlands in the BPE particularly vulnerable to stress due to drying. These effects are more evident in central Alberta where peatlands are close to their hydroclimatic limit (Devito et al., 2005).

In addition to stressors from climate change and wildland fire, boreal peatlands are also subjected to anthropogenic disturbances. There are approximately 5.5 billion barrels of oil that can be mined from Alberta's oilsands, where resource exploration activities often face a conflict between environmental protection and economic benefits (Kits, 2017). Human disturbances from oil and gas exploration and forestry operations often fragment peatlands further, potentially exacerbating or enhancing the intensity of wildfire by altering the soil structure and hydrology of peatland ecosystems, resulting in changes to vegetation successional trajectories (Dabros et al., 2018; Davidson et al., 2020). However, linear disturbance in the form of seismic lines and their impacts on peatlands in combination with climate change and wildland fire presents a no-analogue cumulative disturbance scenario in which we have only relatively recent *a priori* knowledge of how these will interact within peatland ecosystems. Moreover, these natural and anthropogenic drivers (here, drivers are defined as superior complex phenomenon that governs ecosystem change) create pressure on peatland ecosystems causing changes in their biotic and abiotic state (Ficken et al., 2021). This makes it difficult predict future succession trajectories and their impact on other environmental factors within individual peatlands and across the broader extent of the Boreal region (Dabros et al., 2018; Barber et al., 2021).

This chapter will review the literature on how the combination of climate mediated ecosystem changes over time and anthropogenic disturbances by oilsands

industries, in particular, impact peatlands in the western part of the Boreal Plains Ecozone with focus on north-central Alberta. The chapter is divided into the following sections: (1) Climate mediated impacts on peatlands; (2) Impacts of anthropogenic disturbances on peatlands; (3) How peatlands respond to these disturbances; (4) Use of remote sensing to study peatlands; and (5) Recommendations for integrating fieldwork and remote sensing.

## **2.2. CLIMATE MEDIATED IMPACTS TO PEATLANDS**

To address the effects of climate mediated disturbances on peatlands we need to understand changes in the fire regime in the boreal plains and how this impacts the hydrology of peatland ecosystems. These changes are described below:

### **2.2.1 Changes in fire regimes**

With increasing air temperatures, wildland fires in the Boreal Plains Ecozone are occurring more frequently each year, with higher intensity and with greater severity, burning larger areas of forests and peatlands (Flannigan et al., 2000; Wang, 2002; Keeley, 2009). Over the past decade, wildland fires have burned two million hectares on average per year, while extreme fire years can result in the burning of more than seven million hectares (Flannigan et al., 2015). Moreover, climate models predict an increase in spring air temperatures by 2-6 °C and a decrease in late summer precipitation in boreal ecozones, leading to decrease in boreal forest/peatland area and changes in species composition and distribution (Weber and Flannigan, 1997; Walker et al., 2020).



Fire regime is defined as the general temporal and spatial characteristics of fire occurrence over decades to centuries and includes the frequency of fires over a given time period, seasonality of their occurrences, the intensity (or energy) with which they burn, fire severity (an indicator of the impacts of fire on ecosystems/loss of biomass), fire size, and type of fire (Brown et al., 2000; Whitman et al., 2015). These characteristics create a historical summary of the effect of fires on the landscape and help scientist estimate post-fire vegetation dynamics and ecosystem recovery (Whiteman et al., 2019). Historically, fire regimes in western North America were fuel limited with low to moderate severity and frequency (Coop et al., 2020). Moreover, 80% of the area was burned by lightning fires with a fire return interval of 179.9 years (de Groot et al., 2013). Most tree species found in wildfire prone areas exhibit fire adaptive traits such as seedbanks and/or dormant buds along stems or roots which helps plants recover post-fire (Brown et al., 2000).

Despite this general history of fire regimes in North America, climate mediated warming can alter the local post-fire environment such that fire intensity and frequency adjusts beyond the adaptability range of these fire adaptive species, thereby hindering recovery mechanisms (Coop et al., 2020). For example, conifers such as black spruce have semi-serotinous cones that disperse seeds following wildland fires. These trees require fire-free intervals for forests to recover, but due to shorter fire return intervals, fire now sometimes occur before conifers mature, thus post fire seedbank is reduced due to poor seed viability and availability (Coop et al., 2020). Whiteman et al. (2019) found that sites with shorter return intervals ( $\leq 17$  years) had thinner residual organic soil with more deciduous tree species. Deciduous species, such as aspen are less flammable due to

higher moisture content, and have higher dispersal capability due to lightweight seeds, allowing them to recover more rapidly, post-fire (Whiteman et al., 2019; Coop et al., 2020). Hence, deciduous species can replace conifers due to climate mediated disturbances and shorter fire return intervals.

Wildland fires are typically controlled by four factors: weather/climate, fuels, ignition agent, and human activities with the latter having a significant impact more recently (Flannigan et al., 2015). Moreover, weather and climate influence the amount and type of fuel as well as the ignition mechanism. Hence, climate warming will have an immediate effect on fire activity, especially on peatlands that store approximately one third of the global soil carbon (Turetsky et al., 2002). Peatlands have not burned easily in the past because of their moist to wet soil/peat conditions described in Chapter 1. Low severity wildfires from 1980 to 1995 have burned  $1470 \pm 59 \text{ km}^2/\text{year}$  of peatlands, consuming different layers of fuel strata (Schiks et al., 2016). However, recently, peatlands are drying, thereby enhancing fuel sources (Flannigan et al., 2015) and increasing depth of burn  $> 0.20 \text{ m}$  along peatland margins (Lukenbach et al., 2017). Wooded peatlands are also more prone to fires than open or shrubby peatlands, possibly due to the added flammability of black spruce trees and open-air pockets beneath tree roots, which allow fires to smoulder (Turetsky et al., 2002).

Regardless of the existence of trees, peatland fires are dominated by smoldering combustion that burns surface fuels such as non-vascular plants, litter, and ground layers consisting of organic matter and root biomass (Flannigan et al., 2009). Smoldering fires can last for several months and burn deep into peat and organic soil layers (Schik et al 2016). The depth of burn in peatlands is influenced by soil moisture and bulk density,

which can influence water table fluctuations (Hokanson et al., 2016). Higher bulk density results in greater fluctuation of the depth to water table, and during drier periods, can cause greater depth of burn in peatlands, while denser organic matter in peat columns can result in greater burn severity associated with loss of biomass (Benscoter et al., 2011). Hence, peatland fires are mostly moisture limited not fuel limited, thus changes in fire regimes due to climate mediated disturbances that alter fuel moisture will impact fire behavior and post-fire regeneration (Weber and Flannigan, 1997).

### **2.2.2 Changes in peatland hydrology**

Peatlands are moist wetland ecosystems that typically exist in environments that are cool, where precipitation exceeds moisture losses from evapotranspiration (Holden, 2005). Changes in precipitation patterns are more temporally and spatially variable than air temperatures, making the amount of precipitation that will fall in an area difficult to predict (Price et al., 2013). In recent years, peatlands in central Alberta have transitioned to moisture deficit, where evapotranspiration exceeds precipitation for most years (Devito et al., 2005; Waddington et al., 2015). Changes in climate, especially precipitation and atmospheric drying can reduce water inputs and increase evapotranspiration, altering water movement across and below peat surface, thereby changing peatland hydrological fluxes and reducing moisture storage (Holden, 2005; Lukenbach et al., 2016). The internal hydrology of peatlands play an important role in enhancing resilience to natural and anthropogenic disturbances. Hydrology also influences ecosystem processes including nutrient cycling, carbon sequestration, and diffusion of CO<sub>2</sub> and CH<sub>4</sub> from the peat surface to the atmosphere (Holden, 2005; Bridgham et al., 2008).

*Sphagnum* mosses constitute majority of peatland groundcover, inhibit decomposition, and contain hyaline cells, which store moisture and can increase the water storage capacity of peatlands when depth to water table increases (Bu et al., 2013). Hence, peatlands that have a stable water supply via groundwater may have similar pre- and post-fire water table positions, enabling them to be more resilient to climatic and anthropogenic disturbances (Lukenbach et al., 2016). However, peatlands that are hydrologically disconnected (for example, ombrogenous bogs) are more vulnerable to declines in water table position. Higher air temperature and high burn severity can cause a decline in *Sphagnum* species as *Sphagnum* are unable to regenerate on hummocks, or compete with vascular plants, due to changes in post-fire microtopography and hydrology (Benscoter et al., 2005; Dieleman et al., 2015). Drier conditions also promote shrubification of peatlands and can cause transition from *Sphagnum* spp. to feathermoss spp., which have low moisture retention capacity and higher burn severity (reviewed in Nelson et al., 2021).

One method that may be used to understand the impacts of climate change on peatland fire regimes is to examine peatlands that have been disturbed through draining (Sherwood, et al., 2013). While draining is an anthropogenic disturbance, drained peatlands could be an indicator of the loss of water that may occur as a result of climate change. For example, peatlands are drained for silviculture, which can lower the water table by 0.25 m, decreases the hydrological buffers making it difficult for *Sphagnum* moss to recolonize (Kettridge et al., 2015). Peatland drainage of surface and groundwater inputs also cause compaction of the peat profile and reduces peat moisture (Nelson et al., 2021). These act to increase fuel availability for high intensity fires because the peatlands

no longer retain the moisture needed to reduce smouldering beneath the peat surface (Sherwood et al., 2013).

Drained peatlands that are deeply burned can also have fluctuating water table positions in the years since fire (Thompson et al., 2014; Lukenbach et al., 2017; Nelson et al., 2021). A study by Kettridge et al. (2015) found that there was a 77% reduction in moss cover in a post-fire drained fen peatland. The drained fen was also colonized by willow and birch, which had a higher leaf area index than an undrained reference site. Hence, drainage combined with fire provided an indicator of how climate change via drying and lowering of the water table could impact peatlands in the future by altering evapotranspiration fluxes, thereby shifting peatland hydrological balance and impacting vegetation succession (Kettridge et al., 2015; Lukenbach et al., 2016; Nelson et al., 2021).

### **2.3. ANTHROPOGENIC DISTURBANCES TO PEATLANDS**

Peatlands are also impacted by various human disturbances including seismic lines which have long lasting effects on peatland ecosystems. They can also have proximal effects on vegetation recovery by altering peatland biotic and abiotic state. The impacts of these disturbances are described below:

#### **2.3.1 Peatland fragmentation by seismic lines**

Alberta is well-known internationally for its oil and gas reserves, most of which exist in the boreal region of central Alberta and Saskatchewan (Stack et al., 2019).

Oilsands deposits cover 475,000 ha of the boreal zone of Alberta with over 50% of the landscape supporting wetland ecosystems (Rooney et al., 2012). Petroleum exploration is often initiated using seismic lines. These are linear corridors or clearings used since 1960s to explore oil reserves deep below the Earth's surface and can be further classified into conventional (5 – 10 m wide) and low-impact (1.5 – 3 m wide) seismic lines (as defined in Chapter 1). Seismic lines are a dominant disturbance feature in northeastern Alberta (Jordaan, 2012). The mean density of seismic lines is 1.5 km per km<sup>2</sup> however, density can vary to upwards of around 40 km per km<sup>2</sup> in western Canada, which is higher than the density of road networks in Alberta's agricultural zones (Lee and Boutin, 2006; Finnegan et al., 2019). Forested regions are also fragmented by access roads, pipelines, transmission lines, and well pads, which are used to support the oil industry, as well as other natural resources extraction activities such as forest harvesting. Despite this, seismic lines are one of the most prevalent anthropogenic disturbances in North America, constituting approximately 50% of the linear disturbance footprint (Finnegan et al., 2019). Therefore, these often have significant impacts on biodiversity and ecosystem processes in the boreal region (Dabros et al., 2018; Lovitt et al., 2018).

While seismic lines are relatively low impact compared with other types of disturbances, such as in situ and open-pit mining, the installation of seismic lines can have significant influences on the local environment for which they are installed. For example, the construction of seismic lines leads to soil compaction and compression, which makes it difficult for water to penetrate, resulting in the pooling of water near the surface adjacent to and within seismic lines (Dabros et al., 2018). Moreover, increased compaction can decrease the hydraulic conductivity of peat by 75% and increase bulk

density, thereby changing soil morphology (Davidson et al., 2020). These changes can have significant impacts to the local hydro-ecology of the area adjacent to and within the seismic line. For example, Dabros et al. (2018) found that the removal of vegetation and topsoil delays snowmelt and increases albedo of the surface in winter compared to adjacent sites. Also, linear disturbances tend to simplify the microtopography of peatlands by removing hummocks, causing an overall flattening of the peatland surface (Lovitt et al., 2018). For example, Stevenstone et al. (2019) found that seismic lines decreased elevation by 8 cm compared to adjacent forest stands. Comparatively, Lovitt et al. (2018) found that elevation within seismic lines was 2.2 cm lower, on average, compared to adjacent undisturbed peatlands, resulting in shallower water table positions.

Due to changes in abiotic condition, the majority of seismic lines fail to recover back to woody vegetation cover. Water saturated conditions inhibit the development of *Sphagnum* hummocks, which serve as suitable microsites for tree recruitment (van Rensen et al., 2015; Lovitt et al., 2018). Moreover, increased use of seismic lines by off-road vehicles for recreational activities hampers the recovery of conifer seedlings, such as black spruce (Lee and Boutin, 2006; Dabros et al., 2018). In fens, depressed microtopography enhances seismic line flooding and allows moisture tolerant graminoids such as sedges to establish (van Rensen et al., 2015). Sedge dominated fens impact greenhouse gas fluxes by increasing CO<sub>2</sub> and CH<sub>4</sub> emissions associated with the higher respiration rates of these plants (Davidson et al., 2021). Hence, even after 35 years, more than 60% of early seismic line disturbances remained in the landscape, and only 8.2% of these lines recovered to greater than 50% woody vegetation (Lee and Boutin, 2006).

### 2.3.2 Proximal effects of seismic lines

Apart from landscape fragmentation, the establishment of seismic lines also cause edge effects between the linear disturbance (seismic lines) and the adjacent ecosystem. Medium or wide seismic lines alter biotic and abiotic conditions with significant proximal effects on neighboring forest and peatland plant communities (Dabros et al., 2018). Seismic line edges have increased incoming shortwave radiation, due to reduced shading by trees, higher air temperature, and higher soil moisture compared with adjacent peatland/forest ecosystems, thereby impacting the growth and abundance of peatland plant species (Dabros et al., 2017). Moreover, line orientation (N – S vs. E – W) can mitigate or enhance the effect of seismic lines on adjacent peatlands as this alters local micro-climatic factors depending on sun angle, direction of the edge, solar input, and evapotranspiration (Chen et al., 1995; Dabros et al., 2021).

For example, Abib et al. (2019) found that vegetation within 5 to 15 m of seismic lines was shorter with a more open canopy. This may be due to spatial variations in solar radiation where increased light penetration allows deciduous shrubs and herbs to establish on seismic lines while conifer regeneration is generally reduced compared with deciduous species regeneration (Revel et al, 1984). However, vegetation adjacent seismic lines, such as deciduous and coniferous trees were taller than the interior natural forest (Dabros et al., 2018; Abib et al., 2019). Spatial variations in the density of trees and shrubs can increase competition for moisture and nutrients. This can be disadvantageous to shrubs, herbs, and other bryophytes causing reduction in herbaceous cover along the line edges (Dabros et al., 2017). Moreover, wider seismic lines can have greater proximal effects on vegetation height and fractional cover of understory plants up to 100 m (Abib



et al., 2019). In a study by Dabros et al. (2021), they found that light, soil moisture and air temperature did not differ based on edge direction of seismic lines, rather, distance from seismic line explained most of the variability in plant composition.

Since there is no natural analog to these linear disturbances, it is difficult to predict the future successional trajectory within or beyond the seismic lines within boreal ecosystems (Dabros et al., 2018). Based on current median recovery rates, Lee and Boutin (2006) suggest that seismic lines can recover in approximately 112 years if they are not further disturbed. However, with continuous *in situ* oil sands exploration, van Rensen et al. (2015) suggest that one third of the existing seismic lines will fail to regenerate to a height of 3 m even after 50 years. Moreover, the reuse of seismic lines post mining further delays the recovery. This suggest that, while mining permits require functional restoration of the disturbed area, restoring peatlands remains difficult.

While the impacts to peatlands and forests can be extensive, oil sands resource development can also impact human communities as well. For example, Foote, (2012) notes that the installation of seismic lines has interrupted the relationship that local Indigenous people share with the landscape and can have detrimental health impacts on the community (Paul Dana, 2009). Hence, to reduce the effects of landscape fragmentation, old seismic lines should be allowed to recover naturally with minimum human disturbances. Wildland fire may also be able to enhance restoration by promoting secondary succession (Barber et al., 2021).

## 2.4. HOW PEATLANDS RESPOND TO COMBINED DISTURBANCES

Understanding the impacts and responses of boreal peatlands to disturbance is complex because climatic, anthropogenic, and fire disturbances influence peatlands in different ways, which vary over space and through time. Moreover, bogs and fens also burn differently and respond differently to disturbances depending on hydrological, morphological, and vegetation characteristics (as defined in Chapter 1). Post-fire ecosystem response can be quantified from variations in vegetation recovery and changes in carbon flux, which can be indicative of net ecosystem productivity. Canopy cover remains low (below 2 m in height) in the first decade post fire (Bolton et al., 2015) and it takes 2-3 years for shrubs and herbs to colonize (Chen and Popadiouk, 2002), while trees take 3-7 years to establish (Johnstone et al., 2004). However, post-fire vegetation regeneration is highly variable depending on site specific environmental conditions (Bolton et al., 2015; Stalberg et al., 2018).

Both fens and bogs respond differently to cumulative disturbances. Fens in the boreal region are lower in local elevation, compared with surrounding upland forests, and are influenced by slow lateral movement of groundwater, while bogs are slightly upraised and receive water inputs from rain (Chapter 1; Ducks Unlimited Canada, 2015). Seismic lines reduce microtopographic complexity in these peatlands, which is the dominant factor influencing vegetation recovery on these lines (Stevenson et al., 2019). However, wildland fires that burn through seismic lines can improve microtopography in bogs by creating hollow elevations that have higher depth of burn and can increase growth rate on hummocks (Benscoter et al. 2015). Wildland fires can also decrease the moisture level in fens, such that drier conditions cause changes in plant cover driven by changes in water

table position (Weltzin et al, 2003). A few studies have examined the combined impacts of fire and seismic lines on ecosystems, for example Stevenson et al (2019) found no effect of wildland fire on seismic line microtopography. Similarly, Barber et al (2021) found no evidence that wildland fire accelerates vegetation recovery on seismic lines, noting that there was a 21-25% reduction in canopy height on burned seismic lines compared to adjacent forest control plots. On the contrary, Filicetti and Nielsen (2020) found that burned seismic lines in bogs and poor mesic sites had higher regeneration density compared to unburned sites, though wildland fire did not enhance regeneration in poor and rich fens. This suggests site recovery depends on seismic line depression and terrain wetness (Stevenson et al 2019; Filicetti and Nielsen, 2020).

Bogs and fens also vary in terms of species recovery. Stevenson et al., (2019) found that seismic lines in bogs had willow and bog birch regeneration, which are usually found in wetter areas, while poor fens had water sedges and buckbean which are usually associated with the wetter conditions found in rich fens. Similarly, Chasmer et al. (2021) found increased shrub growth in bogs fragmented by anthropogenic disturbances. Hence, bogs typically have lower species richness and can be more subjected to increased shrub cover by as much as 50%, as anthropogenic climate change decreases water table elevations (Weltzin et al., 2003; Bridgham et al, 2008). Moreover, frequent wildland fires and increased drying can create a younger forest mosaic with enhanced regeneration of deciduous upland species such as aspen, which can encroach into peatlands (Thompson et al., 2019; Nelson et al., 2021). Younger deciduous dominated forests store less carbon than mature old growth coniferous stands, causing peatlands to become reduced carbon sinks with the potential to switch to a carbon source rather than a sink (Kashian et al.,

2006). The conceptualization of these feedbacks are summarized in Figure 2.1. However, more research is needed to understand whether wildland fires reverse or accelerate the negative impacts of seismic lines in peatlands, and particularly in climatically sensitive fens.

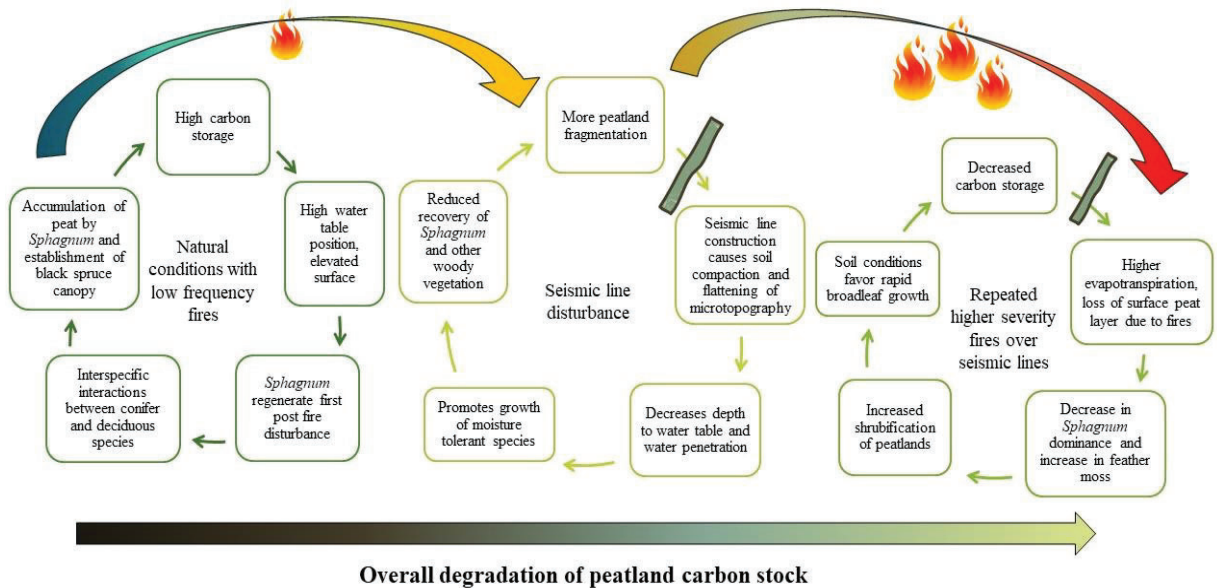


**Figure 2. 1** Peatland feedback response to climatic and anthropogenic disturbances based on known literature (Kettridge et al., 2015; Dabros et al., 2018; Filicetti and Nielsen, 2020; Stevenson et al 2019; Nelson et al., 2021).

## 2.5. USE OF REMOTE SENSING TO STUDY PEATLANDS

Peatlands in the northern and central Canada cover massive land areas and have high variability in environmental factors (Tarnocai and Stolbovoy, 2006). These remote locations can be difficult to access, making field measurements of ecosystem changes difficult and costly. Field work is labor intensive and is often limited temporally by the number of site visits due to the expense of doing repeating fieldwork (Chasmer et al., 2020a). Remote sensing provides a solution to the difficulty associated with doing

fieldwork, by providing an alternative method of measurement, which can be evaluated by fewer field data collections. Remote sensing involves collecting data remotely without touching the objects or measuring them directly, typically sensors that are deployed using ground based, airborne, or spaceborne platforms (Jensen, 2005). Remotely sensed data have a larger spatial coverage, often with some temporal repeatability and can be used to estimate (passive) or measure (active) cumulative effects of natural and anthropogenic disturbances on wetlands by using changes in vegetation as an indicator for a number of environmental processes that might be occurring (Tiner et al., 2015; Chasmer et al., 2020b). Because of this, remote sensing technologies allow scientists and managers to create and monitor wetland inventories in a cost-effective manner (Agrawal and Khairnar, 2019). In recent decades, we have seen the progression from scientific development of sensors and methods to operational use, where agencies are starting to put these into monitoring frameworks by using a combination passive optical sensor (e.g., Sentinel-2 series, Landsat series, MODIS) and active sensors (lidar, synthetic aperture radar (SAR)) to create high spatial resolution wetland maps (Tiner et al., 2015). The changes in passive and active remote sensing and how they have been used in wetland mapping are described below:

### **2.5.1. Passive remote sensing (optical sensors)**

The earliest remotely sensed data included aerial photography, which was realised using balloons and pigeons during the late 1800s and used to delineate landcover boundaries for surveillance. Despite widespread use, aerial photography has quantitative limitations in terms of measuring ground characteristics such as soil moisture, biomass, and water table depths (Tiner et al., 2015). Further, Tiner et al. (2015) found that often

single channel nature of photography severely reduces the ability to apply statistical classification methods. Hence, to improve understanding of the distribution of ecosystems over the Earth's surface (and human impacts on these) optical sensors were developed. Passive sensors detect electromagnetic radiation from the Sun that is absorbed, transmitted, or reflected by objects on Earth. Measurements of electromagnetic radiation is divided into multispectral and hyperspectral sensors (e.g., described in Chasmer et al., 2020a). Multispectral sensors generally detect reflected energy variations across a broad range of wavelengths, while hyperspectral sensors measure reflected radiation across hundreds of discrete narrow bands, both of which provide information on the structural and some biophysical properties about the object (Tiner et al., 2015).

The Landsat program includes a series of multispectral sensors, first launched in 1972, where much of the data collected have widely been used for wetland studies (Chasmer et al., 2020a). Landsat 8, which is the most recent currently operational sensor, recently followed by Landsat 9, launched on September 27<sup>th</sup>, 2021, collects data across a variety of different bands. These include visible, near infrared, thermal infrared, and shortwave infrared, and has a spatial resolution of 30 m for most bands with a panchromatic band with resolution of 15 m (Tiner et al., 2015). The near infrared portion of the electromagnetic spectrum is often used for wetland mapping as vegetation has high reflectance in the near infrared, while water is strongly absorbed in this region, allowing for further differentiation of water and vegetation (Lyon and McCarthy 1995). Landsat series satellites also have multiple data acquisitions per year and data are freely available, which can be used to create relatively long-term time series, allowing scientists to delineate changes in wetland boundaries (Tiner et al., 2015; White et al., 2015). On

average Landsat series have a 70-74 % accuracy in determining wetland class (e.g., bog, fen, marsh, swamp, shallow open water) (Chasmer et al., 2020a). Other sensors have higher spatial resolutions, for example, SPOT has a pixel resolution of 6 m and has slightly higher accuracy (in general, 66-80%) for detecting flooded wetlands, forests and herbaceous vegetation (Töyrä et al., 2002).

Optical sensors can be used to create spectral indices using the pre-and post-fire data to quantify the effect of wildland fire on ecosystems. For example, McCarley et al. (2017) used ratio of shortwave infrared and near infrared reflectance (d74) of Landsat Thematic Mapper to estimate canopy cover loss and found that it was strongly correlated with lidar derived canopy cover change. Also, smoldering fires that cover an area of less than 0.2 ha and occur on the ground surface below the tree canopy are difficult to detect using satellite and airborne sensors because the canopy acts as a blocking agent (Johnston et al., 2018). This makes it difficult for fire management agencies to identify the existence of and control smoldering fires, thereby potentially allowing them to burn deeper ground fuels even when there are no active crown fires.

Apart from multispectral, hyperspectral sensors (AVIRIS, Hyperion, CASI) can be used for mapping and identifying objects based on their spectral signature, across a broad range of electromagnetic wavelengths, typically associated with the molecular or cellular composition of the material (Tiner et al., 2015). Hyperspectral sensors can be used to identify moss species in peatlands (Bubier et al., 1997), determine plant biochemical properties (Schmidt and Skidmore 2003), and water extent and chemistry (Giardino et al., 2015). However, the major limitations of optical sensors are that there is trade-off between spatial and temporal resolution, where typically higher spatial

resolution results in smaller areas covered at the cost of rapid repeat intervals, though this limitation is reducing with satellite constellations of many satellites (e.g., CubeSats). Optical sensors are also sensitive to cloud cover, atmospheric conditions, and shadows with restricted use during daylight hours (Tiner et al., 2015). Moreover, optical sensors measure electromagnetic radiation from objects visible to the sensor, and are unable to measure radiation blocked by vegetation, which makes mapping the full range of ecosystem above ground characteristics difficult (Schmidt and Skidmore 2003; Chasmer et al., 2020a).

### **2.5.2 Active remote sensing (Lidar and SAR)**

Light Detecting and Ranging (LiDAR) is a form of active remote sensing in which the sensor provides its own energy as laser pulses and measures the timing between laser pulse emission and reflection to determine distance to surfaces, thereby creating a three-dimensional point cloud (Wehr and Lohr, 1999; Lim et al., 2003). Lidar technology includes terrestrial, airborne, and spaceborne systems, with wavelengths typically in the visible and near infrared portions of the electromagnetic spectrum. Lidar data are processed to create a digital elevation model (DEM), which has finer spatial resolution than other sensors such as radar-based methods. Greater spatial resolution and vertical accuracy provides an ability to derive canopy and topographic metrics that are useful for quantifying wetland extent and vegetation structure (Hopkinson et al., 2005). The lidar derived point cloud can be separated based on channels (SWIR, NIR, Green) and elevation (ground, low vegetation, high vegetation) which can be used to differentiate tree species (Figure 2.2). Moreover, the advantage of using lidar is that it provides both



horizontal and vertical information that can be used to determine structural attributes of the terrain and vegetation, while optical sensors are limited to horizontal information visible to the sensor (Chasmer et al., 2020a). For example, laser pulse returns can penetrate through forest canopies to the understory, providing more information about vegetation structure than optical imagers (Figure 2.2). The data that are provided can be used for classifying different stages of forest succession (Falkowski et al., 2009), and detecting small (0-4 m<sup>2</sup>) and large (>200 m<sup>2</sup>) changes in canopy over time (Dietmaier et al., 2019). Apart from canopy characteristics, lidar can be used to determine where surface water is likely to accumulate based on locally varying ground surface elevations. This is important for understanding hydrology and for hydrological modelling (Beven and Kirkby 1979; Töyrä et al., 2003).

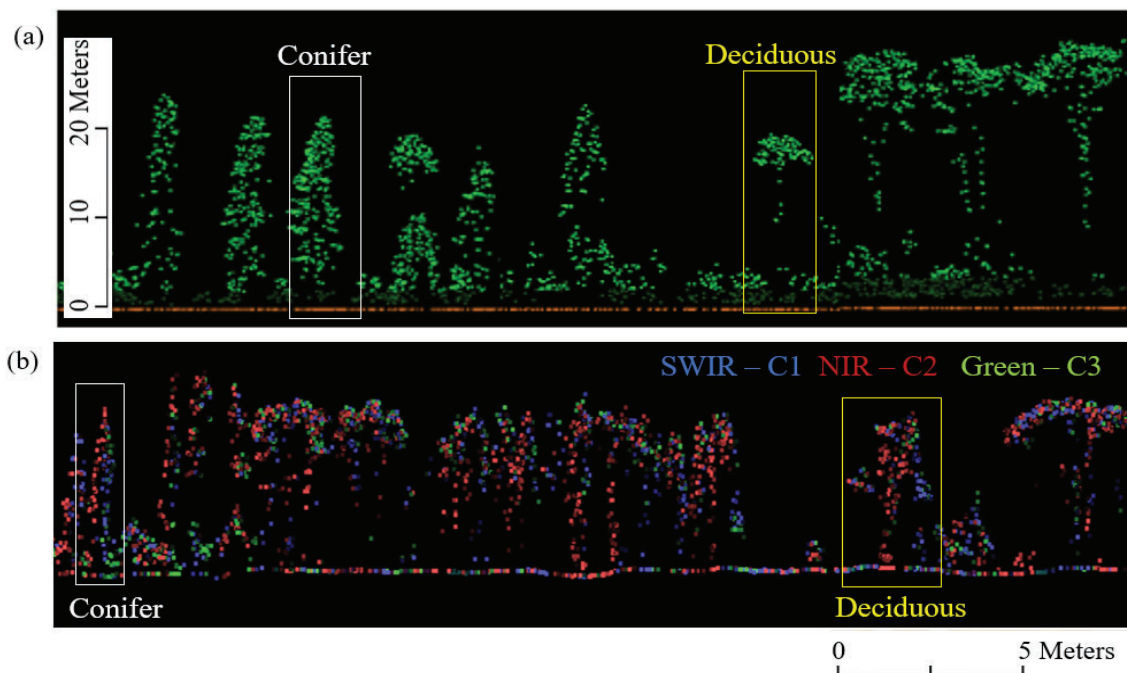


**Figure 2. 2** Lidar point cloud distribution indicating (a) ground normalised returns, where brown is the classified ground surface and green represents all returns above the ground surface; and (b) returns from individual lidar wavelengths/channels (SWIR, NIR, Green).

Synthetic Aperture Radar (SAR) is another active sensor, emitting and receiving wavelengths in the microwave portion of the electromagnetic spectrum, often used for standing water and wetland mapping (White et al., 2015). Unlike optical sensors, radar sensors are not sensitive to poor weather or cloud cover and can collect data regardless of solar illumination (Tiner et al., 2015). Moreover, backscattering of electromagnetic radiation by radars makes this useful for mapping water extent and soil moisture, due to sensitivity to surface texture (White et al., 2014). However, SAR backscattering is impacted by variability in vegetation and surface roughness, which can make it difficult to calculate soil moisture (Millard and Richardson, 2018). Still, using active remote sensing technologies has improve spatial resolution and wetland mapping capabilities.

## **2.6. INTEGRATION OF FIELD AND REMOTE SENSING MEASUREMENTS**

Remote sensing allows spatial observation through proxy indicators of ecosystem changes, however despite this, accuracy of remotely sensed data varies based on sensor limitations and sampling methodology (Chasmer et al., 2020b). Hence, field data are required to validate landcover classifications, within classification accuracies of species, water extents, etc., and improve understanding of future recovery trajectories. Some of the ways field and remote sensing data can be integrated for wetland mapping are: (a) Collect field data for validation (species height, cover, diameter at breast height, understory vegetation characteristics, etc.) using field plots rather than sampling using multiple linear transects. Larger field plots are easier to differentiate in the remotely sensed data and prevent spectral mixing of pixels during classification of species (Chasmer et al., 2020b); (b) Changes in wetland hydrology can be detected using SAR,

but variations in soil moisture needs to be verified on ground using probes or using visual observation of inundation depths (Tiner et al., 2015); and (c) differentiating the transitional boundaries between wetlands, water, and other landcover classes using a global navigation satellite system (GNSS) (Chasmer et al., 2020b). Lastly, field measurements need to be standardized and scaled to the resolution of the sensor such that the attributes captured by the field data are reflected in the remotely sensed data. The following two chapters provide examples of how field data have been used to better understand the impacts of seismic lines and fire on peatlands in the Oil Sands Region of Alberta.

## CHAPTER 3: IDENTIFYING CONIFER TREE VS. DECIDUOUS SHRUB AND TREE REGENERATION TRAJECTORIES IN A SPACE-FOR-TIME BOREAL PEATLAND FIRE CHRONOSEQUENCE USING MULTISPECTRAL LIDAR

\*Humaira Enayetullah<sup>1</sup>, Laura Chasmer<sup>1</sup>, Chris Hopkinson<sup>1</sup>, Dan Thompson<sup>2</sup>, Danielle Cobbaert<sup>3</sup>

<sup>1</sup>*Dept. of Geography and Environment, University of Lethbridge, 4401 University Drive, Lethbridge, AB, T1K 3E3; [humaira.enayetullah@uleth.ca](mailto:humaira.enayetullah@uleth.ca) (H.E.); [laura.chasmer@uleth.ca](mailto:laura.chasmer@uleth.ca) (L.C); [c.hopkinson@uleth.ca](mailto:c.hopkinson@uleth.ca) (C.H.)*

<sup>2</sup>*Canadian Forest Service, Great Lakes Forestry Centre, 1219 Queen Street, Sault Ste. Marie, ON, P6A 2E5; [daniel.thompson@NRCan-RNCan.gc.ca](mailto:daniel.thompson@NRCan-RNCan.gc.ca)*

<sup>3</sup>*Alberta Environment and Parks, 9th Floor, 9888 Jasper Avenue, Edmonton, AB, T5J 5C6; [Danielle.Cobbaert@gov.ab.ca](mailto:Danielle.Cobbaert@gov.ab.ca)*

\*Correspondence: [humaira.enayetullah@uleth.ca](mailto:humaira.enayetullah@uleth.ca) (H.E.); [laura.chasmer@uleth.ca](mailto:laura.chasmer@uleth.ca) (L.C)

*Submitted to Atmospheres special series on Climate-Vegetation Interactions in Northern High Latitudes, November 2021*

### ABSTRACT

Wildland fires and anthropogenic disturbances can cause changes in vegetation species composition and structure in boreal peatlands. These could potentially alter regeneration trajectories following severe fire or through cumulative impacts of climate-mediated drying, fire, and/or anthropogenic disturbance. We used lidar-derived point cloud metrics, and site-specific locational attributes to assess trajectories of post-disturbance vegetation regeneration in boreal peatlands south of Fort McMurray, Alberta, Canada using a space-for-time-chronosequence. The objectives were to: (a) develop methods to identify conifer trees vs deciduous shrubs and trees using multi-spectral lidar data; (b) quantify proportional coverage of shrubs and trees to determine environmental conditions driving shrub regeneration; and (c) determine spatial variations in shrub and tree heights as an indicator of cumulative growth since fire. The results showed that use of lidar-derived structural metrics predicted areas of deciduous shrub establishment (92%

accuracy) and classification of deciduous and conifer trees (71% accuracy). Burned bogs and fens were more prone to shrub regeneration up to and including 38 years after the fire. Transition from deciduous to conifer trees occurred approximately 30 years post-fire. These results improve understanding of environmental conditions that are sensitive to disturbance and impacts of disturbance on northern peatlands within a changing climate.

**Keywords**—remote sensing; machine learning; vegetation classification; climate change; wildland fire

### 3.1 INTRODUCTION

Peatlands constitute 12% of the Canadian landscape and are characterized by slow decomposition of soil organic matter (i.e., peat), having a minimum depth of 40 cm (National Wetland Working Group, 1997; Tarnocai, 2009). They play an important role as climate regulators due to gradual sequestration and storage of atmospheric carbon dioxide (CO<sub>2</sub>) over centuries (Vitt, 1994). It is estimated that northern peatlands store 10 to 16% of terrestrial detrital carbon, with significant amounts found within the Boreal and Subarctic zones of Canada (Tarnocai, 2009).

With increases in air temperature and climatic drying, boreal peatlands in western Canada may be close to reaching their hydroclimatic moisture limit due to changes in hydrology (Tarnocai, 2009; Schneider et al., 2016). Although peatlands have largely been resilient to climatic changes and wildland fire because of their moist soil conditions, many peatlands in the Boreal Plains ecozone of Alberta exist within a sub-humid climate

where evapotranspiration exceeds precipitation during most years (Waddington et al., 2015). Temporal variability in precipitation patterns in this region are characterized by multi-year, below average precipitation combined with short periods of precipitation exceeding the long-term average (Mwale et al., 2009). Interannual variability of precipitation patterns and enhanced drying are expected to increase due to climate change, thus peatlands are becoming more susceptible to wildland fires as their deep soil carbon stores transition from moist organic matter to drier fuels for fire (Flannigan et al., 2015; Schneider et al., 2016; Thompson et al., 2019). Moreover, warmer and drier climate can lengthen the fire season and increase fuel availability, enhancing both the area burned by wildland fire (Thompson et al., 2019) and greater depth of burn (Elmes et al., 2019). To compensate for the drying, precipitation needs to increase by 15% per degree of warming (Flannigan et al., 2015) and so far, the average amount of precipitation, has not increased in the Boreal Plains (Mwale et al., 2009).

Wildland fires are currently one of the major disturbances impacting northern peatlands (Turetsky et al., 2002). It is estimated that fires from 2006-2015 burned approximately 200,000 hectares annually in Alberta (Hanes et al., 2019), releasing large amounts of CO<sub>2</sub> and broad range of pollutants into the atmosphere (Akagi et al., 2011). In response to increasing fire frequency, shifts in forests from mixedwood and conifer to deciduous tree and shrub species have been observed in parts of the Arctic-Boreal region (Stralberg et al., 2018; Wang et al., 2019). Also, permafrost plateaus in northern Canada, dominated by black spruce trees, may transition into treeless bogs and fens as a result of changing climate (Sniderhan and Baltzer, 2016). In the future, climate models predict a warmer, drier climate with increases in fire severity. These changes could result in a

decline in boreal species such as black spruce, and possible transition to younger deciduous species, which may have significant implications to the climate-carbon system by altering carbon dynamics in the northern boreal forests (Amiro et al., 2001; Walker et al., 2020)

The first species to recolonize post-fire are *Sphagnum* mosses due to their low nutrient status and water retention (Lukenbach et al., 2016). However, at higher air temperatures, there is a decline in *Sphagnum* species as they are unable to compete with vascular plants (Dieleman et al., 2015; Caners et al., 2019). Feather mosses have lower subcanopy evapotranspiration rates than *Sphagnum* mosses, which are enhanced due to loss of tree transpiration and poor recovery of subcanopy vascular plants (Kettridge et al., 2017). Similarly, drier conditions and increases in depth to water table can cause encroachment of shrubs into peatlands and transition zones (summarized in Nelson et al., 2021). Canopy cover remains low in the first decade post-fire. It takes about 20-25 years, post-fire, for a black spruce canopy to establish (Bolton et al., 2015). Compared with slow regeneration of trees in forested peatlands, shrubs provide enhanced shading, thereby decreasing the evaporative demand at the peat surface. Shrubs also colonize and grow rapidly in the early years, post-fire, resulting in greater rates of biomass accumulation and aboveground net primary productivity (Alexander et al., 2012; Thompson et al., 2015). In addition to these evaporative influences, shrubs also have high stomatal resistance, increasing conservation of water in the absence of a tree canopy (Thompson et al., 2014; Thompson et al., 2017). Hence, the shrubification of peatlands may cause a shift from *Sphagnum* moss communities to deciduous species often found in upland areas, in peatlands. The expansion of deciduous vegetation into peatlands could

enhance forest-type attributes in peatlands, such as the transitioning from open and treed fens to treed and forested bogs. Enhanced drying could also predispose these ecosystems to more flammable fuel types, observed in Thompson et al., 2019 and reviewed in Nelson et al., 2021.

Despite these changes, often observed in localized studies, shifts in vegetation species, age, and structure are difficult to quantify across large and often remote areas of boreal peatlands and forests using field measurements. In addition to climate mediated drying and fire, peatlands in western Canada have been impacted by anthropogenic disturbances such as draining for resources extraction, including peat harvesting, oil and gas exploration and mining, and other disturbances (Camill et al., 2009; Dieleman et al., 2015). Remote sensing provides an opportunity to quantify the impacts of disturbance on peatlands across larger, spatially continuous areas and greater number of peatlands for which many environmental characteristics, peatland attributes, and proximal influences can be examined. Remotely sensed data can also be examined across ‘space-for-time’ chronosequence which capture differences in structure and productivity with years since disturbance or fire (e.g., Bolton et al., 2017). Although, optical sensors can vary in spatial resolution from a few centimeters (Remote Piloted Aircraft Systems or RPAS, aerial photography) to meters (Sentinel-2, Landsat) to hundreds of meters (MODIS, AVHRR), high-spatial resolution data are typically not freely available. As with all optical imagery, uncertainties can increase associated with varying solar illumination conditions (haze, clouds, etc.) and occlusions from shadows (Agrawal and Khairnar; 2019; reviewed in Chasmer et al., 2020a). Further, vegetation indices derived from optical remote sensing, such as the Normalized Difference Vegetation Index (NDVI), are an indicator of leaf area



in open canopies where there are distinct spectral differences between canopy and ground surface. However, sensitivity in the differences between vegetation indices over time may be reduced in closed canopies associated with mixed pixels and saturation of indices at high leaf area index (Huete and Lui, 1994; Jiang et al., 2006; Montgomery et al., 2019; Vanderhoof et al., 2021).

Active remote sensing using Synthetic Aperture RADAR (SAR) and Light Detection and Ranging (LiDAR) can penetrate through vegetation canopy to provide information about the structure of canopy, understory, and ground surface elevation. Lidar data (terrestrial, airborne, spaceborne) have utility for quantifying structural attributes, such as vegetation height, canopy cover, understory, etc., because of the ranging nature of the technology and the rapidity with which laser pulses are emitted, reflected, and recorded (Wehr and Lohr, 1999; Lim et al., 2003). Moreover, several studies have used lidar technologies for quantifying vegetation structures in peatlands (e.g., Hopkinson et al., 2005; Millard and Richardson, 2018).

In peatlands, conifer and deciduous vegetation may be differentiated within lidar data based on differences in radiation scattering of leaves vs. needles, along with typically round (deciduous) vs. conical (conifer) shape, and the vertical distribution of foliage within the canopy (Ørka et al., 2010; Li et al., 2013; Budei et al., 2018). For example, Ørka et al. (2010) found intensity of single returns from birch species was greater at top of the tree crown while single, first, and last return energy reflected from spruce species were typically more evenly distributed throughout the canopy. Based on the distribution characteristics of return intensity between species, these characteristics may be used to

distinguish between conifer and deciduous, and potentially, different species within these (Ørka et al., 2010; Hopkinson et al., 2016b; Budei et al., 2018).

The combined effects of fire, climate change, and anthropogenic disturbances increases the vulnerability of boreal peatlands in Canada, thereby resulting in decreased carbon sequestration potential in the future. A landscape with fewer robust peatlands will impact ecosystem services such as water retention, flood mitigation, food sources for the northern communities, and other cultural services, (reviewed in Chasmer et al., 2020a) and may enhance CO<sub>2</sub> emissions. Hence, post-fire regeneration trajectories of boreal peatland vegetation species may be an indicator of peatland resilience or sensitivity, depending on the environmental attributes and proximal impacts to individual peatlands.

Here we used a combination of airborne multi-spectral lidar based 3D point cloud structural vegetation metrics, laser pulse intensity variations, active vegetation indices, and site-specific locational attributes to classify the proportion of conifer tree vs. deciduous shrub and tree species within peatlands using a supervised machine learning approach. The goal of this study was to quantify spatial and temporal variations in conifer vs. deciduous shrub/tree communities following fire using a space-for-time-fire chronosequence of 5, 18, 30, and 38 years-post-fire. The objectives of this research were to: (a) determine the utility of multi-spectral lidar for identifying deciduous vs. conifer trees, shrubs, and herbaceous ground cover species; (b) quantify proportional coverage of post-fire shrub vs. tree regeneration within peatlands; and (c) determine the approximate timing of dominance of shrub vs. tree species determined from growth rate within the fire chronosequence. We hypothesize more shrubification in peatlands during the early years

post-fire, and as regenerating forests age, the fuel content shifts from deciduous to conifer, providing more fuels for wildland fire.

## **3.2 MATERIAL AND METHODS**

### **3.2.1 Study area**

The study was conducted ~ 230 km south of Fort McMurray near Wandering River, Alberta (112° 12' 31" W, 55° 37' 46" N) and is a part of the Central Mixedwood subregion of the Boreal Plains ecozone (Figure 3.1). The climate of this region is sub-humid and includes strong seasonal variations with short, warm summers and long, cold winters (Bonan and Shugart, 1989). Air temperature and precipitation decrease throughout the subregion along a northward latitudinal gradient (Alberta Parks, 2015), however, this spatial reduction in moisture is not found within the small area examined here. Field data were collected in August 2020, which was one of the wettest years over the last 100 years, with a cumulative precipitation of 308 mm in Wandering River in July 2020 (Government of Alberta, 2020).

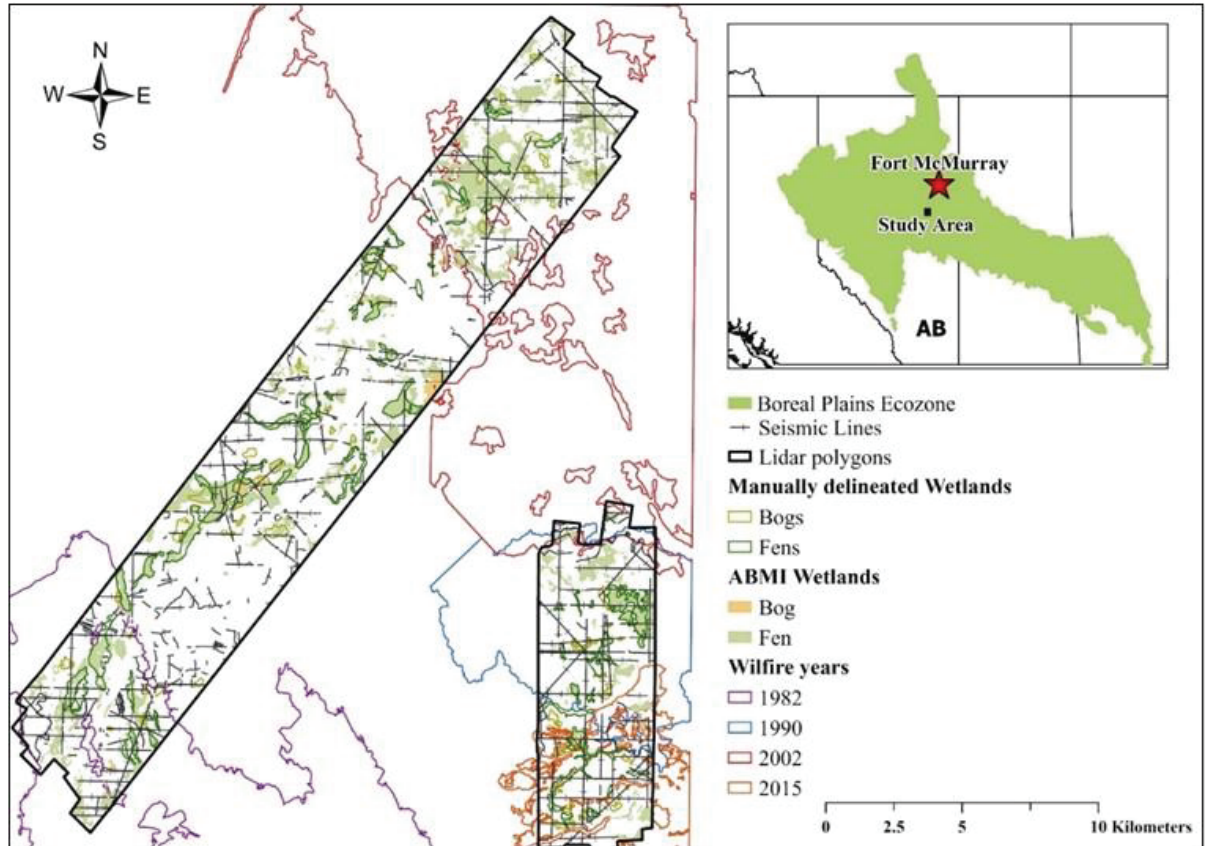


**Figure 3. 1** Location of 5 year, 18 years, 30 years and 38 years since fire chronosequence near Fort McMurray, Alberta surveyed using multi-spectral lidar. The region is within the Boreal Plains ecozone. Areas that have not been burned in the recent history of scientific observation (since ~1930) are found in between the fire scars, predominantly between 1982 and 2002 fires in the western lidar polygon.

Vegetation in the region consists of deciduous tree species including but not limited to *Populus tremuloides* Michx (trembling aspen), *Populus balsamifera* Lyall (balsam poplar), and *Betula papyrifera* Marshall (paper birch). Coniferous tree species include *Picea mariana* Kuntze, and *P. glauca* (Moench) Voss (black and white spruce), and *Pinus banksiana* Lamb. (jack pine). Shrub species include *Prunus virginiana* L. (chokecherry), *Alnus crispa* Pursh (green alder), *Amelanchier alnifolia* Nutt (Saskatoon

berry) and *Symphoricarpos albus* K. Koch (snowberry), with a variety of herbaceous and moss species. More than 50% of the area was dominated by poorly drained fens and bogs (Alberta Parks, 2015) with treed peatlands containing mostly black spruce. Peatland shrub species include but are not limited to *Ledum groenlandicum* Oeder (Labrador tea), *Betula pumila* L. (bog birch), and *Salix* spp. L. (willow species). The surficial geology consists of mostly glacial moraines, stagnant ice moraines, and glaciofluvial deposits (Campbell et al., 2006).

The study areas have a low density of seismic lines: 1.59 km/km<sup>2</sup> (ABMI, 2019) and were burned by fires in 1982, 1990, 2002, and 2015 (Figure 3.1). The older fires in 1982 and 1990 burned 36,996 and 9,451 hectares respectively (Alberta Wildfire, 2019), while fires in 2002 and 2015 burned more than 236,662 and 9,883 hectares respectively and include some unburned islands and partially burned areas.

### **3.2.2 Field data collection**

For validation purposes, shrub and tree heights and species were measured along four transects (three unburned and one burned). The selection of species along seismic lines were used so that laser pulse interactions with the tall trees could be minimized and the plots were homogenous. Species measurements were collected at approximately 4 m intervals along the center of each seismic line and were geographically located using a Garmin Montana 650 handheld GPS ( $n = 202$ ). The Garmin Montana was Wide Area Augmentation System (WAAS)-enabled with a positional accuracy between 0.4 to 1.0 m

(White and Wilson, 2005). Areas adjacent to seismic lines were dominated by black spruce, Labrador tea, and *Sphagnum* moss species (Figure 3.2).

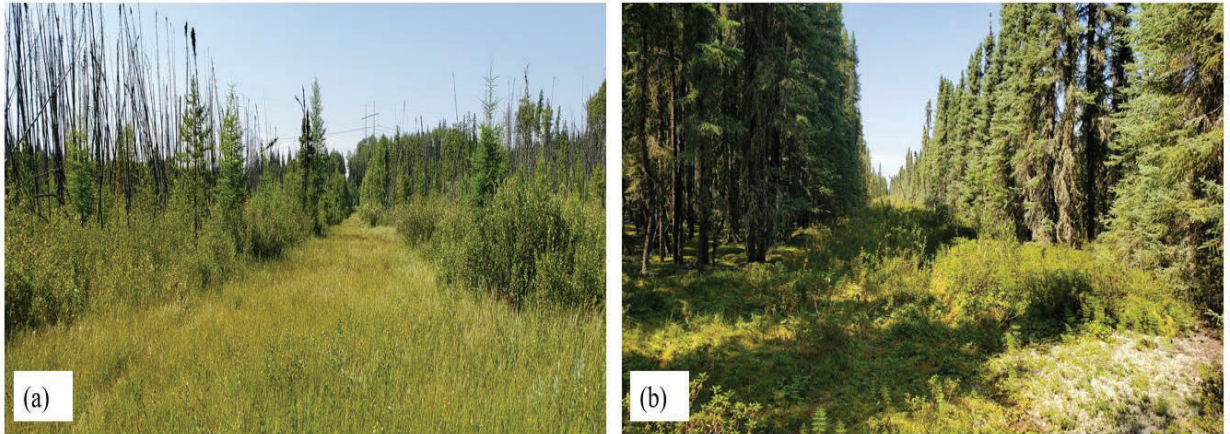


**Figure 3. 2** Examples of seismic line transects for shrub and tree height validation through (a) burned peatland and (b) forest looking into an unburned treed peatland.

### 3.2.3 Lidar data collection

The fire chronosequence and an older, unburned (in recent history) reference area between burn scars was surveyed on August 2<sup>nd</sup>, 2020, by the University of Lethbridge ARTeMiS Lab using the Titan multi-spectral airborne lidar system (Teledyne Optech Inc, Canada). The Titan scanner has three channels (C1, C2, and C3) with laser pulse emission wavelengths of 1550 nm (shortwave infrared, C1), 1064 nm (near infrared, C2) and 532 nm (green, C3), respectively (Hopkinson et al., 2016b). Survey characteristics included a mean flight altitude of 1000 m above the ground surface and pulse repetition frequencies (PRF) of 100KHz per wavelength. The survey covered an area of 220 km<sup>2</sup> with a lateral strip overlap of 50% and an average point density of 6.2 points per square meter.



### 3.2.4 Supplementary geospatial data

In addition to the lidar surveyed areas, we also used additional geospatial layers, including the Human Footprint Inventory for the Oil Sands Monitoring Region circa 2019 (ABMI, 2019). The Human Footprint Inventory (herein, HFI) includes classified seismic lines and other linear disturbances such as pipelines and roads. Peatlands were expertly identified and manually delineated into bogs and fens using the lidar-derived digital elevation model (DEM), Landsat data (pre 2002 to determine pre-fire peatland characteristics for some polygons) and high spatial-resolution World Imagery available through ArcGIS Pro (ESRI, Canada), acquired during approximately maximum foliage cover collected within the last 3-5 years. The digital elevation model was used to identify the lag, found at the transition between bogs and forest, thereby enhancing identification accuracy compared with fens. Peatlands were divided into the following categories for comparative analysis: burned + seismic line fen; burned + seismic line bog; seismic line only fen; seismic line only bog; reference bog; reference fen. A total of 76 bogs (21 unburned, 42 burned, and 13 reference) and 79 fens (22 unburned, 43 burned, and 14 reference) were delineated throughout the two-study area lidar polygons containing the burn chronosequences and unburned areas between them (Figure 3.1).

Shrub and tree locations ( $n = 4000$  in total,  $n = 800$  per each fire chronosequence and unburned area) were manually delineated throughout two study areas within classified peatlands, transition areas, and uplands using (a) high resolution imagery (30 cm pixel resolution) and (b) the lidar derived 99<sup>th</sup> percentile (2 m resolution) of vegetation heights, subdivided into the following categories: deciduous shrubs (0.5 – 3 m); deciduous trees (> 3 m); conifer trees (> 3 m). All vegetation with height greater than

3 m were classified as a “tree”, as defined by the Alberta Wetland Classification System (Government of Alberta, 2015). Manually identified conifer/deciduous trees vs. deciduous shrubs were identified in areas that were more than 100 m from seismic lines to reduce the potential for anthropogenic impacts on vegetation establishment (van Rensen et al., 2015; Abib et al., 2019). Seismic lines in the study area were determined using the HFI layer (ABMI, 2019) for the Oil Sands Monitoring Region

### **3.2.5 Data analysis**

#### **3.2.5.1 Derivation of geospatial layers from lidar**

Lidar point cloud processing and raster analyses were carried out using TerraScan (TerraSolid, Finland), LAStools (RapidLasso, Germany), and ArcGIS Pro (ESRI, Canada). Lidar data returns were classified into ground and non-ground returns using last of many echoes and only echoes in TerraScan. A digital elevation model was generated at 2 m resolution using triangulation with linear interpolation in LAStools. The digital elevation model was also used to calculate Topographic Position Index (TPI), indicating low lying areas and hills in the landscape. TPI was optimized and calculated using a circular search radius of 50 m to capture generalized variations in topography exceeding microtopographic variability. The digital elevation model was also resampled to 5 m cell resolution to calculate local average slope and aspect, similarly, characterizing the more generalized variations in microtopography, but not at the hillslope level. Numerous vegetation structural metrics were calculated based on the distribution of the point cloud, including percent cover, interquartile range, and maximum height within 2 m resolution cells, along with average laser pulse return intensity. All structural metrics were



generated using all returns from all three channels with a height cutoff of > 0.5 m above the ground surface (to ignore groundcover), while intensity metrics were derived using all returns from C1 and C2 only (described in Table 1). In addition to these, Normalized Difference InfraRed index (NDIR) was calculated using C1 and C2 average intensities and was used along with other layers as explanatory rasters to predict areas of conifer or deciduous post-fire regeneration. The NDIR was used to provide a measure of vegetation moisture condition (Ji et al., 2011).

**Table 3. 1** Lidar metrics derived for identifying shrubs and trees using return height above ground greater than 0.5 m. Lidar metrics in bold were used in the final model based on their importance. Other metrics were also generated but were not included in the forest-based classification (described below) because they were highly auto-correlated (Pearson’s correlation  $\geq 0.60$ ). All metrics generated had a cell resolution of  $2 \times 2$  m, except for slope and aspect, which had a resolution of  $5 \times 5$  m, resampled to  $2 \times 2$  m for the random forest classification. C1 = 1550 nm (shortwave infrared, SWIR); C2 = 1064 nm (near infrared, NIR); C3 = 532 nm (green).

Type	Lidar metric	Description
<b>Vegetation Structural Metrics</b>	C123_Max_hgt	Maximum height of all returns from all channels with heights > 0.5m from ground
	C123_Min_hgt	Minimum height of all returns with heights > 0.5m from ground
	<b>C123_IQR_hgt</b>	<b>Interquartile range of height using all returns from all channels with heights &gt; 0.5m from ground. IQR = p75 height – p25 height</b>
	C123_Ske_hgt	Skewness of height values using all returns with heights > 0.5m from ground
	C123_Kur_hgt	Kurtosis of height values using all returns with heights > 0.5m from ground
	<b>C123_Cover</b>	<b>Percent cover using all returns from all channels with heights &gt; 0.5m from ground</b>
<b>Vegetation Laser Return Intensity</b>	C1_Min_int	C1 minimum intensity of returns with heights > 0.5m from ground
	C1_Max_int	C1 maximum intensity of returns with heights > 0.5m from ground
	C1_Ske_int	C1 skewness of intensity values using returns with heights > 0.5m from ground
	C1_Kur_int	C1 kurtosis of intensity values using returns with heights > 0.5m from ground

	<b>NDIR_C1_C2</b>	<b>Normalized Difference InfraRed index using returns with heights &gt; 0.5m from ground calculated using the formula (C1-C2)/(C1+C2)</b>
	C2_Min_int	C2 minimum intensity of returns with heights > 0.5m from ground
	C2_Max_int	C2 maximum intensity of returns with heights > 0.5m from ground
	C2_Ske_int	C2 skewness of intensity values using returns with heights > 0.5m from ground
	C2_Kur_int	C2 kurtosis of intensity values using returns with heights > 0.5m from ground
<b>Environmental/ Topographic</b>	<b>Slope</b>	<b>5 m resolution slope generated based on LasTool generated digital elevation model</b>
	<b>Aspect</b>	<b>5 m resolution aspect generated based on LasTool generated digital elevation model</b>
	<b>TPI</b>	<b>Topographic position index generated using Jenness topographic position tool having a search radius of 50 m</b>

### 3.2.5.2. Extracting lidar derived metrics to field data

Lidar derived vegetation and topographic structural and intensity metrics were extracted for field locations to identify deciduous and conifer tree species, ignoring the ground cover, using 44 out of the 202 homogenous field points with lidar returns (the remainder were removed due to a mixture of vegetation species). Lidar derived percent cover, interquartile range and NDIR were extracted for each species and compared at 2 m grid resolution. Also, average C1 (1550 nm) and C2 (1064 nm) lidar return intensities were examined to identify any differences in return intensity between species (associated with foliage scattering properties).

### 3.2.5.3 Forest-based classification and regression

Forest-based classification and regression was performed in ArcGIS Pro (Version 2.7) following the original methods described in (Breiman, 2001). Forest-based regression is based on a supervised machine learning algorithm that creates multiple decision trees used to create, in this case, a prediction raster of conifer vs. deciduous distribution based on structural and intensity metrics (Table 3.1). Forest-based regression was used because it is non-parametric and does not rely on the user to have *a priori* knowledge of the ecological drivers or characteristics of the prediction/classification outputs (Menze et al., 2009; McCarley et al., 2020). Since the prediction of areas of conifer vs deciduous regeneration were categorical, the model was based on classification trees. The model was first trained using 100, 500, 1500, and 2500 trees including 70% of data that was manually delineated as shrubs vs trees ( $n = 800$  per each fire chronosequence) for training and 30% for validation. The default number of trees for the forest-based regression in ArcGIS Pro is 500, however increasing the number of trees typically improves model accuracy (Belgiu and Drăguț, 2016; ArcGIS Pro, 2020). In this study 1500 trees were used after iterating from 100 to 2500 trees, identified by determining the threshold of the maximum accuracy, such that the maximum accuracy shows little improvement after 1500 trees.

In addition to these, the structural metrics of height and intensity metrics from 1550 nm and 1064 nm laser wavelengths were used as descriptors of conifer vs. deciduous along with environmental drivers of slope, aspect, and topographic position index (TPI), which were used as explanatory variables in the classification (Table 3.1). The model was first trained using all variables listed in Table 3.1. To reduce autocorrelation and model

over-parameterization, explanatory rasters were decreased to the greatest explanatory power using the most important six variables described in Table 3.1. Variable importance was calculated based on Gini coefficient, which was used to eliminate variables with lower importance to create a small subset of important variables that predicted most of the variability in the data. These were used for the final classification (Menze et al., 2009). After training, the model was used to create a prediction raster that classified areas of deciduous shrubs, deciduous trees and conifers in the study areas. The model reported a sensitivity and accuracy value for each category, which were used to assess model performance. Sensitivity measured the number of times the observed category was correctly predicted, and the diagnosis was calculated using a confusion matrix (ArcGIS Pro, 2020).

Using the results of forest-based classification, the proportional cover of shrubs and trees in peatlands was calculated by dividing the classified pixel area by the total peatland area. Pixels within 25 m of seismic lines were not included in the proportional cover of shrubs and trees to reduce the proximal effect of seismic lines on peatlands according to results of (Abib et al., 2019). The cumulative vegetation growth since fire was calculated by averaging 99<sup>th</sup> percentile of vegetation height per cell and resampling this to 5 m using bilinear method in ArcGIS Pro to reduce noise in the vertical data and normalize change across a larger area, resulting in a more generalized height metric. Post-fire standing dead trees/snags were removed by thresholding based on height as these can indicate tall, non-living vegetation in lidar data that is confused with living vegetation. Vegetation greater than 3 m were removed from the 5-year chronosequence, assuming that these were

burned stems (Weider et al., 2009; Bolton et al, 2017). Similar stems were not observed in the older chronosequence sites.

#### **3.2.5.4 Statistical analysis**

Statistical analyses and comparisons between the post-fire chronosequence datasets were performed in SPSS Version 26 (SPSS Inc., USA). Field data were used to identify species differences in vegetation structure and intensity observed using lidar data, within  $1 \times 1$  m areas that had low to no species mixture  $> 0.5$  m. The field data were not normally distributed and were compared using Kruskal-Wallis test. Manually delineated shrub and tree locations/classified information were used to determine the prediction/validation layers within the forest-based regressions, applied separately to each burn area and recently unburned peatlands. A Pearson's correlation matrix of the lidar data derivatives was used to identify and remove correlating variables with correlations greater than 60%. For example, average height (Pearson's correlation  $> 0.96$ ) and standard deviation of height (Pearson's correlation  $> 0.86$ ) were highly correlated with maximum height and were removed from the final model. Moreover, maximum height and interquartile range (IQR, which is the difference between the 25<sup>th</sup> and 75<sup>th</sup> percentiles in the lidar point cloud distribution) had a Pearson's correlation = 0.67 so, maximum height was not included in the final model. Six variables were identified based on importance (Table 3.1) to reduce model overfitting. The lidar derived variables were tested for normality using Kolmogorov-Smirnov and Shapiro-Wilk tests, indicating that data were non-parametric. The difference between proportional cover of deciduous shrubs, deciduous trees and conifer trees in each post-fire year and mean post-fire

vegetation height were not normally distributed and compared using Kruskal-Wallis one way ANOVA.

### **3.3 RESULTS**

#### **3.3.1. Differences in classified conifer and deciduous trees/shrubs using lidar metrics**

Field measurements indicate differences in vegetation structure also observed in lidar data. We found that some deciduous species such as alder and aspen were taller, had greater percent foliage cover, and greater variability in the range of IQR, indicating differences in the distribution of laser returns across the broadest part of the canopy envelope (Figure 3.3). Moreover, the IQR of height and percent cover of foliage were significantly different between black spruce and alder ( $p < 0.05$ ) and black spruce and aspen ( $p < 0.05$ ). This illustrates a broad distribution of returns within deciduous canopies, compared with early regeneration black spruce, which had a narrower distribution of returns within the canopy. In comparison, we found that other deciduous species such as willow and birch had reduced IQR ranging from 0 to 5 m associated with the positioning of returns higher in the canopy compared with black spruce and alder (Figure 3.3a). Significant differences in IQR were found between birch (distribution of returns at the top of the canopy, low IQR range) and alder/aspen (distribution of returns throughout the canopy,  $p < 0.05$ ). Willow had the lowest proportional canopy cover, similar to black spruce and birch, to a lesser extent (Figure 3c), while alder and aspen had the greatest cover in the study areas examined. These were significantly greater than willow ( $p < 0.05$ ). Based on the average reflectance of all returns within grid cells there

was no significant difference observed between conifers and deciduous species ( $p > 0.05$ ) in the ratio of the difference between NIR and SWIR (NDIR) (Figure 3.3b). Average laser return intensities of all returns for individual channels were also observed, where higher SWIR average intensities were observed for alder, aspen, and birch compared to conifers such as black spruce (Figure 3.4), which tend to increase scattering of returns/loss of energy through the canopy. Despite differences between the averages, variability in NIR and SWIR across individual species were also not significantly different ( $p > 0.05$ ), possibly due to other influencing factors including vegetation structure and height, which can impact the number of returns in the canopy.

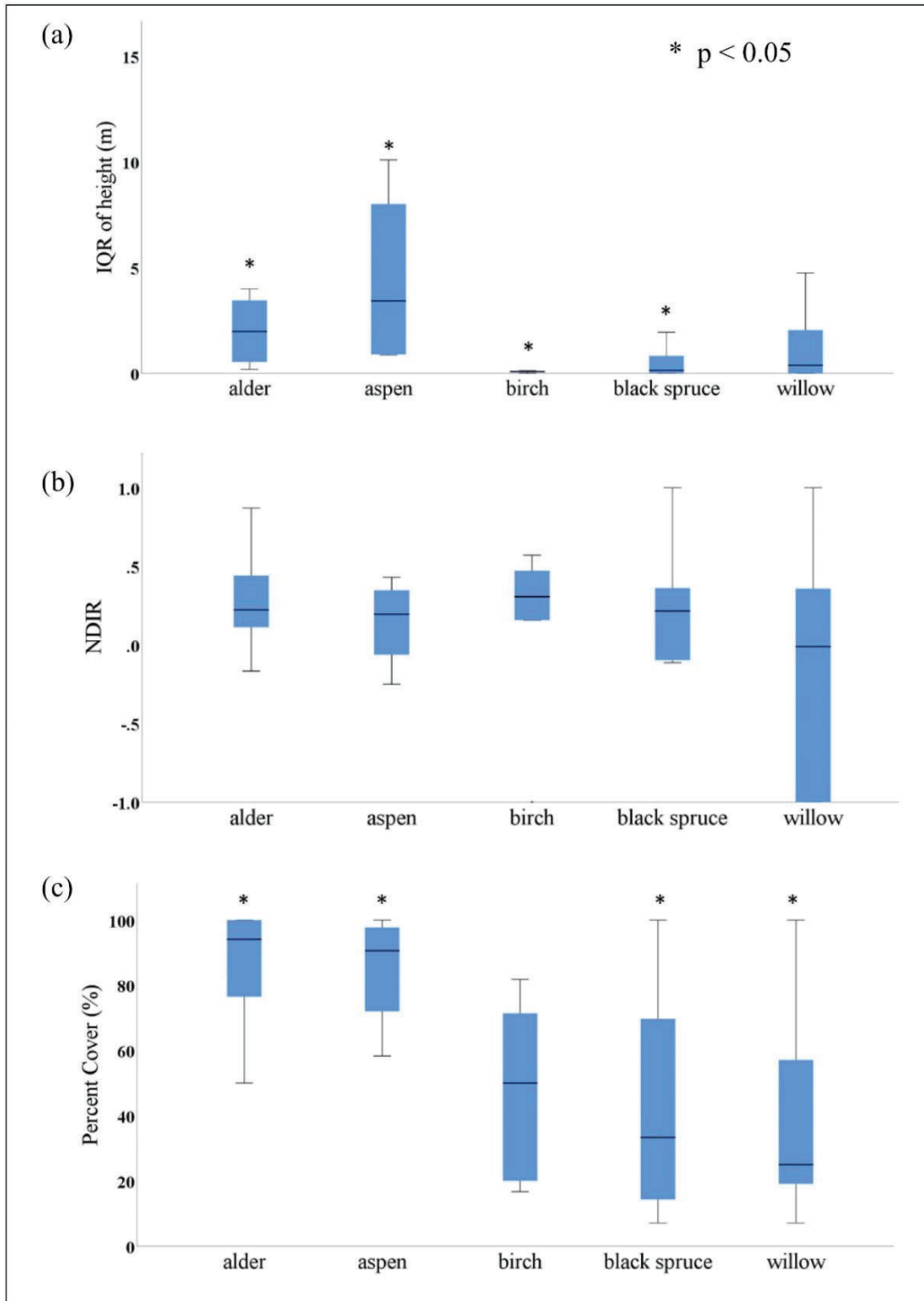


**Figure 3. 3** Box plot of the top four variables a) IQR of height, (b) NDIR, and (c) percent cover used to separate between species. The values are derived from lidar data for deciduous and conifer species identified in unmixed plots in the field ( $n = 44$ ).



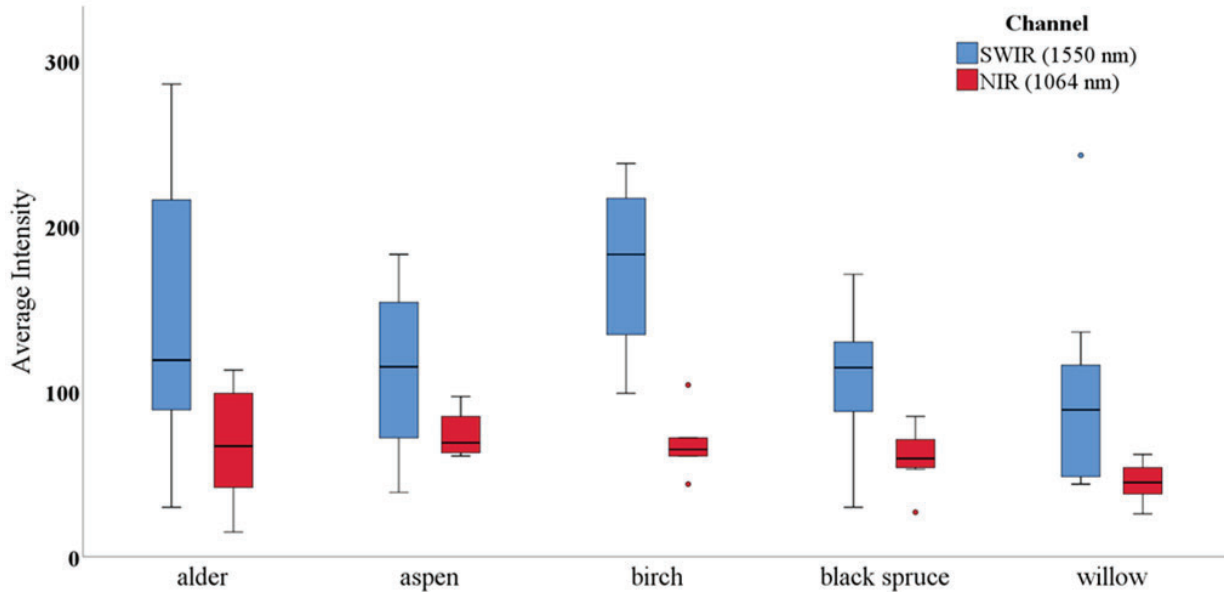


**Figure 3. 4** Average SWIR (shortwave infrared, 1550 nm) and NIR (near infrared, 1064 nm) intensities for field-identified, unmixed pixels with deciduous and conifer species using all returns of SWIR and NIR > 0.5 m ( $n = 44$ ).

### 3.3.2 Classification of conifer vs deciduous shrub/ tree in post-fire peatlands using lidar

Forest-based regression parameterised using manually identified deciduous shrubs, deciduous trees, and conifer trees showed that the structural metric of interquartile range (IQR) of height (the difference between the 25<sup>th</sup> and 75<sup>th</sup> percentiles) was the most important variable for classifying shrub vs. trees, followed by intensity-based metric NDIR; percent cover ranked third. Environmental characteristics associated with local elevation (TPI, slope, and aspect) were less important (Table 3.2). Structural vegetation metrics had a higher importance in burned peatlands and could be used to identify shrubs in absence of a tree canopy. IQR of height was consistently the most important variable for describing shrub vs. tree cover (importance ~ 20% in 5, 18 and 30 YSF), while NDIR and percent cover varied depending on years since fire (Table 3.2).

Separability was greater between variables in burned peatlands compared with unburned ones but was reduced in recently (in the last ~90 years) unburned reference peatlands. Also, the structural variables had reduced importance in the unburned site ( $p > 0.05$ ) because the 3D point cloud structural metrics provided little discriminatory power between established deciduous and conifer canopy. NDIR had the highest importance in unburned sites. Finally, with regards to the establishment of shrubs vs. trees, we found that environmental drivers were similar between burned and unburned sites ( $p > 0.05$ ) (Table 3.2). The combination of derivatives in Table 3.2 provided the most accurate prediction and validation classification compared with field/manually identified deciduous vs. conifers in the areas examined.

**Table 3. 2** Variable importance for each fire chronosequence and unburned area generated using forest-based classification, where YSF refers to years since fire.

<b>Variable Importance (%)</b>	<b>5 YSF</b>	<b>18 YSF</b>	<b>30 YSF</b>	<b>38 YSF</b>	<b>Unburned</b>
<i>IQR height</i>	19.8	19.7	19.9	18.7	18.5
<i>NDIR</i>	17.1	15.6	16.7	15.5	17.9
<i>Percent Cover</i>	15.5	17.1	17.2	18.6	16.0
<i>Aspect</i>	14.9	16.5	15.5	15.5	16.4
<i>TPI</i>	16.6	16.2	15.9	16.1	15.8
<i>Slope</i>	16.1	15.0	14.8	16.7	15.3
	Vegetation structural metric				
	Vegetation laser return intensity				
	Environmental/ Topographic				

The forest-based classification model predicted the spatial distribution of deciduous shrubs, deciduous trees, and conifers to an accuracy of > 95% compared with training data (Table 3.3). However, the ability to predict presence of conifer and deciduous trees in the validation data extracted from the lidar data was reduced (accuracy = 71% for both conifer and deciduous trees) compared with deciduous shrubs (accuracy = 92%). The greatest confusion between training and validation data occurred in areas of mixed deciduous and conifer trees with closed canopies (Table 4). Here we find that deciduous shrubs had the lowest commission error and were mostly correctly identified (omission error of 15%). The highest rate of confusion was associated with a commission error of 33% (conifer trees), while the model had an omission error of 27% and 36% for deciduous and conifer trees, respectively (Table 3.4).

**Table 3. 3** Model performance for the study area. Sensitivity is the percentage of time each observed category was correctly predicted, while accuracy takes into consideration how well each category is predicted and how often it is miscategorised

Training data	Sensitivity (%)	Accuracy (%)
<i>Deciduous shrubs</i>	1.00	<b>0.98</b>
<i>Deciduous trees</i>	0.95	<b>0.96</b>
<i>Conifer trees</i>	0.96	<b>0.96</b>
Validation data	Sensitivity (%)	Accuracy (%)
<i>Deciduous shrubs</i>	0.92	<b>0.92</b>
<i>Deciduous trees</i>	0.66	<b>0.71</b>
<i>Conifer trees</i>	0.62	<b>0.71</b>

**Table 3. 4** Confusion matrix of forest-based regression between deciduous shrubs, deciduous trees, conifers within burned and recently unburned peatlands.

	Deciduous shrubs	Deciduous trees	Conifer trees	Commission Error	Omission Error
Deciduous shrubs	<b>150</b>	5	7	0.07	0.15
Deciduous trees	12	<b>239</b>	102	0.32	0.27
Conifer trees	14	84	<b>197</b>	0.33	0.36

Numbers in bold represents the number of correctly identified groups compared with validation

Using forest-based classification, a prediction raster was generated with a pixel resolution of 2 m. The classification predicted more deciduous shrub presence in the areas burnt in 5 year and 18-year since fire (YSF) compared with the older burned sites and recently unburned peatlands. (Figure 5). Most deciduous trees were found throughout the 30 year and 38-year sites within the chronosequence, while unburned areas were predicted to have greater areas of peatland containing conifers (Figure 3.5). Using the topographic metrics, we found that deciduous shrubs in peatlands were found in areas with shallow slopes (0 - 3°) in both burned and unburned sites determined using the random forest classification. Approximately 1% of flat to shallow slope areas in unburned peatlands had deciduous shrubs vs. 6% area coverage of conifers. Similarly, burned shallow slope areas within peatlands had 1-2% area coverage of deciduous shrubs, with a decrease in conifer trees to 1-2%. Comparatively, upland and transition areas with north facing steep slopes (> 25°) were dominated by mixedwood stands of conifer and deciduous trees while south facing slopes were dominated by deciduous trees (Figure 3.5).

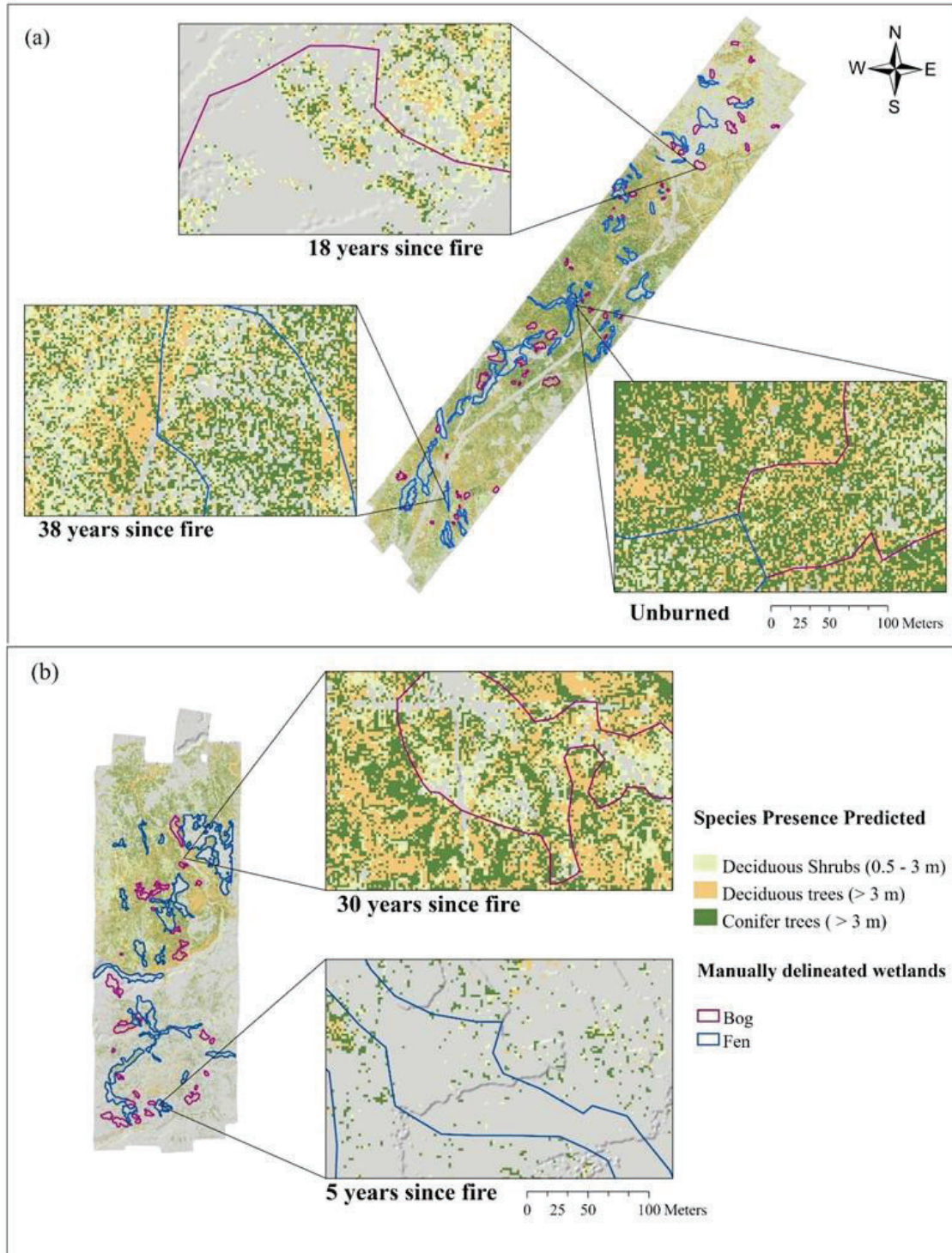


**Figure 3. 5** Prediction raster generated for (a) western lidar polygon including vegetation regeneration 18 YSF, 38 YSF, and recently unburned peatlands and (b) eastern lidar polygon including vegetation regeneration 5 YSF and 30 YSF. No data areas shaded in grey represent vegetation height less than 0.5 m. These low vegetation areas are typically representing ground cover, Labrador tea, and herbaceous species.

### **3.3.3 Proportional of conifer and deciduous shrubs and/or trees in post-fire peatlands**

Bogs had an overall higher proportional coverage of deciduous shrubs, deciduous trees, and conifer trees (Figure 3.6), while higher area coverage of deciduous shrubs were found in fens in the burned sites. Bogs and fens that have not been burned within recent scientific records (reference sites) had higher proportional cover of conifers compared to deciduous species, ranging from 6.6% in fens to 11.3% in bogs, overall. The highest proportion of conifers were found in reference peatlands (average = 10.5% in fens, and average = 11.5% in bogs) that have not been disturbed by natural and/ or anthropogenic disturbance (Figure 3.6). In the 30 years since fire (YSF), bogs had the highest proportional area coverage of deciduous trees, which decreased significantly after that period (Figure 3.6a,  $p < 0.05$ ). Differences in proportional area coverage of deciduous shrubs and conifers were also significant ( $p < 0.05$ ) within all post fire years except between the 30 YSF and 38 YSF.

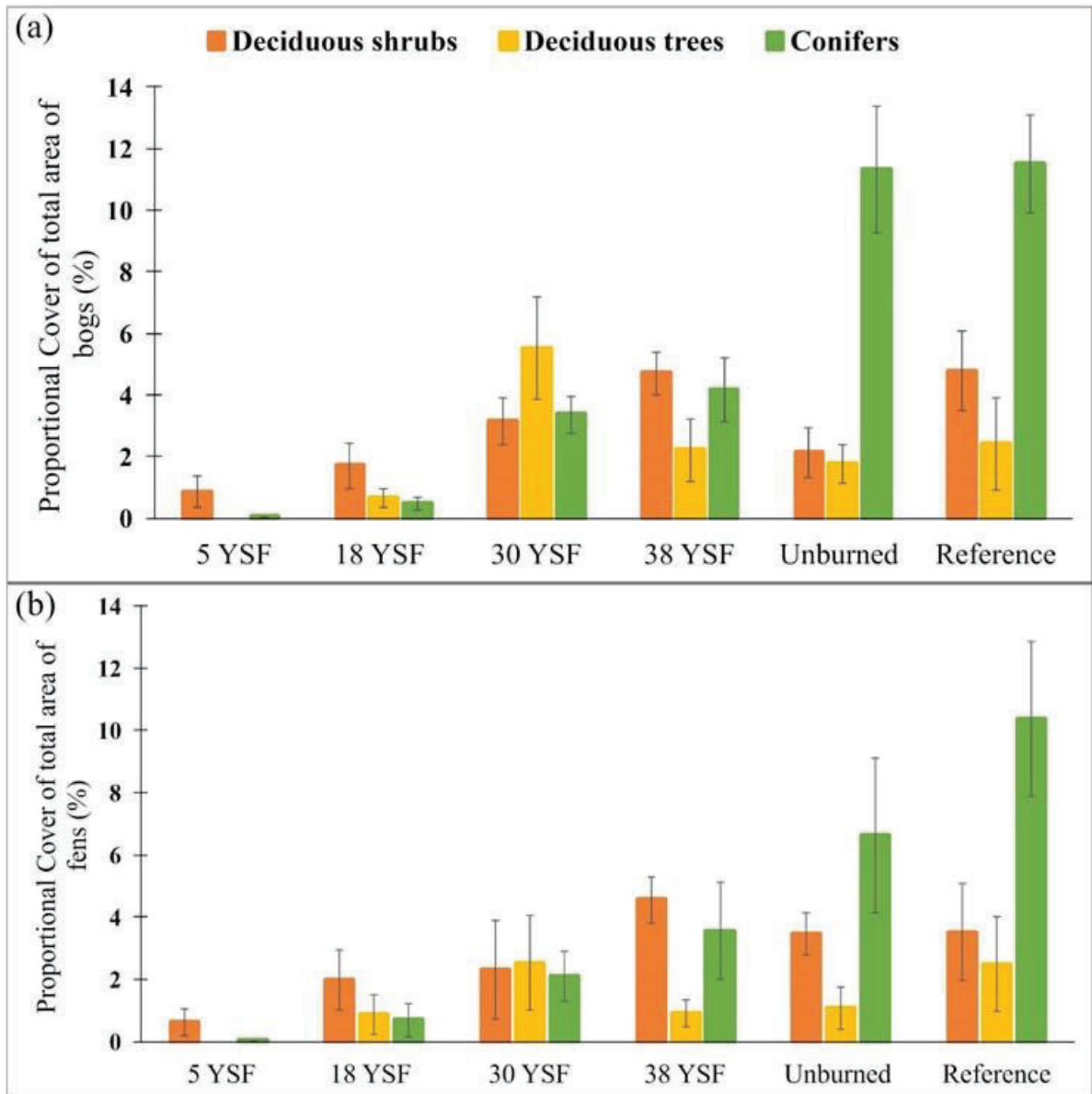


**Figure 3. 6.** Proportional cover of wetland conifer vs. deciduous species per fire chronosequence, in (a) bogs and (b) fens



On the other hand, fens were more prone to post-fire shrub regeneration, having the highest proportional cover of deciduous shrubs (average = 4.6%) observed at 38 years since fire. The difference in proportional cover of deciduous shrubs was at each period since fire within peatlands (5 YSF, 30 YSF, 38 YSF, and unburned fens ( $p < 0.05$ )), associated with a gradual increase in the proportion of shrubs in the years following fire. Shrubs were also greater following fire at 38 YSF than unburned sites that had been anthropogenically disturbed and undisturbed reference sites. Interestingly, the proportional cover of deciduous trees was significantly greater at 30 YSF compared with 38 YSF (Figure 3.6b,  $p < 0.05$ ), however, similar differences did not occur in conifers. Differences between years in deciduous cover may be associated with other influencing environmental factors, such as surficial geology.

### **3.3.4 Cumulative growth of conifers vs deciduous tree and shrubs in the years since fire**

In the years since fire, we find that the cumulative growth of shrubs and trees within bogs and fens has increased over time, resulting in a chronosequence-based growth curve (Figure 3.7). Vegetation within both bogs and fens appeared to follow a logistic growth curve with significantly taller vegetation in unburned bogs compared to fens ( $p < 0.05$ ). Also, the vegetation height in bogs and fens was statistically significant between all YSF, except between the 30 YSF and 38 YSF ( $p > 0.05$ ). The regeneration growth rate of vegetation was also slower in fens than bogs. We also observed shorter vegetation heights in the 38 YSF (average = 3.6 m, stdev  $\pm 1.8$ ) compared to the 30 YSF



(average = 3.8, stdev  $\pm 1.7$ ) suggesting poor growth conditions possibly due to other environmental factors not examined here.

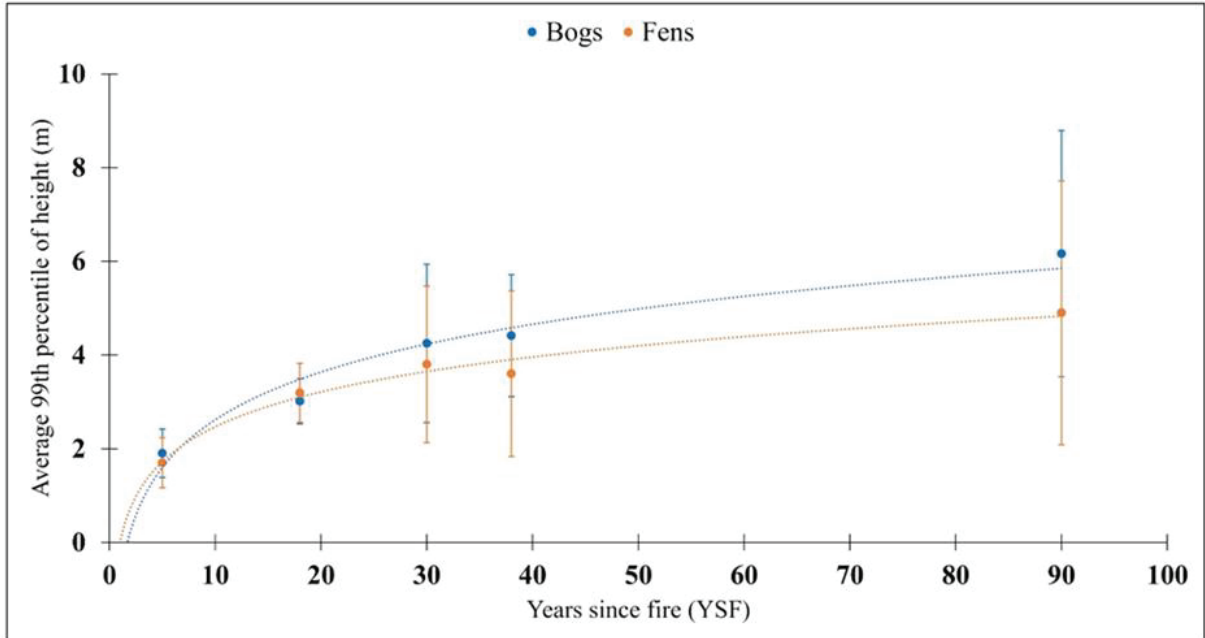


**Figure 3. 7** Average vegetation height (at 99<sup>th</sup> percentile of lidar returns) with stand age for boreal peatland fire chronosequence ( $R^2 = 0.96$  for bogs,  $R^2 = 0.98$  for fens). Unburned peatlands are plotted with an arbitrary stand age of  $90 \pm 10$  years, though there may be many more years since the last fire, but not determined in the field and not included in the recent history of scientific observation (since  $\sim 1930$ ).

### 3.4 DISCUSSION

#### 3.4.1 Use of lidar to identify conifers and deciduous trees and shrubs

In this study, we demonstrated the use of high spatial resolution lidar data and machine learning to identify conifer and deciduous shrubs/trees in a post-fire peatland chronosequence. Lidar-based point cloud structural and intensity metrics were used to predict areas of conifer and deciduous regrowth with relatively high accuracy compared with manually identified trees and shrubs in high spatial resolution optical imagery

(Table 3.3, Figure 3.5). The interquartile range (IQR) of the point cloud distribution between the 25<sup>th</sup> and 75<sup>th</sup> percentile provided the greatest descriptor of shrub vs. trees, especially in the burned chronosequence where sites were recently disturbed by fire over the last 5 to 38 years (Table 3.2). IQR may be an indicator of the volume of biomass, and therefore, differences in the distribution of this biomass between conifers/deciduous shrubs and trees (Hopkinson et al., 2016b; Figure 3.3). The intensity-based Normalized Difference Infrared Index (NDIR) is ranked second as it is sensitive to reflectance differences between leaf vs. needle foliage (Table 3.2). Despite its importance in the random forest model, at the species level, we found no significant differences in NDIR when compared with field data. This is likely due to the spatial resolution of cells and low point density, while larger cell sizes often include a mixture of species/deciduous and conifers, which can skew return intensities resulting in weakness in the NDIR as a discriminatory variable. Budei et al. (2018) found that NDIR ratios capture differences in chlorophyll (NIR) and water content (SWIR) of the leaves, thus, providing greater separability. Moreover, deciduous species had higher NDIR ratios than conifer species because broadleaf species have spherical crown structure and larger cross-sectional area, which provides greater reflectance in NIR (Hopkinson et al., 2016b; Budei et al., 2018). While differences exist between conifer and deciduous vegetation in more recently burned sites, the structural and intensity metrics were not significantly different in unburned areas where late successional species dominate.

Through the forest-based classification, we also found that the model resulted in reduced sensitivity of identification of deciduous trees vs. conifers trees, which may be due to overlapping crowns (Table 3.4, Budei et al., 2018). Our results produced an

overall validation accuracy of 71% for both deciduous trees and conifers (Table 3.3, Figure 3.5, based on structural, intensity, and topographic inputs). Similarly, Li et al. (2013) found that lidar point clouds were influenced by compactness of tree crown and vertical distribution of tree crown, increasing errors when separating aspen and jack pine.

In addition to structural metrics, topographic derivatives may be used to indicate where trees and shrubs grow following fire (Table 3.2, Figure 3.5). While not direct measures of energy receipt and moisture, these are influencing factors of areas that receive more (south facing) or less (north facing) energy and greater (low-lying, closer to water table) and higher (further from water table) topo-environmental conditions that may enhance or deter growth. For example, Thompson et al. (2019) found that in shrub dominated peatlands a water table decline below 40 cm can cause surface vegetation to dry, making the ecosystem more flammable. Hence, these structural, environmental, and intensity-based variables can be determined from multi-spectral lidar to better understand the range and combination of environmental drivers impacting boreal peatland vegetation succession.

### **3.4.2 Changes in proportional coverage of conifers and deciduous tree/shrubs**

In this study, we found higher proportional coverage of deciduous shrubs in the early years post-fire overall (Figure 3.6). Similarly, Alexander et al., (2012) found deciduous trees and shrubs in interior Alaska had high aboveground net primary productivity and high deciduous snag biomass with years since fire, while black spruce stands had slower rates of biomass accumulation. Bogs are typically hydrologically

disconnected (Waddington et al., 2015; Devito et al., 2017, while others found increased depth to water table in bogs and poor fens due to climate-mediated drying, providing ideal conditions for shrubs to grow (Waddington et al., 2015; Chasmer et al., 2021). However, in older burned bogs (38 YSF), we observed an increase in proportional coverage of conifers to 4.1% indicating suitable microsites for black spruce establishment (Jean et al., 2020).

There is also a lag in vegetation response to wildfires, creating younger forests with more deciduous dominated species over time, which are less flammable (Johnstone et al., 2004; Johnstone and Chapin III, 2006; Stralberg et al., 2018). For example, it takes about two to three years following fire for shrubs to colonize (Beck et al., 2011), while deciduous species dominate peatlands and other boreal ecosystems including pre-disturbance forest ecosystems in the first 10-20 years of succession (Boucher et al., 2006; Figure 3.6). Deciduous tree species typically die off during the intermediate stages of stand succession due to density dependent factors and shifts in dominance towards conifers also observed in older post-fire years and unburned peatlands (Figure 3.6). Unburned peatlands typically have more heterogeneous eco-hydrological conditions, with large hydrological differences occurring between peatland margins and centers (Waddington et al., 2015; Morison et al., 2021). Unburned bogs in both areas surveyed by lidar had the greatest proportional cover of conifers, possibly because moist bog sites underlain with mineral soils beneath *Sphagnum* mosses provided suitable microsites for conifer seedling establishment (Johnstone and Chapin III, 2006; Bolton et al., 2017; Jean et al., 2020). Thus, differences in site hydrology (either spatial or temporal) can result in difference in the relative deciduous and conifer proportion. Here, we found that it is

approximately between 18- and 30-years post-fire where there is a transition from deciduous trees to conifer trees observed. After 30 years, we observed a reduction in proportional cover of deciduous trees in bogs and fens (Figure 3.6).

### **3.4.3 Spatial variation in vegetation height in bogs and fens**

Growth curves have been applied to understand the biomass accumulation with stand age. The cumulative growth curve follows the different stages of boreal mixedwood succession: stand initiation dominated by deadwood, stem exclusion and canopy transmission during the intermediate stages and gap dynamics in old growth (Chen and Popadiouk, 2002; Harper et al., 2005). Here we used growth curve to determine variations in vegetation growth in bogs and fens. Although bogs and fens have similar range of vegetation heights within the first five years since fire (Figure 3.7), we found a greater rate of cumulative growth of woody vegetation in the later stages of stand succession in bogs compared with fens with time since fire. This may be associated with lifecycle influences on bog species regeneration, especially where bogs are dominated by black spruce, which have semi-serotinous cones and a half life of 4.4 to 16.2 years (Harper et al., 2005; Bolton et al., 2017). Fires often do not burn all available biomass entirely, with some residual leaves/needles, deadwood, snags, and mosses remaining. These act as a preferred seedbed for conifer seedling establishment, often requiring 5-10 years for post-fire establishment (Johnstone and Chapin III, 2006; Jean et al., 2020). On the other hand, fens may be more sensitive to changes in hydrology due to drainage, road disturbance, or sustained drought, where a moderate drop in water table can make it difficult for *Sphagnum* spp. to colonize, resulting in enhanced broadleaf species

establishment (Sherwood et al., 2013; Kettridge et al., 2015). Deciduous seedling recruitment occurs in the first decade post fire, through reproduction via root suckers (aspen) and seed stump sprouts (birch), which are shade intolerant (Chen and Popadiouk, 2002). However, deciduous species typically experience thinning in the second decade of stand development, resulting in density dependent mortality and replacement by conifers (Johnstone et al., 2004; Bolton et al., 2013; Bolton et al., 2017). Hence, bogs outcompete fens in terms of vegetation regeneration (Figure 3.7), and overtime, growth rate decreases in mature stands to the point of stabilization.

#### **3.4.4 Use of remote sensing and possible limitations**

Remote sensing of wetlands provides a broad range of information that could be used to enhance field measurements. Although field sampling provides insights and measurements of the complex environmental and physical processes that are occurring, it can be labor intensive and expensive (Chasmer et al., 2020b). Cumulative impacts of natural and anthropogenic disturbances can be estimated using remotely sensed data, when calibrated/validated using field measurements. These datasets provide an opportunity to estimate (optical) or sample (lidar) vegetation structural characteristics beyond plots via classification and change detection methods (Chasmer et al., 2020b). Active remote sensing using lidar provides better estimates of structural attributes such as tree height. Lidar can be used for individual tree segmentation (St-Onge et al., 2015) and separating shrub canopy from ground layers (Zhuang et al., 2015) at accuracies that are comparable or potentially better than field structural mensuration methods.

In this study, we used a combination of lidar and field measurements to identify trees and shrubs. However, despite the collection of 202 species along seismic line transects, there were not enough field points to run forest-based classification to genus level, as random forest requires hundreds to thousands of measurements to parameterise the full distribution of the variability of shrub and tree characteristics. To reduce the implications of pixel mixtures on structure/intensity metrics, only homogenous plots were used, reducing the sample size to 44 micro-plot locations. Despite data density reduction, these plots were useful for identifying differences in structural variability between species observed in Figures 3.3 and 3.4 using lidar data. We observed some variability in 3D structure in deciduous (aspen, alder, willow, and birch) and conifer species (black spruce) based on the influences of branching structures and foliage on the point cloud distribution (Li et al., 2013). To train the random forest model, 4000 manually delineated image-based locations of deciduous vs. conifers, were used. Despite this, we expect that there may be some misidentification of shrubs and trees from high spatial resolution imagery. For example, it was more difficult to identify deciduous shrubs due to potential impact of shadows, which occlude shrubs, such as overstory canopies. One way to improve this study would be to use an object-oriented classification, which could include structural attributes such as tree crown shape and crown area to height ratio to better distinguish between conifer and deciduous shrubs and trees (Zahidi et al., 2015; Budei et al., 2018). Though this could enhance uncertainty when applied to early post-fire vegetation regeneration as small stature individuals may be missed within objects and requiring division of structures within pixels similar to spectral unmixing. Moreover, vegetation height was used to measure post-fire cumulative growth however, other

metrics could also be used including allometrically derived biomass (Hopkinson et al., 2016a) and/or foliage or total area coverage (Bolton et al., 2017). Although the cumulative vegetation growth in peatlands follows a logistic curve to maturity, there remains some uncertainty which could be improved by adding intermediate chronosequence data or YSF to the curve (e.g., between 18 and 30 years).

### **3.5 CONCLUSION**

This study explored the use of airborne multi-spectral lidar data to identify deciduous shrubs/trees and conifers in a space-for-time post-fire chronosequence boreal peatland environment using forest-based classification. Using a supervised machine learning model deciduous shrubs were classified to 92% accuracy, while deciduous trees and conifers were classified to 71% accuracy for both, respectively, compared with validation data. The structural variables of interquartile range (IQR) followed by NDIR, and percent cover provided more discriminatory power than topographic metrics particularly in the burned areas. The results of the forest-based classification illustrated high shrubification in recently burned peatlands, particularly in the 5 and 18 YSF, while conifers dominate the unburned peatlands and uplands. We also found that there was more shrubification in fens compared to bogs, though there was some evidence to suggest a transition between 18 and 30-year post-fire from deciduous to conifer tree species. These results indicate that, as regenerating forests age, they become more flammable because the fuel content shifts from deciduous to conifer, providing more fuels for wildland fire. Early post-fire deciduous regeneration in peatlands may reduce the movement of fire across the landscape. Deciduous shrubification associated with climatic



change in more mature peatland ecosystems could have mixed implications for fire, by reducing flammability (due to the moisture content of leaves) but also drying out peat through evaporative losses. Greater understanding of climate-mediated changes in post-fire peatlands will be critically important for assessing peatland resilience and fire behaviour in the future.

## **ACKNOWLEDGEMENTS**

Funding for this project was provided to H. Enayetullah by Alberta Graduate Excellence Scholarship, University of Lethbridge Graduate Assistantship, and Northern Scientific Training Program (NSTP). This research was also supported by the Oil Sands Monitoring Program, Alberta Environment and Parks, and Canada Wildfire NSERC SPG-N provided to L. Chasmer. The Titan lidar was purchased with a grant to C. Hopkinson from Western Economic Diversification Canada. Field equipment was purchased using a Canadian Foundation for Innovation grant to C. Hopkinson and L. Chasmer. Wildland fire research has also been supported by a NSERC Discovery Grant to L. Chasmer. We would also like to thank Chinyere Ottah and Nick Cuthbertson for assistance in the field and Maxim Okhrimenko for airborne survey and lidar data processing.

## **CHAPTER 4. IMPACTS OF SEISMIC LINE DISTURBANCE ON POST-FIRE REGENERATION IN A SPACE-FOR-TIME BOREAL PEATLAND FIRE CHRONOSEQUENCE USING MULTISPECTRAL LIDAR**

### **ABSTRACT**

Seismic lines are the dominant anthropogenic disturbance in the boreal forest of Alberta fragmenting over 1900 km<sup>2</sup> of peatland area and accounting for more than 80% of all anthropogenic disturbance in this region. There is limited regeneration along this fragmented landscape due to changes in ecohydrological conditions. However, wildland fires over seismic lines may improve recovery by initiating secondary succession and enhancing peatland microtopography. Here we used a combination of seismic line and vegetation structural characteristics derived from multi-spectral lidar to better understand and quantify post-disturbance vegetation recovery in 155 boreal peatlands in Alberta, Canada. The goal of this study was to determine whether wildland fires that burn over seismic lines in peatlands lead towards regeneration of woody vegetation adjacent to seismic lines over time by altering the local environment in the years following fire. The objectives of this study were: (a) assess how the spatial distribution of deciduous (shrub and tree) vs. conifer (tree) vegetation varies within and with proximity to seismic lines, including near (0-30 m from seismic line edges), intermediate (30-60 m), and far (60-90 m) distances from seismic lines within a fire chronosequence of 5, 18, 30, and 38 years since fire (YSF); and (b) determine the important peatland (class, shape, area, etc.) and anthropogenic disturbance (width, proportional area, year since disturbance, etc.) characteristics with years since fire in boreal peatlands. The results showed greater deciduous shrub regeneration adjacent to seismic lines in the early years post-fire, while

taller deciduous trees were found in more mature post-fire peatlands, suggesting that wildland fires improve site conditions that promote woody vegetation regeneration adjacent to seismic lines in the years following fire in peatlands. Although seismic lines have a small footprint, they had long lasting effects on vegetation regeneration, particularly on fens with shorter woody vegetation found adjacent to seismic lines in fens compared to bogs. With regards to environmental and anthropogenic correlates (indicating possible drivers) of vegetation change, incoming solar radiation and seismic line age were the most strongly associated co-factors in enhanced shrubification. This suggests that prolonged periods of incoming solar radiation were the most important factors impacting post-fire and post seismic line succession. Environmental and anthropogenic variables explained approximately 54% of the total variance for both bogs and fens, suggesting that localized factors also likely contribute to post-disturbance vegetation characteristics.

**Keywords** - linear disturbances; vegetation succession; remote sensing; cumulative impacts

#### **4.1 INTRODUCTION**

Boreal peatlands cover large surface areas in western Canada and play an important role in carbon sequestration via slow accumulation of biomass within peatland mosses (Kuhry et al., 1993; Vitt, 1994). However, within the next century, climate models predict a 1-2 °C increase in summer air temperatures (Weber and Flannigan,

1997), which will increase drying of boreal peatlands and cause changes to their hydrology (Thompson et al., 2017). Although wildland fires are regarded as the most prevalent disturbance driving ecosystem change in the Boreal Plains Ecozone (Burton et al., 2008), climate change has contributed by altering fire regimes, impacting vegetation succession trajectories and carbon balance (de Groot et al., 2013; Jones et al., 2021). Wildland fires cause a reduction in belowground C stores in peatlands and alter soil organic matter by burning deep into peatlands that have been exposed to drying and increased depth to water table (Davidson et al., 2019). Mean fire return intervals in North America range from 167-180 years, however with climate change, wildland fires in the boreal region are occurring more frequently, on average every 35-120 years (de Groot et al., 2013; Natural Resources Canada, 2017). Moreover, with increased fire risk, Whitman et al. (2019) found shorter fire return intervals less than 30 years in recently burned areas. In the years following wildland fire, there can be a lag in woody vegetation regeneration and a decrease in vegetation Net Ecosystem Production (NEP). It can take 3 to 7 years for trees to establish, and up to 20 to 25 years for the tree canopy to mature due to changes in soil conditions and nutrient levels (Johnstone et al., 2004; Johnstone and Chapin III, 2006; Bolton et al., 2015). Also, in Chapter 3 we found that burned bogs and fens were more prone to deciduous shrub regeneration, while it takes more than 30-years following a fire to transition from deciduous to conifer dominated trees.

Additionally, peatlands are fragmented by anthropogenic disturbances including seismic lines, which are used for oil and gas resource exploration (Dabros et al., 2018). Oilsands deposits cover 142,200 km<sup>2</sup> of northern Alberta, most of which are found as deep bitumen deposits which are extracted using *in-situ* methods (Stack et al., 2019),

which include a network of linear features including seismic lines, well sites, access roads, and pipelines. These are relatively low impact disturbances compared to surface mining, which fully removes ecosystem components (e.g., soils, vegetation) and leaves behind a polygonal footprint of bare ground mine sites, tailing ponds, and end-pit lakes (Jordaan 2012). Despite this, about 80% of Oil Sands resources are currently extracted using *in-situ* methods (Jordaan 2012). Seismic lines disturb over 1900 km<sup>2</sup> of peatlands, causing the organic soils and mosses within seismic lines to become more compacted than within areas that have not been disturbed by seismic lines, due to the mulching of trees and driving over the land surface with heavy machinery (Dabros et al., 2018; Stack et al., 2019). Seismic lines are also warmer due to greater reception of incoming shortwave solar radiation, which can alter vegetation succession trajectories, depending on hydrological limitations (Stack et al 2019; Stevenson et al., 2019). Wider seismic lines (> 3m) have greater impact on soil characteristics: they increase soil bulk density and have higher soil moisture content due to shallower water tables (Davidson et al., 2020). Moreover, seismic lines that cut through permafrost terrain can cause rapid degradation/thaw of permafrost resulting in deeper depths to frost table (the seasonally thawed layer) and the potential for a linear, permafrost free corridor, connecting peatlands and increasing groundwater connectivity and movement to rivers (Braverman and Quinton, 2016).

The majority of seismic lines installed in the last 30 - 40 years show little to no recovery to forested state, post disturbance due to slow regeneration, local uses (as trails, for hunting and all terrain vehicle use), and continuous industrial activity (Lee and Boutin, 2006; Lovitt et al., 2018). However, provincial governments, including the

Government of Alberta require restoration to enhance post-disturbance vegetation recovery to pre-disturbance ecosystem characteristics of forests and peatlands (Saraswati et al., 2020). Despite low ecosystem recovery success, areas within seismic lines have higher productivity in terms of understory species and mosses. Increased incoming solar radiation and decreased competition for nutrients allows for greater diversity of herbaceous and deciduous shrub establishment (Revel et al., 1984). For example, Revel et al (1984) found that seismic lines had about 80% herbaceous cover and 41% moss cover with few trees compared to adjacent forest stands that had more than 50% tree cover and decreased herb cover. Similarly, Davidson et al (2021) found that seismic lines had higher peak greenness and were dominated by moisture tolerant sedges and willows in fens, while *Sphagnum fuscum* dominated seismic lines in bogs. Also, seismic lines had enhanced decomposition with low Carbon to Nitrogen (C: N) ratios (Davidson et al., 2020). Despite enhanced productivity, dominance of graminoids and sedges caused greater greenhouse gas emissions due to the high respiration rate of sedges, producing more CH<sub>4</sub> than mosses (Schmidth et al., 2021; Davidson et al., 2021).

As of August 2021, there were 42,403 active wells used in *in situ* petroleum extraction projects in Alberta (Alberta Energy Regulator, 2021), creating additional fragmentation of peatlands. The impacts of these relatively low-intensity disturbances on the broader landscape requires further understanding, especially over a large number of environmentally variable peatlands. However, it is difficult to quantify the cumulative impacts of seismic lines, fires, and climate change due to constraints in the ability, time, and cost associated with field data collection. Collecting measurements over a few peatlands may not represent the broad range of environmental characteristics and can be

influenced by subjective errors, such as accessibility (Chasmer et al., 2020a). Remote sensing provides an alternative for long-term monitoring of the impacts of seismic lines and other low intensity disturbances, fire, and climate change across broad areas of peatland-forest ecosystems. Further, lidar data, which is acquired by measuring the emission and reception of laser pulses from aircraft (Lim et al., 2003), can be used to quantify the three-dimensional characteristics of vegetation and ground-surface elevation. Vertical and horizontal changes in vegetation structure with time since disturbance provide measurements of canopy characteristics, which can be used as proxy indicators of ecosystem response (e.g., changes in water, nutrients), and recovery, post-disturbance (Abib et al., 2019). Cameras on Unmanned Aerial Vehicles (UAV) provides a cost-effective alternative for measuring vegetation height using overlapping photos, which can be used to create dense three-dimensional point clouds along linear disturbances (Chen et al., 2017). The elevational data provided by both lidar, and UAV photogrammetry can be used to map micro-topography and estimate the depth to the water table, assumed in areas of low-lying relief (e.g., hollows, Lovitt et al., 2018). The combination of field measurements with remote sensing technologies can be used to quantify broader ecological impacts of seismic lines. Although the impacts of seismic lines on upland forests are well known (Lee and Boutin, 2006; van Rensen et al., 2015; Dabros et al., 2018; Finnegan et al., 2019; Davidson et al., 2020), there is relatively little research on the impact of these disturbances on peatland ecosystems, and how these ecosystems recover following fire and anthropogenic disturbance. A recent study, for example, by Barber et al. (2021) found significantly reduced vegetation heights within seismic lines in peatlands that had been burned in 2001 and 2002 compared with undisturbed peatlands,

however, little is known about vegetation recovery across multiple sites and years since fire.

The goal of this study is to use airborne lidar to determine whether wildland fires that burn over seismic lines in peatlands result in the regeneration of woody vegetation adjacent to seismic lines relative to peatlands that are fragmented by seismic lines only. The objectives are: (a) assess how the spatial distribution of deciduous and conifer vegetation varies within seismic lines and with distances from seismic lines in peatlands that had individually burned 5, 18, 30, and 38 years ago, based on a post-fire burn chronosequence, compared with recently unburned and undisturbed ‘mature’ reference peatlands and (b) determine the primary environmental and anthropogenic drivers of post-fire and post-seismic line vegetation growth in boreal peatlands with time since fire. We hypothesize that there will be higher deciduous regeneration proximal to seismic lines as a proxy indicator of changes in resource availability and abiotic factors compared with undisturbed parts of peatlands. Furthermore, seismic line attributes combined with incoming solar radiation and soil moisture availability (determined using topographic and vegetation proxy indicators) will influence vegetation regeneration trajectories.

## **4.2. MATERIAL AND METHODS**

### **4.2.1 Study area**

The area of study is located ~ 230 km south of Fort McMurray near Wandering River, Alberta (112° 12' 31" W, 55° 37' 46" N) and within the Central Mixedwood subregion of the Boreal Plains Ecozone (Figure 4.1). The Boreal Plains is one of the



driest ecozones in Canada with strong seasonal variations in temperature (Bonan and Shugart, 1989). Peatlands include bogs and fens, which cover more than 50% of the area (Alberta Parks, 2015). Vegetation in this region is dominated by pure and mixed forest of coniferous (*Picea* spp. and *Pinus banksiana*), and broadleaf deciduous species (*Populus tremuloides*, *Populus balsamifera*, and *Betula papyrifera*). Understory shrub species include but are not limited to *Prunus virginiana*, *Alnus* spp., *Amelanchier alnifolia*, *Symphoricarpos* spp., *Ledum groenlandicum*, *Betula pumila*, and *Salix* spp. with a variety of herbaceous and moss species. The surficial geology is characterized by glacial deposits consisting of mostly glacial moraines, stagnant ice moraines, and glaciofluvial deposits (Campbell et al., 2006).

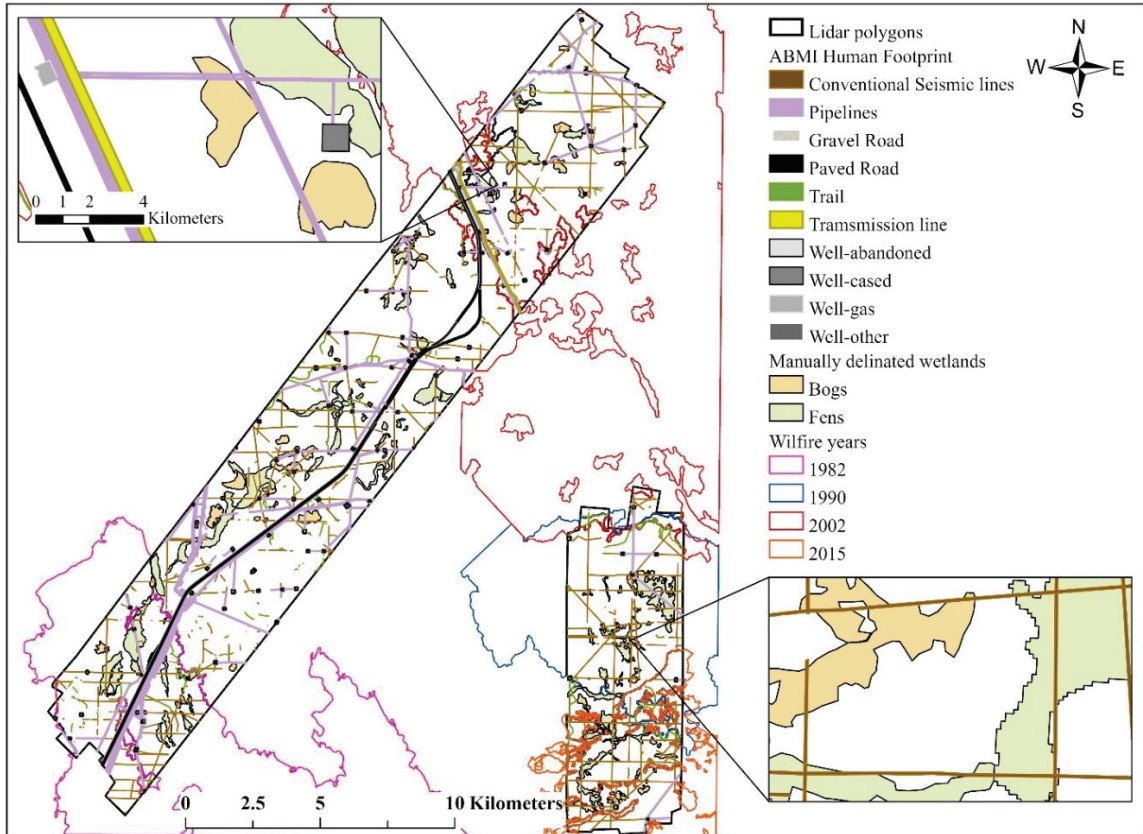


**Figure 4. 1** Location of lidar survey polygons near Fort McMurray, Alberta that have been temporarily or permanently disturbed by industrial land use activities. Areas that have not been burned in the recent history of scientific observation (since ~1930) are found in between the fire scars, predominantly between 1982 and 2002 fires in the western lidar polygon, while the eastern lidar polygon was burned by fires in 1990 and 2015.

Lidar survey areas had a low density of seismic lines of 1.59 km/km<sup>2</sup> (ABMI, 2019) and were burned by fires in 1982, 1990, 2002, and 2015, which are used to assess post-fire regeneration with age since fire, assuming relatively similar environmental conditions (Figure 4.1). Seismic lines found in these areas were 6 m wide and were classified as conventional seismic lines based on Human Footprint Inventory. The majority of seismic lines were constructed in 2002, with an average period available for vegetation regeneration of 18 years in the burned areas and 15 years (constructed in

2005) in the unburned areas. Moreover, some peatlands were fragmented by ~ 4 m wide trails, 10 to 20 m wide underground/ aboveground pipelines used to transport petrochemicals, and adjacent 100 m × 100 m well-pads and were included in the anthropogenic footprint (ABMI, 2019). Finally, there was a 38 m wide transmission line corridor that intersected the eastern lidar polygon with towers and poles for transmitting high voltage electricity (ABMI, 2019). Vegetation within these linear disturbances consisted mostly of mosses and herbaceous ground cover with *Salix spp.* and *Alnus spp.* growing on seismic lines and intersections with well pads (from field data and in Revel et al., 1984).

#### **4.2.2 Lidar data collection and processing**

Airborne lidar data from the fire chronosequence was collected by the ARTeMiS Lab (University of Lethbridge) using the Titan multi-spectral airborne lidar system (Teledyne Optech Inc, Canada). The Titan scanner is multi-spectral, three channel (Channel 'C' herein C1, C2, and C3) system with laser pulse emissions at 1550 nm (shortwave infrared, C1), 1064 nm (near infrared, C2), and 532 nm (green, C3), respectively (Hopkinson et al., 2016b; Chasmer et al., 2017). Survey characteristics included a mean flight altitude of 1000 m above ground and a pulse repetition frequency (PRF) of 100KHz per channel. The survey polygons covered an area of 220 km<sup>2</sup> with a lateral strip overlap of 50% and an average point density of 6.2 points per square meter (Chapter 3). Lidar data were used to derive elevation and canopy characteristics from within burned and unburned peatlands.

Lidar returns were classified into ground and non-ground returns using last of many echoes and only echoes in TerraScan (TerraSolid, Finland). A digital elevation model and a digital surface model was generated at 2 m pixel resolution in LAStools (RapidLasso, Germany). To determine variations in vegetation height a Canopy Height Model was created by calculating the difference between the digital surface model and the digital elevation model. Various interpolation techniques were used in LAStools to derive vegetation structural metrics including average percent cover, 95<sup>th</sup> and 99<sup>th</sup> percentile of height (described in Chapter 3). These were then used to determine topographic and stand characteristics of peatlands, years since fire and seismic line impact using ArcGIS Pro (ESRI, Canada).

#### **4.2.3 Supplementary geospatial data**

Additional geospatial layers were used to quantify the distribution of seismic lines and other anthropogenic disturbances within peatlands. These included the Human Footprint Inventory for the Oil Sands Monitoring Region circa 2019 (ABMI 2019), which was created using SPOT 6 imagery. The edges of seismic lines and other linear disturbances including trails, pipelines, and well pads were manually delineated using the human footprint inventory as a guide (ABMI, 2019) and in greater detail by using the canopy height model, which indicates shorter vegetation, which occurs within seismic lines, compared with that of the surrounding forests and peatlands. These linear disturbances were together treated as total anthropogenic disturbances. Seismic line age was calculated by subtracting the year seismic line was installed from the year when lidar data were collected, in this case, 2020. Also, seismic line direction (NS vs. EW) and total

percentage of peatland area fragmented by these anthropogenic disturbances were also calculated as these can influence amount of soil moisture and incoming solar radiation (Abib et al., 2019).

Peatlands were expertly identified based on shape and vegetation characteristics using high spatial resolution imagery (Earth Data) in ArcGIS circa 2018. These were approximately outlined and delineated into bogs and fens described in Chapter 3 and were used for comparative analysis. A total of 155 peatlands (sample size,  $n = 76$  bogs and  $n = 79$  fens) were identified and used for the study. Within classified peatland shapes, peatland forms were also determined and classified into open, shrubby, and treed peatlands based on the shrub and tree classification developed in Chapter 3. However, it is difficult to predict whether the recently burned peatlands were open or shrubby before fire due to lack of pre-fire data.

To integrate proportions of open, shrub, and treed cells within each peatland (classification described in Chapter 3), a simple height-based metric was used based on the Alberta Wetland Classification System (Government of Alberta, 2015). To determine proportional cover of open, shrub, and treed cells within each peatland, cells with a vegetation height  $< 0.5$  m were re-classed with an arbitrary value of “0”, representing the ‘open’ class because these cells contained vegetation that was shorter than 0.5 m. Cells that included vegetation with heights of 0.5 to 3 m (determined from the canopy height model) were re-classed with an arbitrary value of “1”, indicating vegetation which was assumed to represent shrubs with a height of 0.5 to 3 m. However, the shrub class might include juvenile trees in early stages of succession as the canopy height model is divided based on height. All cells with vegetation heights  $> 3$  m (assumed to be deciduous or

conifer trees) were re-classed arbitrarily with a value of “2”. These were then multiplied by the proportional cover calculated in Chapter 3 and zonal average was calculated for each peatland. The zonal average was then divided into three equal segments or groups representing the three proportions. If the average cell value within the peatland group was between 0 and 0.66, then the peatland was classified as “open” assuming that there were more open areas than shrubs or trees. If the average was between 0.67 and 1.32, then it was classified as “shrubby”, assuming a greater proportion of shrubs. If the average was between 1.33 and 2, then peatlands with these characteristics were classified as “treed” peatlands, assuming a higher proportion of trees within peatlands. The open, shrubby, treed classification was used as an index of combined height and proportional cover akin to a generalized metric of ‘volume’ to determine how different peatland types regenerate and how the amount of biomass changes

To better understand the localised environmental conditions in which vegetation regenerates, lidar derived digital surface model was used to calculate incoming solar radiation in watt hours per m<sup>2</sup> for an annual period of one year (January to December), as a proxy indicator of maximum energy receipt as well as the general ‘northness’ of peatland orientation. The digital surface model was standardized to range between 0 (at 90/270 degrees) and 1 at 0/360 degrees, whereas the opposite scale is used for 90 to 180 degrees and 180 degrees to 270 degrees (ranging from 0 to -1). Using the digital surface model provides information regarding areas of illumination and shadows based on vegetation structure. Here, north facing slopes receive less solar radiation and retain more moisture, which support coniferous trees and cast shadows further reducing incoming energy (Prévost and Raymond, 2012).

Other environmental variables include topographic position index (TPI), which was calculated using the digital elevation model by applying a circular search radius of 50 m to capture variations in general peatland microtopography. TPI was assumed to indicate where parts of the peatland surface were closer to or further from the water table based on topographic undulations. Furthermore, the average slope of the peatland was calculated by resampling the digital elevation model to 5 m cell resolution as lower resolution cells provide a more generalized variation of the surface topography. These data layer outputs were generated in ArcGIS Pro using area solar radiation TPI (Jenness, 2006), and slope tools (ArcGIS Pro, 2020).

#### **4.2.4 Data Analysis**

##### **4.2.4.1 Seismic line buffer analysis**

The difference in vegetation structure adjacent to seismic lines was quantified using buffer analysis, which provides a proxy measure of the impact of landscape fragmentation on peatlands. For the buffer analysis, three ring buffers each of width 30 m were created along each individual manually delineated seismic line as it extended into each adjacent peatland. Seismic lines can have proximal effects up to 100 m and wide seismic lines can influence vegetation height up to 60 m from seismic lines (Abib et al., 2019). To address this, the buffers were categorized based on distance from seismic lines as: near (0 – 30 m), intermediate (30 – 60 m), and far (60 – 90 m), such that each buffer was of equal width (an example of which is shown in Figure 4.2). A total of 190 seismic lines were identified and used per buffer ( $n = 80$  for bogs, and  $n = 110$  for fens). Average



vegetation height for deciduous shrubs, deciduous trees, and conifer trees within each peatland were determined using the shrub and tree classification described in Chapter 3 for each buffer distance and within each peatland, excluding open areas without shrubs or trees. Average deciduous shrub, deciduous tree, and conifer tree heights were also extracted for reference peatlands (unburned with no seismic lines) and were treated as control sites. In some areas, standing dead, burned stems from the previous fires were observed in the lidar data, thereby artificially increasing canopy height (and an over exaggeration of post-fire regeneration). To remove the influence of standing dead stems, any vegetation heights in the canopy height model greater than 6 m (within each 2 m grid cell resolution, thus exceeding the circumference of dead tree stems) was removed from post-fire lidar data within 5 year, 18 year, 30 year, and 38 year burn scars by classifying these to represent a ‘null’ data class. Heights of > 6 m were chosen as this was the maximum height observed in unburned peatlands based on lidar point cloud distribution and canopy height model.

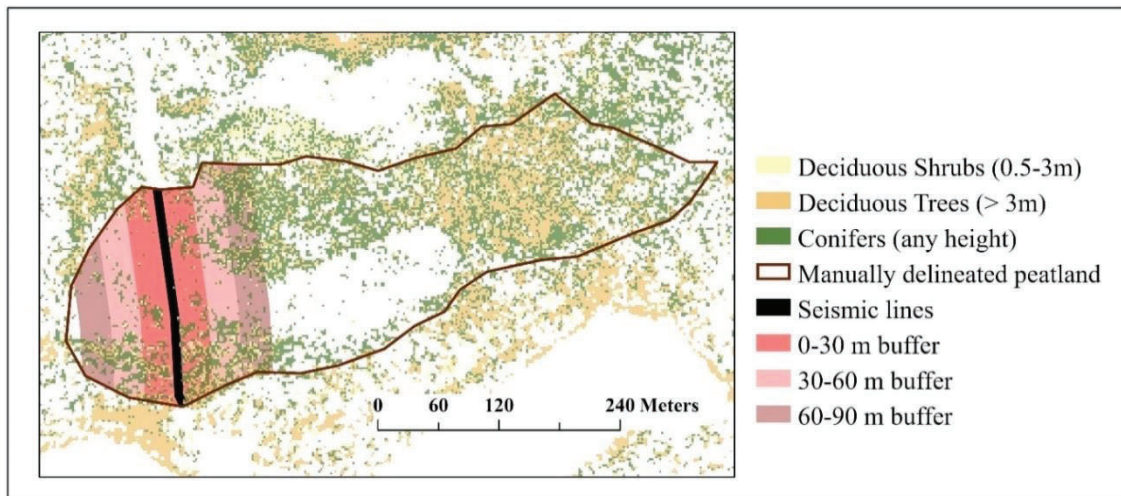


**Figure 4. 2** Example for a single peatland of near (0 – 30 m), intermediate (30 – 60 m), and far (60 – 90 m) buffers along manually delineated seismic lines within peatlands used to quantify the proximal effects of seismic lines on vegetation regeneration.



All statistical analyses were performed in SPSS Version 26 (SPSS Inc., USA). Lidar derived variables were tested for normality using Kolmogorov-Smirnov and Shapiro-Wilk tests, which showed that data were non-parametric. Vegetation heights across the seismic line buffers within peatlands were compared using Kruskal-Wallis one-way ANOVA, to determine if statistically significant differences exist with distance from seismic lines.

#### **4.2.4.2 Principal Component Analysis**

To identify potentially important general peatland natural/morphological and anthropogenic drivers of post-disturbance succession, a principal component analysis (PCA) was used. PCA is defined as a dimension reduction approach in which new variables are constructed from original variables without losing the original information, thereby maintaining high data variance (Jolliffe, 1990). For example, in a PCA, the first principal component (PC) is a linear function that contains the highest variance and therefore, highest eigenvalue, while the second PC explains the maximum possible variance, while remaining uncorrelated with the first PC (Jolliffe, 1990; Liu et al., 2003). Hence, PCA was used to identify the interactions between different environmental and anthropogenic correlates associated with post-fire succession. This method efficiently combines information from features and reduces data redundancy.

Within the PCA analysis, vegetation height was treated as the dependent variable and various environmental/ natural characteristics, such as peatland slope, area, TPI, and

incoming solar radiation, were treated as explanatory variables as this influence post- fire vegetation height within each peatland by altering moisture and energy budget (Gignac and Dale, 2007; Méndez-Toribio et al., 2016). Anthropogenic characteristics such as seismic line age, seismic line direction, and total area fragmented by linear disturbances were also included as explanatory variables as these can also impact the rate of vegetation regeneration (assumed using a descriptor of height) within peatlands (van Rensen et al., 2015; Abib et al., 2019). The final variables used within the PCA are described in Table 4.1. Variables were standardized first using (1) to remove the arbitrariness of the units and give equal weightage to all variables (Jolliffe, 1990).

$$X' = \frac{x_i - \bar{x}}{S_{x_i}} \quad (1)$$

where  $X'$  stands for the standardized dependent variable,  $x_i$  is the dependent variable,  $\bar{x}$  is the mean of the dependent variable, and  $S_{x_i}$  is the standard deviation of the dependent variable. Standardizing the variables also helps preserve correlation between variables and ensure that the total variance is 1 (Liu et al., 2003).

**Table 4. 1** Explanatory variables used in PCA analysis.

Variable	Description	Mechanism/ Hypothesis	Range	
			Bogs	Fens
<b>TPI (m)</b>	Topographic Position Index (TPI), calculated using the 2 m digital elevation model by applying a circular search radius of 50 m, low lying areas had negative values, positive values indicate hills, while values near 0 are flat	Negative TPI may be an indicator that the ground surface is closer to the top of the water table, which may result in less woody vegetation recovery.	-1.27 to 0.69	-5.63 to 1.69

<b>Peatland slope (degrees)</b>	Average peatland slope calculated using 5 m digital elevation model	Peatlands with greater sloped surfaces, might have a higher growth rate since fire and greater area coverage associated with drainage and evaporative losses adjacent to seismic lines, which may result in preferential growth of taller vegetation.	0.32 to 4.04	0.36 to 7.08
<b>Peatland area (m<sup>2</sup>)</b>	Peatland area in m <sup>2</sup>	Natural and anthropogenic factors vary between peatlands based on peatland size (area). Smaller peatlands are more vulnerable to greater disturbances and vegetation height changes.	2538.55 to 292147.55	5979.12 to 1375497.74
<b>Incoming solar radiation (WH/ m<sup>2</sup>)</b>	Incoming solar radiation in watt hours per m <sup>2</sup> calculated using 2 m digital surface model	Areas adjacent to seismic line would have more incoming solar radiation compared to closed canopies allowing vegetation to receive more sunlight and enhancing growth	986.59 to 3465.94	718.16 to 3372.41
<b>Percent cover (%)</b>	Percent cover generated using all returns from all channels with heights > 0.5 m from ground	Low percent cover may be an indicator of open canopies that are more disturbed with less time for recovery compared to peatlands with higher percent cover.	10.73 to 90.88	14.03 to 92.18
<b>Seismic line age (years)</b>	Age of seismic line in years, calculated by subtracting the year the line was installed from the year lidar data was collected	Taller vegetation found within and adjacent to older seismic lines as these have more time for woody vegetation recovery compared to younger seismic lines	0 to 37	0 to 37

		that have vegetation in the early stages of succession.		
<b>Anthropogenic peatland fragmentation (%)</b>	Percentage of peatland area fragmented by seismic lines, well pads, trails, and pipelines	More fragmented peatlands will have less vegetation recovery due to changes in hydrology and peatland microtopography.	0 to 15.9	0 to 10.47

The PCA was carried out in SPSS using factor reduction analysis tools. The variables were checked for auto correlation and collinearity using a correlation matrix and variance inflation factors (VIF), respectively. A correlation score of greater than 0.8 and VIF greater than 15 suggest that the variables are correlated and are subjected to collinearity (Liu et al., 2003). These variables were removed from the final model and total variance was accounted for based on eigenvalues. The eigenvalues were then used to create a component matrix with varimax rotation to visualize how the variables cluster (Jolliffe, 1990). Varimax rotation was chosen as the rotation method because it is an orthogonal rotation that attempts to maximize the variance for each component. For this analysis, eigenvalues >1.0 were considered as significant and the varimax factors loadings on each PC were measured. If the values were > 0.75, the factor was considered as “strong” loading factor. While values ranging from 0.50-0.75 were considered as “moderate”, and values range from 0.30-0.49 were considered as “weak” factor loadings (Jolliffe, 1990).

## 4.3. RESULTS

### 4.3.1 Influence of seismic lines on conifer and deciduous shrub and/or trees heights

Descriptive statistics and the canopy height model provided an enhanced ability to visualize the differences between tree and shrub canopy characteristics within both bogs and fens. Here we found that seismic lines, well pads, and other linear features had little to no regeneration within them in from 5 years to 38 years since fire (YSF), and especially in unburned peatlands (Figure 4.3). Peatlands, on average, had shorter vegetation compared to upland areas. Peatlands also had higher proportional cover of conifers, especially in older burned scars (of 30 and 38 YSF) and in unburned peatlands (Figure 4.3, Table 4.2). Moreover, the average height of vegetation found within peatlands was similar between 30 YSF and the 38 YSF, indicating reduced rate of growth as trees begin to mature (Chapter 3). The greatest average vegetation canopy height observed in undisturbed/ reference bogs and fens was  $4.2 \text{ m} \pm 0.8$  and  $4.1 \text{ m} \pm 1.4$ , respectively (Table 4.2) suggesting poor growth conditions in these peatlands due to localized environmental factors, regardless of disturbance, though these conditions would require verification using field measurements.

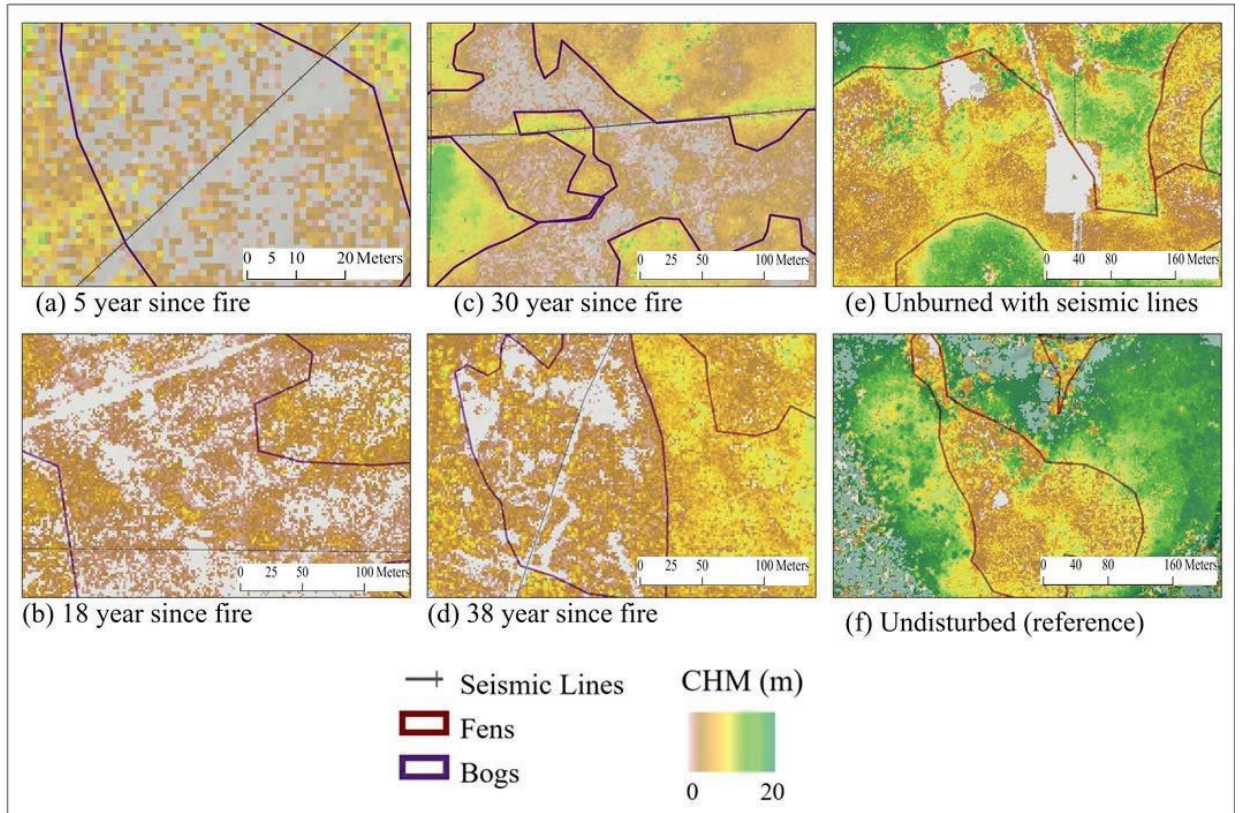


**Figure 4. 3** Canopy height model for example peatlands found in the study area. Upland and transitional areas have taller vegetation while peatlands fragmented by seismic lines have vegetation height less than 6 m.

**Table 4. 2** Average vegetation descriptive characteristics determined for peatland classes/ fire age for burned chronosequence and unburned peatlands.

	<b>Disturbance</b>	<b>Number of open, shrubby, and treed peatland</b>	<b>Hgt (m)</b>	<b>Stdev (m)</b>	<b>Deci shrub (%)</b>	<b>Deci trees (%)</b>	<b>Conifer (%)</b>	<b>Anthro disturb (%)</b>
<b>BOGS</b>	5 YSF + seismic line (n = 10)	0 open 6 shrubby 4 treed	1.06	0.74	0.51	0.00	0.01	3.43
	18 YSF + seismic line (n = 12)	4 open 8 shrubby 0 treed	2.14	0.24	2.18	0.83	0.51	3.30
	30 YSF + seismic line (n = 10)	0 open 1 shrubby 9 treed	2.83	0.31	4.78	7.68	4.98	5.56

	38 YSF + seismic line ( <i>n</i> = 10)	0 open 6 shrubby 4 treed	2.77	0.48	4.75	2.29	3.88	4.54
	Unburned + seismic line ( <i>n</i> = 21)	0 open 1 shrubby 20 treed	3.84	0.98	2.76	1.85	12.56	5.92
	Reference ( <i>n</i> = 13)	0 open 0 shrubby 13 treed	4.21	0.81	4.77	2.41	11.48	0
<b>FENS</b>	5 YSF + seismic line ( <i>n</i> = 12)	1 open 4 shrubby 7 treed	1.02	0.66	1.11	0.00	0.02	1.72
	18 YSF + seismic line ( <i>n</i> = 10)	3 open 7 shrubby 0 treed	2.21	0.17	2.81	1.18	1.14	2.32
	30 YSF + seismic line ( <i>n</i> = 11)	0 open 4 shrubby 7 treed	2.43	0.28	5.61	5.37	3.59	2.60
	38 YSF + seismic line ( <i>n</i> = 10)	0 open 5 shrubby 5 treed	2.63	0.49	5.13	1.10	4.11	1.70
	Unburned + seismic line ( <i>n</i> = 22)	1 open 5 shrubby 16 treed	3.29	0.91	3.30	1.64	9.28	3.47
	Reference ( <i>n</i> = 14)	1 open 1 shrubby 12 treed	4.13	1.44	3.51	2.49	10.35	0

Hgt = average height, Stdev = standard deviation of height, Deci shrub = proportional cover of deciduous shrubs, Deci trees = proportional cover of deciduous trees, Conifer = proportional cover of conifers, Anthro disturb = proportion of peatland area fragmented by linear disturbances including seismic lines

In the years following wildland fire, we found that significant differences in vegetation height of deciduous shrubs, and deciduous and conifer trees between fires within peatlands ( $p < 0.05$  in all cases). Along seismic line buffers, deciduous shrubs were first to recover in bogs, post-fire and had higher average vegetation height with distance from seismic lines in 5 and 18 YSF (Figure 4.4). However, we also observed that the average variability of deciduous shrub heights within peatlands decreased with years



since fire as competition between herbaceous vegetation/forbs and shrubs increased. Deciduous and conifers trees overtake deciduous shrubs at about 18 YSF, on average, however, we did not observe any significant differences in vegetation height with distance from seismic lines ( $p > 0.05$ ). In younger, post-fire sites (e.g., at 5 years since fire), we found that fire was the dominant influence on regeneration at these sites, corroborating results in Barber et al. (2021).

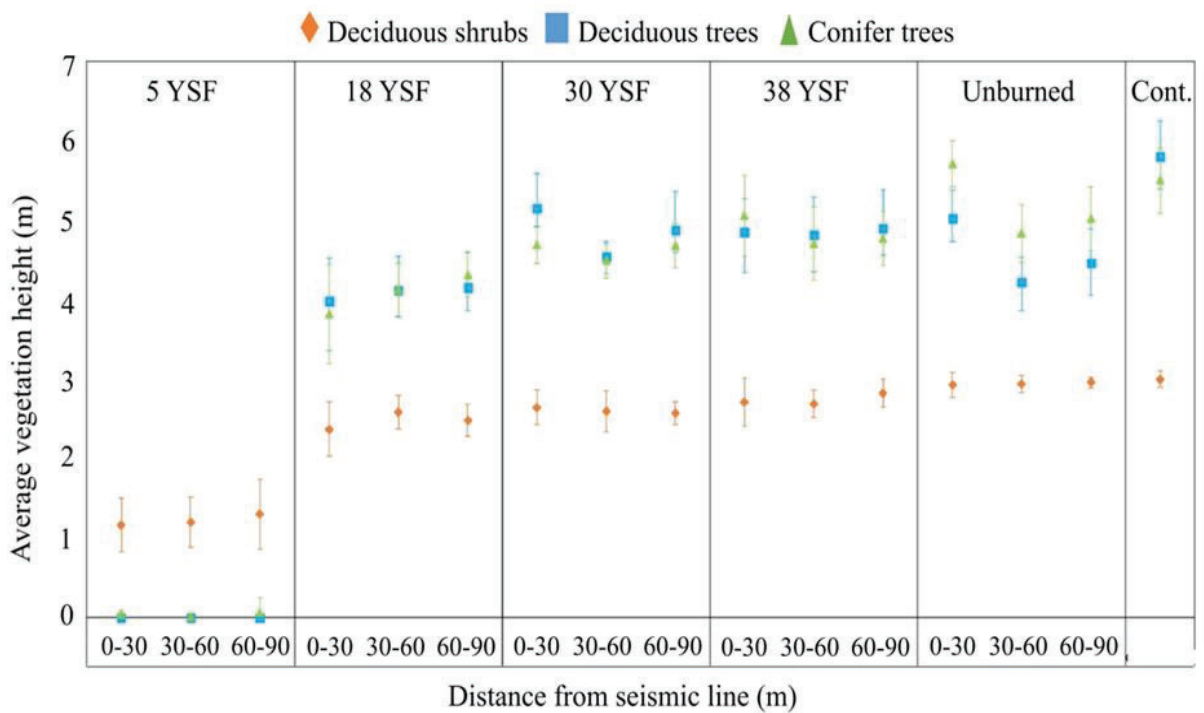


**Figure 4.4** Variation in vegetation height in bogs for deciduous shrubs, deciduous trees, and conifers trees across burn chronosequence and with distance from seismic lines. Whiskers represent the standard deviation of height within each period/buffer, whereas the symbols represent the average height. Here Cont. ae reference peatlands that are unburned with no seismic lines.

In older burned scars in bogs (30 and 38 YSF), there was an increase in vegetation height of deciduous trees and conifers adjacent to seismic lines, however tree heights decreased beyond 30 m from seismic lines within older (vegetation), burned peatlands.



Similarly, in unburned bogs, there was a significant ( $p < 0.05$ ) increase in vegetation height in both deciduous and conifer trees adjacent to seismic lines (0-30 m buffer). Average tree heights declined as the distance from seismic line increases to 60 m and 90 m. Unburned areas near seismic lines had the tallest conifer trees of any bog examined (average = 5.7 m, stdev  $\pm$  0.29), while the tallest deciduous trees (average = 5.2 m, stdev  $\pm$  0.43) were found within 30 m adjacent to seismic lines at sites burned 30 years ago (Figure 4.4), suggesting that deciduous species regenerate at a faster rate post-fire.

Differences in height between deciduous and conifer trees were significant ( $p < 0.05$ ) within all unburned bogs with seismic lines and with distances from seismic lines. However, when burned bogs with seismic lines were compared, we found no statistically significant differences in deciduous and conifer tree heights with distance from seismic lines ( $p > 0.05$ ). This illustrates that post-fire regeneration likely dominates vegetation rate of regeneration in the early years of succession more than distance from seismic lines within these peatlands.

On the other hand, fens had shorter deciduous and conifer tree heights with less variability in deciduous shrub height as years since fire increased (Figure 4.5). Similar to bogs, we found enhanced shrubification of fens along seismic lines in the first 5 YSF, while deciduous and conifers trees became more established (and could be identified) by 18 YSF. The tallest deciduous trees (average = 4.9 m, stdev  $\pm$  0.54) and conifer trees (average = 5.1 m, stdev  $\pm$  0.41) were found adjacent to seismic lines within 0 – 30 m in the 30 YSF and 38 YSF respectively (Figure 4.5). Tree heights decreased as the distance from seismic lines increased to 30 – 60 m and 60 – 90 m. However, height of deciduous and conifer trees were lower in the unburned seismic line buffers, especially at 0 – 30 m

buffer from seismic lines in more mature sites (38 YSF and unburned areas,  $p < 0.05$ ). This suggests that seismic lines had more detrimental impact on fens, based on the growth of deciduous shrubs and trees. Overall, height of deciduous shrubs, deciduous trees, and conifer trees were significantly different between each period since fire within peatlands (5 YSF, 18 YSF, 30 YSF, 38 YSF, and unburned fens ( $p < 0.05$ )) but not with distance from seismic lines.

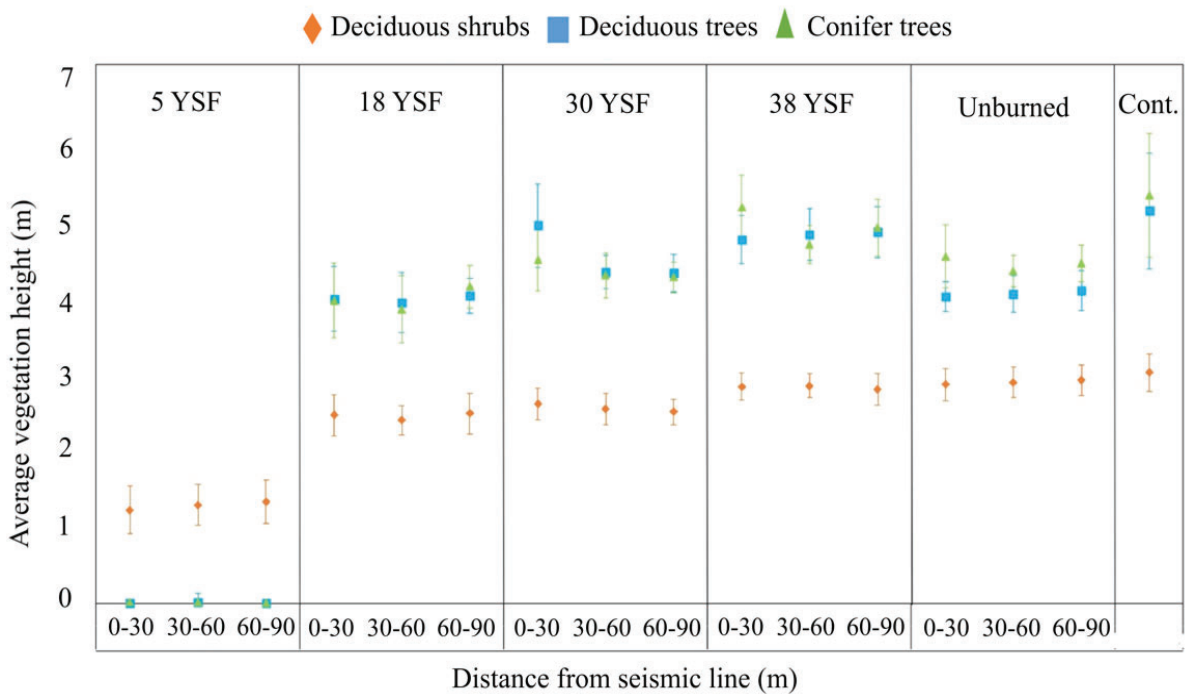


**Figure 4. 5** Variation in vegetation height in fens for deciduous shrubs, deciduous trees, and conifers trees across burn chronosequence and with distance from seismic lines. Whiskers represent the standard deviation of height within each period/buffer, whereas the symbols represent the average height. Here Cont. ae reference peatlands that are unburned with no seismic lines

#### 4.3.2 Anthropogenic/environmental correlates of vegetation succession in peatlands

General peatland characteristics and anthropogenic influences, including age and width of seismic lines were compared within a PCA to identify correspondence between

these and post-fire vegetation growth as well as dominance of shrubs vs. trees within bog and fen peatlands. Here we found that the seven explanatory variables (described in Table 4.3) were not strongly correlated with each other (correlation coefficient less than 0.8). Also, variables had a variance inflation factor (VIF) of less than 5, suggesting that there was no collinearity in the model. PCA results showed that PC1 explained 34% of the variance of average vegetation characteristics of peatlands (bogs and fens together), while PC2 explained 20% of the variance (Table 4.4).

**Table 4.3** Correlation matrix of the explanatory variables used.

	Peatland area (m <sup>2</sup> )	Seismic line age (years)	Percentage of peatland area fragmented by anthropogenic disturbance (%)	TPI	Peatland Slope	Incoming Solar radiation (WH/m <sup>2</sup> )	Percent cover (%)
Peatland area (m <sup>2</sup> )	1.00	-	-	-	-	-	-
Seismic line age (years)	0.05	1.00	-	-	-	-	-
Percentage of peatland area fragmented by anthropogenic disturbance (%)	-0.11	0.27	1.00	-	-	-	-
TPI	0.17	0.05	-0.04	1.00	-	-	-
Peatland Slope	-0.21	0.06	-0.01	-0.24	1.00	-	-
Incoming Solar radiation (WH/m <sup>2</sup> )	0.29	0.25	0.02	0.21	-0.38	1.00	-
Percent cover (%)	-0.19	-0.34	-0.07	-0.10	0.20	-0.67	1.00

**Table 4. 4** Total variance explained by each component.

Component	Initial Eigenvalues			Extraction Sums of Squared Loadings		
	Total	% of Variance	Cumulative %	Total	% of Variance	Cumulative %
<b>PC1</b>	2.23	33.91	33.91	2.23	33.91	33.88
<b>PC2</b>	1.37	19.60	53.51	1.37	19.60	53.51
<b>PC3</b>	0.95	11.94	65.45			
<b>PC4</b>	0.84	11.57	77.02			
<b>PC5</b>	0.77	11.02	88.04			
<b>PC6</b>	0.54	7.76	95.80			
<b>PC7</b>	0.29	4.20	100.00			

Extraction Method: Principal Component Analysis.

Hence, these two principal components accounted for 54% of the variability in vegetation height, while the remaining variability could be due to localized or ecological factors, possibly associated with local moisture conditions, and other local drivers. When components were plotted for combined bogs and fens using varimax rotation, incoming solar radiation had the strongest loading on PC1 followed by peatland slope and area. Similarly, seismic line age and percentage of peatland area fragmented by anthropogenic disturbance had the greatest loading on PC2 (Table 4.5). Percent of vegetation cover was negatively correlated with these variables and had a moderate loading on both components. Based on the groupings of the drivers, PC1 represents morphological/natural environmental drivers and PC2 represents anthropogenic disturbance drivers of vegetation height variability within peatlands (Table 4.5).

**Table 4. 5** Rotated component matrix for the PCA.

	Component	
	PC1	PC2
Incoming Solar radiation (WH/m <sup>2</sup> )	0.72	
Peatland Slope	-0.66	
Peatland area (m <sup>2</sup> )	0.61	
TPI	0.53	
Seismic line age (years)		0.79
Percent cover (%)	-0.53	-0.63
Percentage of peatland area fragmented by anthropogenic disturbance (%)		0.61

Extraction Method: Principal Component Analysis.  
Rotation Method: Varimax with Kaiser Normalization.

Using PCA scores, the relationship between environmental and anthropogenic characteristics was evident based on clustering and loading vectors. The visualization identified four groups of clusters: reference peatlands that had a strong positive loading on PC1, unburned peatlands that had a strong negative loading on PC2, 5 YSF peatlands that had a strong negative loading on PC1, and 18 YSF peatlands that had a strong positive loading on PC2 (Figure 4.6). Negative values indicate an inverse correlation between component and original variables, while positive values indicate a positive correlation. Remaining peatlands had variable loading of environmental and anthropogenic components and might be influenced by other, possibly more localized environmental driving mechanisms. Further, separation of peatlands into open, shrubby, and treed forms, regardless of year since fire, indicated differences in component loadings depending on class: bogs vs. fens (Figure 4.7). Shrubby and open bogs that were burned had a strong positive loading on PC2, while shrubby burned fens had a strong negative loading on PC1. However, both reference bogs and fens had a strong positive

loading on PC1 due to lack of seismic line influences, while unburned peatlands with seismic lines loaded strongly on PC2, illustrating separation between environmental and anthropogenic drivers of variations in vegetation heights in the years since fire. Hence, the environmental component (PC1) had the greatest impact during the early and later stages of succession, while anthropogenic components (PC2) dominated after early competition (at 18 to 30 YSF), but before trees had established.

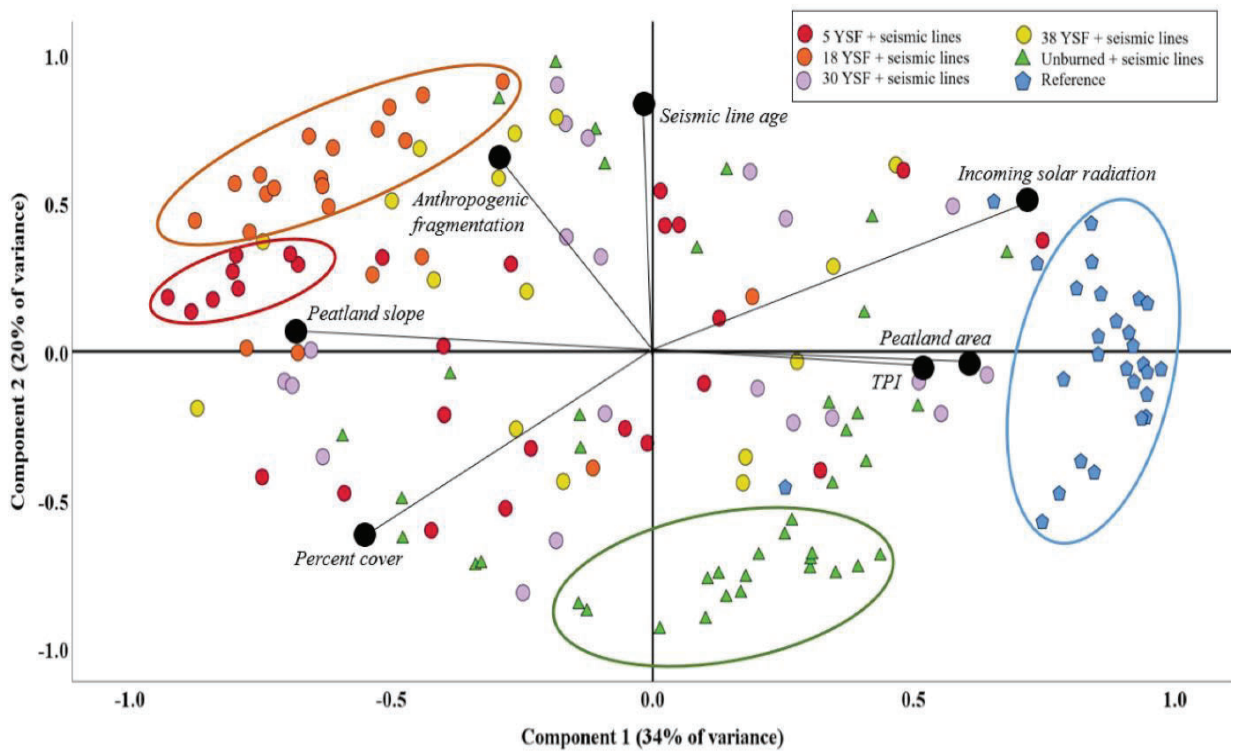


**Figure 4. 6** Plots of scaled peatland explanatory attribute score and arrows of loadings for the first two principal components (PC1 34% and PC2 20% of variance) of PCA for both bogs and fens. The length of their respective arrows illustrates the component loadings of the indices, while individual bogs and fens found in the study area are also included ( $n = 155$ ). Circles represent strong clustering of bogs and fens that cluster with years since fire.

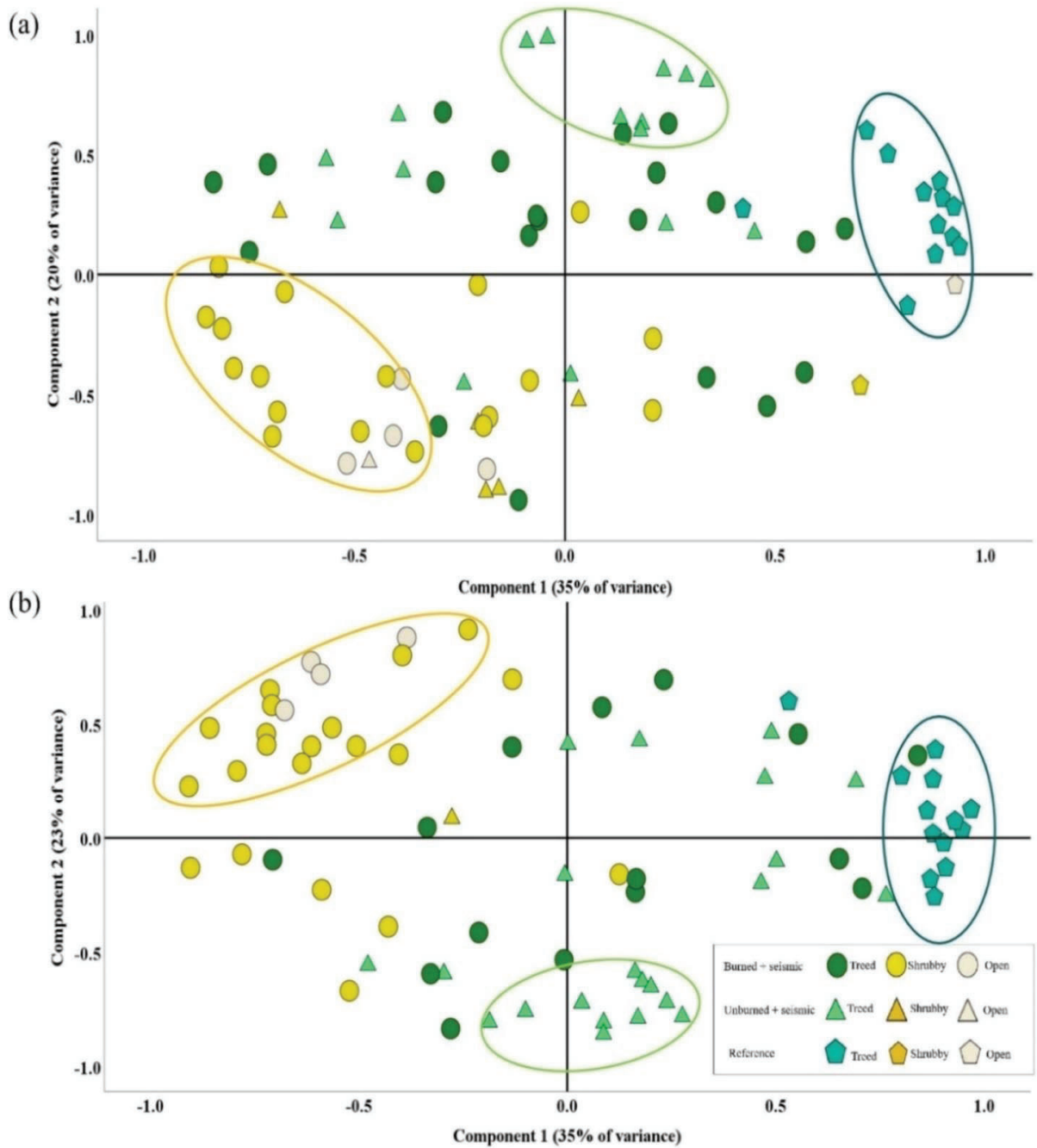


**Figure 4.** 7 PCA loading plots for (a) fen only ( $n = 79$ ) (b) bogs only ( $n = 76$ ) based on peatland type: open, shrubby, and treed. Circles represent strong clustering of some bog and fen forms (open, shrubby, treed).

## 4.4 DISCUSSION

### 4.4.1. Interaction between seismic lines and vegetation response

This study illustrates that peatland vegetation successional trajectories can be determined using lidar derived canopy metrics. These can be used to quantify the impact of seismic lines using vegetation height as an indicator of environmental changes that drive variations in height within peatlands. Lidar derived canopy height models were used to visualize areas of vegetation regeneration and also, describe variations in proportional cover of deciduous shrub, deciduous trees, and conifer trees (Table 4.2). Based on the canopy height model, vegetation height varies from near zero in seismic lines to 20 m in the upland forests (Figure 4.3), though the impacts of seismic lines on upland forests were not considered in this study. Variations in the height of vegetation, indicated by the canopy height model exists likely due to a combination of the construction of seismic lines, compression due to heavy machinery, resulting in the lowering of the surface elevation, and reduced depth to water table (Dabros et al., 2017; Stevenson et al., 2019). This may result to the loss of suitable microsites for regeneration associated with changing soil moisture and thermal regimes (Dabros et al., 2018).

Wide seismic lines can have proximal effects on vegetation height, especially in peatlands, which have slow regeneration leading to changes in vegetation structure and above ground biomass (Bolton et al., 2015; Gibson et al., 2016). Here we observe that seismic lines with variable width also have vegetation that is taller than reference sites, especially in fens (Figure 4.5). Previous studies have found that burned seismic lines are characterized by an open canopy of moss and graminoid cover and can be subject to



establishment failure (Barber et al., 2021). Others found that boreal ecosystems with seismic lines can recover to low understory cover characterized by shrubs and herbaceous vegetation (Lee and Boutin, 2006; Finnegan et al., 2019). Moreover, Davidson et al. (2021) found that areas disturbed by seismic lines greened at a faster rate, 1 – 3 weeks earlier, compared to reference peatlands. Similarly, our results showed that in the early years since fire (5 YSF) in bogs and fens, deciduous shrubs are the first to regenerate. Deciduous trees and conifer trees grow adjacent to seismic lines, reaching average vegetation heights of about 4 m by 18 YSF. When compared to burned peatlands with seismic lines, vegetation heights can be up to 1 m taller in seismic-disturbed peatlands that have not burned (Figures 4.4 and 4.5). Hence, wildland fire is the dominant influence on regeneration within peatlands that initiate secondary succession. In these peatlands, vegetation heights do not vary greatly with distance from seismic lines ( $p > 0.05$ ), further demonstrating the importance of fire in these environments, especially as vegetation regenerates at similar rates.

Within bogs, we found greater vegetation regeneration in areas adjacent to burned seismic lines to that in fens. Furthermore, burned seismic lines in fens within older burned scars (30 YSF and 38 YSF) had greater deciduous tree and conifer tree regeneration compared to unburned seismic lines (Figure 4.5), suggesting that seismic lines have a potentially more damaging and long-lasting effect on fens. Wildland fire within peatlands containing seismic lines can diminish these negative impacts by releasing seeds stored in seedbanks for conifers and enhancing vegetative regeneration of competitive deciduous species (Chen and Popadiouk, 2002; Day et al., 2020). Seismic lines have long-term detrimental effect on fens because the construction of seismic lines

causes an overall flattening of the peatland microtopography, eliminating hummocks and hollows (Lieffers et al. 2017; Filicetti and Nielsen, 2020). This results in a decrease in the depth of the water table making seismic lines wetter and lower compared to the surrounding peatland, restricting tree recruitment (Lovitt et al., 2018).

On the other hand, the cumulative impacts of wildland fire and seismic lines in bogs, promoting deciduous and conifer tree regeneration adjacent to seismic lines, especially as time since fire increases (Figure 4.4). Since bogs are ombrogenous and dominated by black spruce, areas adjacent to burned seismic lines provide suitable microsites for the establishment of conifer seedlings, post-fire, which were observed (approaching adolescence to maturity) at peatlands burned 38 years ago (Figure 4.4; Filicetti and Nielsen, 2020). Unburned peatlands with seismic lines had the tallest conifers adjacent to seismic lines. Tree heights decreased significantly ( $p < 0.05$ ) with distance from seismic lines, suggesting that seismic lines have a less severe impact on bogs, overall.

At 30 years since fire, deciduous trees were taller and not highly variable with distance from seismic lines in unburned peatlands. This provides evidence that peatlands with seismic lines that burn could result in enhanced deciduous regeneration that are similar in vegetation characteristics as those areas adjacent to seismic lines in unburned peatlands. Hence, wildland fires that burn through seismic lines may increase depth of the water table over time, thereby enhancing conditions for woody vegetation growth (Benscoter et al., 2015; Filicetti and Nielsen, 2020). Changes in hydrology, especially enhanced drying, promotes more rapid regeneration following fire with taller deciduous trees in the decades following fire, compared to peatlands that have remained unburned.

In conclusion, wildland fires over seismic lines were the dominant force driving succession in the initial years following fire. Fire also allows vegetation near seismic lines to recover to similar trajectories as undisturbed peatlands that have not been burned or fragmented by seismic lines (Figure 4.4; Figure 4.5).

#### **4.4.2 Interaction between the primary drivers of vegetation growth**

Among all environmental/ morphological variables examined in this study (on average for each peatland), incoming solar radiation was the strongest driver of vegetation growth adjacent to seismic lines. This was demonstrated by the highest loading on PC1 compared to other topographical drivers, including average peatland slope and TPI (Table 4.5). Greater canopy openness by conventional seismic lines increases light penetration adjacent to seismic lines, creating an opportunity for competition and vegetation establishment likely with fewer limitations adjacent to peatlands, compared to areas that are furthest from seismic line influences. This was observed in some peatlands burned 5 years prior to data collection, resulting in strong loading on PC1, dominated by deciduous shrubs (Figure 4.6). Also, greater amounts and prolonged periods of incident solar radiation increases air and soil temperatures as well as water fluxes (Holland and Steyn, 1975), decreasing resource competition among species (Revel et al., 1984). Deciduous and conifer tree height differences reduce further from seismic lines as proximal effects decrease (Dabros et al., 2017; Abib et al., 2019). Similar to Abib et al. (2019), vegetation that is 60-90 m from seismic lines becomes more similar in height to that found in unburned and undisturbed (reference) peatlands.

Similarly, age of seismic lines has the strongest loading on the anthropogenic component, PC2, compared to percentage of area fragmented by linear disturbances and seismic line direction. Vegetation is often taller adjacent to older seismic lines (Abib et al., 2019). Within peatlands that were burned 18 years ago, these are strongly influenced by anthropogenic factors, loading strongly on PC2. Interestingly, in this area, peatlands also have an average seismic line age of 18 years as well (ABMI, 2019), indicating that seismic lines in some peatlands may have been constructed either just before or just after the fire. Within peatlands that had burned 30 and 38 years ago, we find that these tend to have variable loading of environmental and seismic line characteristics, possibly indicating other, perhaps more localised environmental factors influencing vegetation regeneration (Figure 4.6), which should be explored further in future studies.

Hence, there is dominance of deciduous shrubs and trees immediately adjacent to seismic lines (up to 30 YSF) with higher proportions of conifer trees further from seismic lines, indicating that the seismic lines are having an influence on vegetation succession. This is also reflected in burned peatlands that are open or shrubby, having strong loading/impacts of seismic line characteristics along PC2 (Figure 4.7). These may also recover more rapidly due to abiotic conditions, especially in the early years following disturbance (Davidson et al., 2021). While, in unburned peatlands, wildland fire is not a major driver of vegetation distribution. Here, vegetation is at a more mature stage of succession, so trees will be dominantly impacted by seismic lines only (and climatic changes impacting all peatlands in the area), observed by the strong loading of unburned treed peatlands on PC2 (Figure 4.6). Recovery of vegetation on seismic lines is slow and

may take decades to establish pre - disturbance conditions suitable for tree regeneration (Lee and Boutin, 2006; Abib et al., 2019).

#### **4.4.3 Limitations**

Although lidar data are better than other remotely sensed data, such as optical/multispectral imagery, for explaining structural variability (Hopkinson et al., 2016), forest succession can be more accurately and more completely explained by field measurements of seedling count, tree diameter, site conditions (Barber et al., 2021). However, field measurements are limited due to time and cost, whereas the ability to map post-fire and seismic line impacts for more than 150 peatlands would not be easily possible using field methods alone. Moreover, juvenile trees and shrubs were not separated in this study and there was 30% classification error in the tree and shrub classification (in Chapter 3) which might impact vegetation height of conifer and deciduous trees. This study is also limited to the use of morphological and anthropogenic variables, which only explain 54% of the variability, suggesting that the remaining variability is localized (Table 4.4) and needs to be assessed using on-site characteristics and/or more localised thematic information. Moreover, extrinsic drivers such as wind and water inputs into the peatlands were not considered, which can influence site conditions and seedbank availability. To improve this model, localized environmental variables such as peatland hydrological characteristics, soil moisture, and life stage conditions of deciduous and conifer species should be considered in future studies.

## 4.5 CONCLUSION

This study demonstrates the use of multi-spectral lidar for quantifying vegetation recovery adjacent to seismic lines using a fire chronosequence approach. These results suggest that wildland fires improve site conditions for woody vegetation regeneration, especially deciduous shrubs and trees adjacent to seismic lines in the years following fire in peatlands. However, once seismic lines have been constructed through peatlands, we find no significant differences in vegetation structures as distance from seismic lines increase. This could indicate that seismic lines have lasting effects on peatlands, not only within seismic lines, but also across the broader peatland as a whole. Also, peatland morphological/ environmental and anthropogenic components explained 54% of the variability, with little difference between 30 YSF and 38 YSF. However, PCA identifies and groups broad ecosystem changes between peatlands within the fire chronosequence. This suggests that peatlands with seismic lines in later year succession might be impacted by other more localised factors such as warming and peatland abiotic conditions. In addition, shrubby and open peatlands that are burned are more prone to seismic line impacts and can regenerate more rapidly compared to treed peatlands. Therefore, greater burn severity might further mitigate the impacts of seismic lines in peatlands, especially seismic lines that are older.

## Chapter 5: CONCLUSIONS

### 5.1 Summary of research

This research aimed to assess the cumulative impacts of wildland fire, seismic lines, and climate change on peatlands in northern Alberta, using a chronosequence approach. It was motivated by the need to understand how peatland ecosystems recover post disturbance and how wildland fires affect seismic lines regeneration.

The first objective used airborne lidar data to determine how wildland fire affects the regeneration trajectory of conifer vs. deciduous shrub/tree communities in seismic line-disturbed and burned/ unburned peatlands using space-for-time-chronosequence of 5 years, 18 years, 30 years, 38 years since fire (YSF), along with recently unburned peatlands. Our results suggest that using lidar-derived structural metrics in combination with field data allowed us to predict areas of deciduous shrub establishment with 96% accuracy and to identify deciduous trees and conifers with 74% accuracy. Canopy structural, laser pulse intensity, and topographic variables were important for discriminating between conifers and deciduous shrub/trees. Within the fire chronosequence we showed that burned bogs and fens were more prone to shrub regeneration up to and including 38 years after the fire.

The second objective examined the combined effects of fire and seismic line fragmentation to answer the question of whether wildland fires that burn over seismic lines in peatlands result in regeneration of woody vegetation adjacent to seismic lines compared to peatlands fragmented by seismic lines only. Our findings showed that areas adjacent to seismic lines had greater deciduous shrub regeneration in the early years post-

fire, and taller deciduous trees were found in more mature post-fire peatlands (30 to 38 YSF). This suggests that secondary succession via wildland fires promote woody vegetation regeneration adjacent to seismic lines compared to peatlands fragmented by seismic lines alone. Fens were more sensitive to changes in ecohydrology due to flattening of peatland microtopography and had less woody vegetation regeneration adjacent to seismic lines compared to bogs. Post-fire and post seismic line succession were largely driven by incoming solar radiation and seismic line age.

Hence, using a fire chronosequence approach we were able to quantify changes in vegetation structure over time by measuring changes in deciduous vs conifer vegetation. The increased shrubification of peatlands in response to climate mediated drying and anthropogenic disturbances may alter the vegetation structure and composition in peatlands. However, wildland fires over seismic lines can improve conditions adjacent to these lines for tree recruitment, seismic lines continue to leave an ecological footprint, particularly in fens, which is difficult to restore naturally. Thus, seismic lines remained visible after 38 years after fire.

## **5.2 Recommendations and future directions**

This research showed that seismic lines have long-term effects on peatlands, particularly fens. Hence, we recommend that the development of seismic lines should be avoided in fens, including limiting the construction and use of conventional as well as low impact seismic lines. Mounding (defined as a technique to create mounds by digging holes and filling it with soil) can be used as a restoration technique to create elevated



microsites (resembling hummocks) that have increased depth to water table and improve growing conditions for revegetation (Dabros et al., 2018).

For future research, the field methodology needs to be improved. Here, field data were only collected in transects along seismic lines. This could be improved by using vegetation plots perpendicular to seismic lines along peatlands, which would provide more detail about vegetation structure as these changes with distance from the edge of the seismic line, similar to what was measured using lidar. Also, peatland microtopography plays an important role in determining the recovery of seismic lines and can be quantified using high-precision hydrostatic altimeters, which measure sub-centimeter changes in elevation (Stevenson et al., 2019). Other abiotic factors such as wind, air temperature, and soil moisture should also be measured as it influences vegetation regeneration.

## REFERENCES

- Abib, T. H., Chasmer, L., Hopkinson, C., Mahoney, C., and Rodriguez, L. C. E. 2019. Seismic line impacts on proximal boreal forest and wetland environments in Alberta. *Sci Total Environ*, 658, 1601-1613. <https://doi.org/10.1016/j.scitotenv.2018.12.244>
- ABMI. 2019. Human Footprint Inventory enhanced (HFIE) for the Oil Sands Region: Wall-to-Wall Human Footprint Inventory enhanced for the Oil Sands Region. Edmonton, AB: Alberta Biodiversity Monitoring Institute and Alberta Human Footprint Monitoring Program, Retrived March 24, 2021 from <https://abmi.ca/home/data-analytics/da-top/da-product-overview/Data-Archive/Land-Cover.html>
- Agrawal, S., and Khairnar, G. B. 2019. A comparative assessment of remote sensing imaging techniques: Optical, SAR and Lidar. *The International Archives of the Photogrammetry, XLII-5-W3*, 1-6. <https://doi.org/10.5194/isprs-archives-XLII-5-W3-1-2019>
- Akagi, S. K., Yokelson, R. J., Wiedinmyer, C., Alvarado, M. J., Reid, J. S., Karl, T., Crounse, J. D., and Wennberg, P. O. 2011. Emission factors for open and domestic biomass burning for use in atmospheric models. *Atmospheric Chemistry and Physics*, 11(9), 4039-4072. <https://doi.org/10.5194/acp-11-4039-2011>
- Alberta Energy Regulator. 2021. Active In Situ Scheme Approval Well List. Retrived August 20, 2021 from <https://www.aer.ca/providing-information/data-and-reports/activity-and-data/active-in-situ-scheme-approval-well-list>
- Alberta Parks. 2015. Natural Regions and Subregions of Alberta. A Framework for Alberta's Parks. Alberta Tourism, Parks and Recreation. Edmonton, Alberta. Retrieved March 26, 2021 from <https://www.albertaparks.ca/media/6256258/natural-regions-subregions-of-alberta-a-framework-for-albertas-parks-booklet.pdf>
- Alberta Wildfire. 2019. Spatial wildfire data. Retrived March 26, 2021 from <http://wildfire.alberta.ca/resources/historical-data/spatial-wildfire-data.aspx>
- Alexander, H. D., Mack, M. C., Goetz, S., Beck, P. S. A., and Belshe, E. F. 2012. Implications of increased deciduous cover on stand structure and aboveground carbon pools of Alaskan boreal forests. *Ecosphere*, 3(5), art45-21. <https://doi.org/10.1890/ES11-00364.1>
- Alonzo, M., Morton, D. C., Cook, B. D., Andersen, H., Babcock, C., and Pattison, R. 2017. Patterns of canopy and surface layer consumption in a boreal forest fire from repeat airborne lidar. *Environmental Research Letters*, 12(6), 65004.
- Amiro, B. D., Ian MacPherson, J., Desjardins, R. L., Chen, J. M., and Liu, J. 2003. Post-fire carbon dioxide fluxes in the western Canadian boreal forest: Evidence from

- towers, aircraft and remote sensing. *Agricultural and Forest Meteorology*, 115(1), 91-107. [https://doi.org/10.1016/S0168-1923\(02\)00170-3](https://doi.org/10.1016/S0168-1923(02)00170-3)
- Amiro, B. D., Todd, J. B., Wotton, B. M., Logan, K. A., Flannigan, M. D., Stocks, B. J., Mason, J. A., Martell, D. L., and Hirsch, K. G. 2001. Direct carbon emissions from Canadian forest fires, 1959-1999. *Canadian Journal of Forest Research*, 31(3), 512-525. <https://doi.org/10.1139/cjfr-31-3-512>
- ArcGIS Pro. 2020. How Forest-based Classification and Regression works. Retrived April 1, 2021 from <https://pro.arcgis.com/en/pro-app/latest/tool-reference/spatial-statistics/how-forest-works.htm>
- Barber, Q. E., Bater, C. W., Dabros, A., Pinzon, J., Nielsen, S. E., and Parisien, M. A. 2021. Persistent impact of conventional seismic lines on boreal vegetation structure following wildfire. *Canadian Journal of Forest Research*. [ in press]
- Beck, P. S. A., Goetz, S. J., Mack, M. C., Alexander, H. D., Jin, Y., Randerson, J. T., and Loranty, M. M. 2011. The impacts and implications of an intensifying fire regime on Alaskan boreal forest composition and albedo. *Global Change Biology*, 17(9), 2853-2866. <https://doi.org/10.1111/j.1365-2486.2011.02412.x>
- Benscoter, B. W., Greenacre, D., and Turetsky, M. R. 2015. Wildfire as a key determinant of peatland microtopography. *Canadian Journal of Forest Research*, 45(8), 1132-1136. doi:10.1139/cjfr-2015-0028
- Benscoter, B. W., Kelman Wieder, R., and Vitt, D. H. 2005. Linking microtopography with post-fire succession in bogs. *Journal of Vegetation Science*, 16(4), 453-460. <https://doi.org/10.1111/j.1654-1103.2005.tb02385.x>
- Benscoter, B., Thompson, D., Waddington, J., Flannigan, M., Wotton, B., De Groot, W., and Turetsky, M. 2011. Interactive effects of vegetation, soil moisture and bulk density on depth of burning of thick organic soils. *International Journal of Wildland Fire*, 20(3), 418-429.
- Belgiu, M., and Drăguț, L. 2016. Random forest in remote sensing: A review of applications and future directions. *ISPRS Journal of Photogrammetry and Remote Sensing*, 114, 24-31. <https://doi.org/10.1016/j.isprsjprs.2016.01.011>
- Beven, K.J. and M.J. Kirkby. 1979. A physically based, variable contributing area model of basin hydrology. *Hydrological Sciences Journal* 24:43–69.
- Bolton, D. K., Coops, N. C., Hermosilla, T., Wulder, M. A., and White, J. C. 2017. Assessing variability in post-fire forest structure along gradients of productivity in the Canadian boreal using multi-source remote sensing. *Journal of Biogeography*, 44(6), 1294-1305. <https://doi.org/10.1111/jbi.12947>
- Bolton, D. K., Coops, N. C., and Wulder, M. A. 2013. Measuring forest structure along productivity gradients in the Canadian boreal with small-footprint Lidar.

*Environmental monitoring and assessment*, 185(8), 6617-6634.  
<https://doi.org/10.1007/s10661-012-3051-9>

- Bolton, D. K., Coops, N. C., and Wulder, M. A. 2015. Characterizing residual structure and forest recovery following high-severity fire in the western boreal of Canada using Landsat time-series and airborne lidar data. *Remote Sensing of Environment*, 163, 48-60. <https://doi.org/10.1016/j.rse.2015.03.004>
- Bonan, G. B., and Shugart, H. H. 1989. Environmental Factors and Ecological Processes in Boreal Forests. *Annual review of ecology and systematics*, 20(1), 1-28. <https://doi.org/10.1146/annurev.es.20.110189.000245>
- Boucher, D., Gauthier, S., and Grandpré, L. D. 2006. Structural changes in coniferous stands along a chronosequence and a productivity gradient in the northeastern boreal forest of Québec. *Écoscience*, 13(2), 172-180. <https://doi.org/10.2980/i1195-6860-13-2-172.1>
- Boutin, C., and Carpenter, D. 2017. Assessment of wetland/upland vegetation communities and evaluation of soil-plant contamination by polycyclic aromatic hydrocarbons and trace metals in regions near oil sands mining in Alberta. *Science of The Total Environment*, 576, 829-839. doi: 10.1016/j.scitotenv.2016.10.062
- Braverman, M., and Quinton, W. L. 2016. Hydrological impacts of seismic lines in the wetland-dominated zone of thawing, discontinuous permafrost, Northwest Territories, Canada. *Hydrological Processes*, 30(15), 2617-2627. <https://doi.org/10.1002/hyp.10695>
- Breiman, L. 2001. Random forests. *Machine Learning*, 45(1), 5-32. <https://doi.org/10.1023/A:1010933404324>
- Bridgman, S. D., J. Pastor, B. Dewey, J. F. Weltzin, and K. Updegraff. 2008. Rapid carbon response of peatlands to climate change, *Ecology*, 89(11), 3041-3048, doi:10.1890/08-0279.1.
- Brown, James K.; Smith, Jane Kapler, eds. 2000. Wildland fire in ecosystems: effects of fire on flora. Gen.Tech. Rep. RMRS-GTR-42-vol. 2. Ogden, UT: U.S. Department of Agriculture, Forest Service, Rocky Mountain Research Station. 257 p.
- Brubaker, K. M., Johnson, Q. K., and Kaye, M. W. 2018. Spatial patterns of tree and shrub biomass in a deciduous forest using leaf-off and leaf-on lidar. *Canadian Journal of Forest Research*, 48(9), 1020-1033. doi:10.1139/cjfr-2018-0033
- Bu, Z.-J., Zheng, X.-X., Rydin, H., Moore, T., Ma, J., 2013. Facilitation vs. competition: Does interspecific interaction affect drought responses in Sphagnum? *Basic Appl. Ecol.* 14 (7), 574-584. <https://doi.org/10.1016/j.baae.2013.08.002>

- Bubier, J. L., Rock, B. N., and Crill, P. M. 1997. Spectral reflectance measurements of boreal wetland and forest mosses. *Journal of Geophysical Research: Atmospheres*, 102(D24), 29483-29494. <https://doi.org/10.1029/97JD02316>
- Budei, B. C., St-Onge, B., Hopkinson, C., and Audet, F.A. 2018. Identifying the genus or species of individual trees using a three-wavelength airborne lidar system. *Remote Sensing of Environment*, 204, 632-647. <https://doi.org/10.1016/j.rse.2017.09.037>
- Burton, P.J., Parisien, M. A., Hicke, J. A., Hall, R. J., and Freeburn, J. T. 2008. Large fires as agents of ecological diversity in the North American boreal forest. *International Journal of Wildland Fire* 17, 754–67.
- Bush, E. and Lemmen, D.S. 2019. Canada’s Changing Climate Report; Government of Canada, Ottawa, ON. 444 p. [https://changingclimate.ca/site/assets/uploads/sites/2/2020/06/CCCR\\_FULLREPORT-EN-FINAL.pdf](https://changingclimate.ca/site/assets/uploads/sites/2/2020/06/CCCR_FULLREPORT-EN-FINAL.pdf)
- Camill, P., Barry, A., Williams, E., Andreassi, C., Limmer, J., and Solick, D. 2009. Climate-vegetation-fire interactions and their impact on long-term carbon dynamics in a boreal peatland landscape in northern Manitoba, Canada. *Journal of Geophysical Research*, 114(G4). <https://doi.org/10.1029/2009jg001071>
- Campbell, J., E., Fenton, M., M., and Pawlowicz, J., G. 2006. Surficial geology of the Pelican lake area (NTS83P). Retrived March 23, 2021 from <https://ags.aer.ca/publication/dig-2002-0017>
- Canadian Councils of Resource Ministers. 2014. Boreal Plains Ecozone+ evidence for key findings summary. Canadian biodiversity: Ecosystem status and trends 2010. Evidence for key findings summary report No. 12. Ottawa, ON. ix + 106 p. <http://www.biodivcanada.ca/default.asp?lang=En&n=137E1147-1>
- Caners, R. T., Crisfield, V., and Lieffers, V. J. 2019. Habitat heterogeneity stimulates regeneration of bryophytes and vascular plants on disturbed minerotrophic peatlands. *Canadian Journal of Forest Research*, 49(3), 281-295. <https://doi.org/10.1139/cjfr-2018-0426>
- Chasmer, L., Cobbaert, D., Mahoney, C., Millard, K., Peters, D., Devito, K., Brisco, B., Hopkinson, C., Merchant, M., Montgomery, J., Nelson, K., and Niemann, O. 2020a. Remote Sensing of Boreal Wetlands 1: Data Use for Policy and Management. *Remote Sensing*, 12(8). <https://doi.org/10.3390/rs12081320>
- Chasmer, L., and Hopkinson, C. 2017. Threshold loss of discontinuous permafrost and landscape evolution. *Glob Chang Biol*, 23(7), 2672-2686. <https://doi.org/10.1111/gcb.13537>
- Chasmer, L., Lima, E. M., Mahoney, C., Hopkinson, C., Montgomery, J., and Cobbaert, D. 2021. Shrub changes with proximity to anthropogenic disturbance in boreal wetlands determined using bi-temporal airborne lidar in the oil sands region,

Alberta Canada. *The Science of the Total Environment*, 780, 146638-146638.  
<https://doi.org/10.1016/j.scitotenv.2021.146638>

- Chasmer, L., Mahoney, C., Millard, K., Nelson, K., Peters, D., Merchant, M., Hopkinson, C., Brisco, B., Niemann, O., Montgomery, J., Devito, K., and Cobbaert, D. 2020b. Remote sensing of boreal wetlands 2: Methods for evaluating boreal wetland ecosystem state and drivers of change. *Remote Sensing (Basel, Switzerland)*, 12(8), 1321. <https://doi.org/10.3390/rs12081321>
- Chen, S., McDermid, G., Castilla, G., and Linke, J. 2017. Measuring vegetation height in linear disturbances in the boreal forest with UAV photogrammetry. *Remote Sensing (Basel, Switzerland)*, 9(12), 1257. <https://doi.org/10.3390/rs9121257>
- Chen, H. Y., and Popadiouk, R. V. 2002. Dynamics of North American boreal mixedwoods. *Environmental Reviews*, 10(3), 137-166.  
<https://doi.org/10.1139/a02-007>
- Cheng, C. S., Auld, H., Li, Q., and Li, G. 2012. Possible impacts of climate change on extreme weather events at local scale in south-central Canada. *Climatic Change*, 112(3), 963-979. <https://doi.org/10.1007/s10584-011-0252-0>
- Clymo, R. S. 1984. The limits to peat bog growth. *Philosophical transactions of the Royal Society of London. Series B, Biological sciences*, 303(1117), 605-654.  
<https://doi.org/10.1098/rstb.1984.0002>
- Coop, J. D., Parks, S. A., Stevens-Rumann, C. S., Crausbay, S. D., Higuera, P. E., Hurteau, M. D., Tepley, A., Whitman, E., Assal, T., Collins, B. M., Davis, K. T., Dobrowski, S., Falk, D. A., Fornwalt, P. J., Fulé, P. Z., Harvey, B. J., Kane, V. R., Littlefield, C. E., Margolis, E. Q., North, M., Parisien, M.-A., Prichard, S., & Rodman, K. C. (2020). Wildfire-driven forest conversion in western North American landscapes. *Bioscience*, 70(8), 659-673.  
<https://doi.org/10.1093/biosci/biaa061>
- Dabros, A., Higgins, K. L., and Pinzon, J. 2021. Seismic line edge effects on plants, lichens and their environmental conditions in boreal peatlands of northwest Alberta (Canada). *Restoration Ecology*, <https://doi.org/10.1111/rec.13468>
- Dabros, A., James Hammond, H.E., Pinzon, J., Pinno, B., and Langor, D. 2017. Edge influence of low impact seismic lines for oil exploration on upland forest vegetation in northern Alberta (Canada). *Forest Ecology and Management*, 400, 278-288. <https://doi.org/10.1016/j.foreco.2017.06.030>
- Dabros, A., Pyper, M., and Castilla, G. 2018. Seismic lines in the boreal and arctic ecosystems of North America: environmental impacts, challenges, and opportunities. *Environmental Reviews*, 26(2), 214-229. <https://doi.org/10.1139/er-2017-0080>



- Davidson, S. J., Goud, E. M., Goud, E. M., Franklin, C., Nielsen, S. E., and Strack, M. 2020. Seismic Line Disturbance Alters Soil Physical and Chemical Properties Across Boreal Forest and Peatland Soils. *Frontiers in earth science (Lausanne)*, 8. <https://doi.org/10.3389/feart.2020.00281>
- Davidson, S. J., Goud, E. M., Malhotra, A., Estey, C. O., Korsah, P., and Strack, M. 2021. Linear disturbances shift boreal peatland plant communities toward earlier peak greenness. *Journal of Geophysical Research: Biogeosciences*, 126, e2021JG006403. <https://doi.org/10.1029/2021JG006403>
- Davidson, S. J., Van Beest, C., Petrone, R., and Strack, M. 2019. Wildfire overrides hydrological controls on boreal peatland methane emissions. *Biogeosciences*, 16(13), 2651-2660. <https://doi.org/10.5194/bg-16-2651-2019>
- Day, N. J., White, A. L., Johnstone, J. F., Degré-Timmons, G. É., Cumming, S. G., Mack, M. C., Turetsky, M. R., Walker, X. J., and Baltzer, J. L. 2020. Fire characteristics and environmental conditions shape plant communities via regeneration strategy. *Ecography (Copenhagen)*, 43(10), 1464-1474. <https://doi.org/10.1111/ecog.05211>
- de Groot, W. J., Flannigan, M. D., and Cantin, A. S. 2013. Climate change impacts on future boreal fire regimes. *Forest Ecology and Management*, 294, 35-44. <https://doi.org/10.1016/j.foreco.2012.09.027>
- Devito, K. J., Creed, I. F., Fraser, C. J. D. 2005. Controls on runoff from a partially harvested aspen-forested headwater catchment, Boreal Plain, Canada. *Hydrological Processes* 19, 3–25.
- Devito, K. J., Hokanson, K. J., Moore, P. A., Kettridge, N., Anderson, A. E., Chasmer, L., Hopkinson, C., Lukenbach, M. C., Mendoza, C. A., Morissette, J., Peters, D. L., Petrone, R. M., Silins, U., Smerdon, B., and Waddington, J. M. 2017. Landscape controls on long-term runoff in subhumid heterogeneous boreal plains catchments. *Hydrological Processes*, 31(15), 2737-2751. <https://doi.org/10.1002/hyp.11213>
- Dieleman, C. M., Branfireun, B. A., McLaughlin, J. W., and Lindo, Z. 2015. Climate change drives a shift in peatland ecosystem plant community: implications for ecosystem function and stability. *Glob Chang Biol*, 21(1), 388-395. <https://doi.org/10.1111/gcb.12643>
- Dietmaier, A., McDermid, G. J., Rahman, M. M., Linke, J., and Ludwig, R. 2019. Comparison of lidar and digital aerial photogrammetry for characterizing canopy openings in the boreal forest of northern Alberta. *Remote Sensing*, 11(16). doi:10.3390/rs11161919
- Ducks Unlimited Canada. 2015. Field Guide of Boreal Wetland Classes in the Boreal Plains Ecozone of Canada. Retrived May 15, 2020 from

<https://www.ducks.ca/resources/industry/field-guide-of-boreal-wetland-classes-in-the-boreal-plains-ecozone-of-canada/>

- Elmes, M. C., Thompson, D. K., Sherwood, J. H., and Price, J. S. 2018. Hydrometeorological conditions preceding wildfire, and the subsequent burning of a fen watershed in Fort McMurray, Alberta, Canada. *Natural Hazards and Earth System Sciences*, 18(1), 157-170. <https://doi.org/10.5194/nhess-18-157-2018>
- Falkowski, M. J., Evans, J. S., Martinuzzi, S., Gessler, P. E., and Hudak, A. T. 2009. Characterizing forest succession with lidar data: An evaluation for the inland northwest, USA. *Remote Sensing of Environment*, 113(5), 946-956. doi:10.1016/j.rse.2009.01.003
- Ficken, C. D., Cobbaert, D., and Rooney, R. C. 2019. Low extent but high impact of human land use on wetland flora across the boreal oil sands region. *The Science of the Total Environment*, 693, 133647-133647. <https://doi.org/10.1016/j.scitotenv.2019.133647>
- Ficken, C. D., Connor, S. J., Rooney, R., and Cobbaert, D. 2021. Drivers, pressures, and state responses to inform long-term oil sands wetland monitoring program objectives. *Wetlands Ecology and Management*, <https://doi.org/10.1007/s11273-021-09828-2>
- Filicetti, A. T., and Nielsen, S. E. 2018. Fire and forest recovery on seismic lines in sandy upland jack pine (*Pinus banksiana*) forests. *Forest Ecology and Management*, 421, 32-39. <https://doi.org/10.1016/j.foreco.2018.01.027>
- Filicetti, A. T., and Nielsen, S. E. 2020. Tree regeneration on industrial linear disturbances in treed peatlands is hastened by wildfire and delayed by loss of microtopography. *Canadian Journal of Forest Research*, 50(9), 936-945. <https://doi.org/10.1139/cjfr-2019-0451>
- Finnegan, L., Pigeon, K. E., and MacNearney, D. 2019. Predicting patterns of vegetation recovery on seismic lines: Informing restoration based on understory species composition and growth. *Forest Ecology and Management*, 446, 175-192. <https://doi.org/10.1016/j.foreco.2019.05.026>
- Flannigan, M., Stocks, B., Turetsky, M., and Wotton, M. 2009. Impacts of climate change on fire activity and fire management in the circumboreal forest. *Global Change Biology*, 15(3), 549-560.
- Flannigan, M. D., Stocks, B. J., and Wotton, B. M. 2000. Climate change and forest fires. *Science of the Total Environment*, 262(3), 221-229. doi:10.1016/S0048-9697(00)00524-6
- Flannigan, M. D., Wotton, B. M., Marshall, G. A., de Groot, W. J., Johnston, J., Jurko, N., and Cantin, A. S. 2015. Fuel moisture sensitivity to temperature and



- precipitation: Climate change implications. *Climatic Change*, 134(1-2), 59-71. doi:10.1007/s10584-015-1521-0
- Foote, L. 2012. Threshold considerations and wetland reclamation in Alberta's mineable oil sands. *Ecology and Society*, 17(1), 35
- Giardino, C., Bresciani, M., Valentini, E., Gasperini, L., Bolpagni, R., and Brando, V. E. 2015. Airborne hyperspectral data to assess suspended particulate matter and aquatic vegetation in a shallow and turbid lake. *Remote Sensing of Environment*, 157, 48-57. <https://doi.org/10.1016/j.rse.2014.04.034>
- Gibson, C. M., Turetsky, M. R., Cottenie, K., Kane, E. S., Houle, G., and Kasischke, E. S. 2016. Variation in plant community composition and vegetation carbon pools a decade following a severe fire season in interior Alaska. *Journal of Vegetation Science*, 27(6), 1187-1197. <https://doi.org/10.1111/jvs.12443>
- Gignac, L.D., and Dale, M.R.T., 2007. Effects of size, shape, and edge on vegetation in remnants of the upland boreal mixed-wood forest in agro-environments of Alberta, Canada. *Can. J. Bot.* 85, 273–284. <https://doi.org/10.1139/B07-018>.
- Gorham, E. 1991. Northern peatlands: Role in the carbon cycle and probable responses to climatic warming, *Ecol. Appl.*, 1, 182–195.
- Government of Alberta. 2015. Alberta Wetland Classification System. Retrieved July 11, 2020 from <https://open.alberta.ca/publications/9781460122587>
- Government of Alberta. 2020. Current and historical Alberta weather station data viewer. Retrived July 10, 2021 from <https://acis.alberta.ca/weather-data-viewer.jsp>
- Government of Alberta. 2021. The Alberta Human Footprint Monitoring Program (AHFMP) – A Historical Overview of Geophysical Exploration in Alberta. Retrived Aug 5, 2021 from <https://open.alberta.ca/dataset/615e27ef-89c7-4245-a299-a868eb3f0a36/resource/a0419862-603d-467a-91ae-a42000c7a218/download/aep-ahfmp-historical-overview-geophysical-exploration-2021-07.pdf>
- Group, N.W.W. 1997. *The Canadian Wetland Classification System*, 2nd ed.; Wetlands Research Centre, University of Waterloo: Waterloo, ON, Canada.
- Hanes, C. C., Wang, X., Jain, P., Parisien, M., Little, J. M., and Flannigan, M. D. 2019. Fire-regime changes in Canada over the last half century. *Canadian Journal of Forest Research*, 49(3), 256-269. <https://doi.org/10.1139/cjfr-2018-0293>
- Harper, K. A., Bergeron, Y., Drapeau, P., Gauthier, S., and De Grandpré, L. 2005. Structural development following fire in black spruce boreal forest. *Forest Ecology and Management*, 206(1), 293-306. <https://doi.org/10.1016/j.foreco.2004.11.008>

- Hawkins, E., Ortega, P., Suckling, E., Schurer, A., Hegerl, G., Jones, P., Joshi, M., Osborn, T. J., Masson-Delmotte, V., Mignot, J., Thorne, P., and van Oldenborgh, G. J. 2017. Estimating changes in global temperature since the preindustrial period. *Bulletin of the American Meteorological Society*, 98(9), 1841-1856. <https://doi.org/10.1175/BAMS-D-16-0007.1>
- Helbig, M., Chasmer, L. E., Desai, A. R., Kljun, N., Quinton, W. L., and Sonnentag, O. 2017. Direct and indirect climate change effects on carbon dioxide fluxes in a thawing boreal forest–wetland landscape. *Global Change Biology*, 23(8), 3231-3248
- Hokanson, K.J., Lukenbach, M.C., Devito, K.J., Kettridge, N., Petrone, R.M., Waddington, J.M., 2016. Groundwater connectivity controls peat burn severity in the boreal plains: Groundwater controls peat burn severity. *Ecohydrology* 9 (4), 574–584. <https://doi.org/10.1002/eco.1657>.
- Holden, J. 2005. Peatland hydrology and carbon release: Why small-scale process matters. *Philosophical transactions of the Royal Society of London. Series A: Mathematical, physical, and engineering sciences*, 363(1837), 2891-2913. <https://doi.org/10.1098/rsta.2005.1671>
- Holland, P.G., and Steyn, D.G. 1975. Vegetational responses to latitudinal variations in slope angle and aspect. *Journal of Biogeography*, 2, 179–183. <https://doi.org/10.2307/3037989>.
- Hopkinson, C., Chasmer, L., Barr, A. G., Kljun, N., Black, T. A., and McCaughey, J. H. 2016a. Monitoring boreal forest biomass and carbon storage change by integrating airborne laser scanning, biometry and eddy covariance data. *Remote Sensing of Environment*, 181, 82-95. <https://doi.org/10.1016/j.rse.2016.04.010>
- Hopkinson, C., Chasmer, L., Colville, D., Fournier, R. A., Hall, R. J., Luther, J. E., Milne, T., Petrone, R. M., and St-Onge, B. 2013. Moving Toward Consistent ALS Monitoring of Forest Attributes across Canada: A Consortium Approach. *Photogrammetric engineering and remote sensing*, 79(2), 159-173.
- Hopkinson, C., Chasmer, L., Gynan, C., Mahoney, C., and Sitar, M. 2016b. Multisensor and Multispectral LiDAR Characterization and Classification of a Forest Environment. *Canadian Journal of Remote Sensing*, 42(5), 501-520. <https://doi.org/10.1080/07038992.2016.1196584>
- Hopkinson, C., Chasmer, L. E., Sass, G., Creed, I. F., Sitar, M., Kalbfleisch, W., and Treitz, P. 2005. Vegetation class dependent errors in lidar ground elevation and canopy height estimates in a boreal wetland environment. *Canadian Journal of Remote Sensing*, 31(2), 191-206. <https://doi.org/10.5589/m05-007>
- Huete, A. R., and Liu, H. Q. 1994. An error and sensitivity analysis of the atmospheric- and soil-correcting variants of the NDVI for the MODIS-EOS. *IEEE Transactions*

*on Geoscience and Remote Sensing*, 32(4), 897-905. <https://doi.org/10.1109/36.298018>

- Ireson, A. M., Barr, A. G., Johnstone, J. F., Mamet, S. D., van der Kamp, G., Whitfield, C. J., Michel, N. L., North, R. L., Westbrook, C. J., DeBeer, C., Chun, K. P., Nazemi, A., and Sagin, J. 2015. The changing water cycle: The boreal plains ecozone of western Canada. *Wiley Interdisciplinary Reviews. Water*, 2(5), 505-521. <https://doi.org/10.1002/wat2.1098>
- Ingram, H.A.P., 1978. Soil layers in mires: function and terminology. *J. Soil Sci.* 29 (2), 224–227.
- Jean, S. A., Pinno, B. D., and Nielsen, S. E. 2020. Early Regeneration Dynamics of Pure Black Spruce and Aspen Forests after Wildfire in Boreal Alberta, Canada. *Forests*, 11(3). <https://doi.org/10.3390/f11030333>
- Jenness, J. 2006. Topographic Position Index (tpi\_jen.avx) extension for ArcView 3.x, v. 1.3a. Jenness Enterprises. Available at: <http://www.jennessent.com/arcview/tpi.htm>. Kasischke
- Jensen J.R. 2005. Introductory Digital Image Processing: A Remote Sensing Perspective, 3<sup>rd</sup> Ed., Upper Saddle River, Prentice-Hall, 525p.
- Ji, L., Zhang, L., Wylie, B. K., and Rover, J. 2011. On the terminology of the spectral vegetation index (NIR – SWIR)/(NIR + SWIR). *Int. J. Remote Sens.*, 32, 6901-6909
- Jiang, Z., Huete, A. R., Chen, J., Chen, Y., Li, J., Yan, G., and Zhang, X. 2006. Analysis of NDVI and scaled difference vegetation index retrievals of vegetation fraction. *Remote Sensing of Environment*, 101(3), 366-378. <https://doi.org/10.1016/j.rse.2006.01.003>
- Johnston, J., Johnston, L., Wooster, M., Brookes, A., McFayden, C., and Cantin, A. 2018. Satellite detection limitations of sub-canopy smouldering wildfires in the North American boreal forest. *Fire*, 1(2). doi:10.3390/fire1020028
- Johnstone, J. F., and Chapin III, F. S. 2006. Effects of Soil Burn Severity on Post-Fire Tree Recruitment in Boreal Forest. *Ecosystems (New York)*, 9(1), 14-31. <https://doi.org/10.1007/s10021-004-0042-x>
- Johnstone, J. F., Chapin III, F. S., Foote, J., Kemmett, S., Price, K., and Viereck, L. 2004. Decadal observations of tree regeneration following fire in boreal forests. *Canadian Journal of Forest Research*, 34(2), 267-273. <https://doi.org/10.1139/x03-183>
- Jolliffe, I. T. 1990. Principal component analysis: A beginner's guide — I. Introduction and application. *Weather*, 45(10), 375-382. <https://doi.org/10.1002/j.1477-8696.1990.tb05558.x>

- Jones, E., Chasmer, L., Devito, K., Rood, S., and Hopkinson, C. 2021. Hydro-ecological impacts of shortening fire return intervals on regenerating Boreal peatlands and transition zones using integrated in situ sampling and lidar approaches. *Ecohydrology*, [undergoing revisions]
- Jordaan, S. M. 2012. Land and water impacts of oil sands production in alberta. *Environmental Science & Technology*, 46(7), 3611-3617. <https://doi.org/10.1021/es203682m>
- Kashian, D. M., Romme, W. H., Tinker, D. B., Turner, M. G., and Ryan, M. G. 2006. Carbon storage on landscapes with stand-replacing fires. *Bioscience*, 56(7), 598-606. [https://doi.org/10.1641/0006-3568\(2006\)56\[598:CSOLWS\]2.0.CO;2](https://doi.org/10.1641/0006-3568(2006)56[598:CSOLWS]2.0.CO;2)
- Kasischke, E. S., and Turetsky, M. R. 2006. Recent changes in the fire regime across the North American boreal region—Spatial and temporal patterns of burning across Canada and Alaska. *Geophysical Research Letters*, 33(9), L09703-n/a. <https://doi.org/10.1029/2006GL025677>
- Keeley, J., E. 2009. Fire intensity, fire severity and burn severity: a brief review and suggested usage. *International Journal of Wildland Fire*, 18, 116-126. <https://doi.org/10.1071/WF07049>
- Kettridge, N., Lukenbach, M. C., Hokanson, K. J., Hopkinson, C., Devito, K. J., Petrone, R. M., Mendoza, C. A., and Waddington, J. M. 2017. Low Evapotranspiration Enhances the Resilience of Peatland Carbon Stocks to Fire. *Geophysical Research Letters*, 44(18), 9341-9349. <https://doi.org/10.1002/2017gl074186>
- Kettridge, N., Turetsky, M. R., Sherwood, J. H., Thompson, D. K., Miller, C. A., Benscoter, B. W., Flannigan, M. D., Wotton, B. M., and Waddington, J. M. 2015. Moderate drop in water table increases peatland vulnerability to post-fire regime shift. *Sci Rep*, 5, 8063. <https://doi.org/10.1038/srep08063>
- Kimmel, K., and Mander, Ü. 2010. Ecosystem services of peatlands: Implications for restoration. *Progress in Physical Geography*, 34(4), 491-514. <https://doi.org/10.1177/0309133310365595>
- Kits, G. J. 2017. Good for the economy? an ecological economics approach to analyzing Alberta's bitumen industry. *Ecological Economics*, 139, 68-74. <https://doi.org/10.1016/j.ecolecon.2017.04.020>
- Kuhry, P., B. J. Nicholson, L. D. Gignac, D. H. Vitt, and S. E. Bayley 1993. Development of Sphagnum-dominated peatlands in boreal continental Canada. *Can. J. Bot.*, 71(1), 10–22, doi:10.1139/b93-002
- Lee, P., and Boutin, S. 2006. Persistence and developmental transition of wide seismic lines in the western Boreal Plains of Canada. *J Environ Manage*, 78(3), 240-250

- Lenton, T. M., Held, H., Kriegler, E., Hall, J. W., Lucht, W., Rahmstorf, S., and Schellnhuber, H. J. 2008. Tipping elements in the earth's climate system. *Proceedings of the National Academy of Sciences - PNAS*, 105(6), 1786-1793. <https://doi.org/10.1073/pnas.0705414105>
- Li, J., Hu, B., and Noland, T. L. 2013. Classification of tree species based on structural features derived from high density LiDAR data. *Agricultural and Forest Meteorology*, 171-172, 104-114. <https://doi.org/10.1016/j.agrformet.2012.11.012>
- Lieffers, V. J., Caners, R. T., and Ge, H. 2017. Re-establishment of hummock topography promotes tree regeneration on highly disturbed moderate-rich fens. *J Environ Manage*, 197, 258-264. <https://doi.org/10.1016/j.jenvman.2017.04.002>
- Lim, K., P. Treitz, M.A. Wulder, B. St-Onge, and M. Flood. 2003. LiDAR remote-sensing of forest structure. *Progress in Physical Geography*, 27, 88–106
- Liu, R. X., Kuang, J., Gong, Q., and Hou, X. L. 2003. Principal component regression analysis with spss. *Computer Methods and Programs in Biomedicine*, 71(2), 141-147. [https://doi.org/10.1016/S0169-2607\(02\)00058-5](https://doi.org/10.1016/S0169-2607(02)00058-5)
- Lovitt, J., Rahman, M. M., Saraswati, S., McDermid, G. J., Strack, M., and Xu, B. 2018. UAV Remote Sensing Can Reveal the Effects of Low-Impact Seismic Lines on Surface Morphology, Hydrology, and Methane (CH<sub>4</sub>) Release in a Boreal Treed Bog. *Journal of Geophysical Research: Biogeosciences*, 123(3), 1117-1129.
- Lukenbach, M. C., Devito, K. J., Kettridge, N., Petrone, R. M., and Waddington, J. M. 2016. Burn severity alters peatland moss water availability: implications for post-fire recovery. *Ecohydrology*, 9(2), 341-353. <https://doi.org/10.1002/eco.1639>
- Lukenbach, M. C., Hokanson, K. J., Devito, K. J., Kettridge, N., Petrone, R. M., Mendoza, C. A., Granath, G., Waddington, J. M., and Sveriges lantbruksuniversitet. 2017. Post-fire ecohydrological conditions at peatland margins in different hydrogeological settings of the boreal plain. *Journal of Hydrology (Amsterdam)*, 548, 741-753. <https://doi.org/10.1016/j.jhydrol.2017.03.034>
- Lyon, J. and J. McCarthy. 1995. *Wetland and Environmental Applications of GIS*. Lewis Publishers, New York.
- McCarley, T. R., Hudak, A. T., Sparks, A. M., Vaillant, N. M., Meddens, A. J. H., Trader, L., Mauro, F., Kreitler, J., and Boschetti, L. 2020. Estimating wildfire fuel consumption with multitemporal airborne laser scanning data and demonstrating linkage with MODIS-derived fire radiative energy. *Remote Sensing of Environment*, 251. <https://doi.org/10.1016/j.rse.2020.112114>
- McCarley, T. R., Kolden, C. A., Vaillant, N. M., Hudak, A. T., Smith, A. M. S., Wing, B. M., . . . and Kreitler, J. 2017. Multi-temporal lidar and Landsat quantification of

- fire-induced changes to forest structure. *Remote Sensing of Environment*, 191, 419-432. doi:10.1016/j.rse.2016.12.022
- Méndez-Toribio, M., Meave, J.A., Zermeño-Hernández, I., and Ibarra-Manríquez, G. 2016. Effects of slope aspect and topographic position on environmental variables, disturbance regime and tree community attributes in a seasonal tropical dry forest. *J. Veg. Sci.* 27, 1094–1103. <https://doi.org/10.1111/jvs.12455>.
- Menze, B. H., Kelm, B. M., Masuch, R., Himmelreich, U., Bachert, P., Petrich, W., and Hamprecht, F. A. 2009. A comparison of random forest and its gini importance with standard chemometric methods for the feature selection and classification of spectral data. *BMC Bioinformatics*, 10(1), 213-213. <https://doi.org/10.1186/1471-2105-10-213>
- Millard, K., and Richardson, M. 2018. Quantifying the relative contributions of vegetation and soil moisture conditions to polarimetric C-Band SAR response in a temperate peatland. *Remote Sensing of Environment*, 206, 123-138. <https://doi.org/10.1016/j.rse.2017.12.011>
- Morison, M., Beest, C., Macrae, M., Nwaishi, F., and Petrone, R. 2021. Deeper burning in a boreal fen peatland 1-year post-wildfire accelerates recovery trajectory of carbon dioxide uptake. *Ecohydrology*, 14(3). <https://doi.org/10.1002/eco.2277>
- Montgomery, J., Brisco, B., Chasmer, L., Devito, K., Cobbaert, D., Hopkinson, C., 2019. SAR and Lidar Temporal Data Fusion Approaches to Boreal Wetland Ecosystem Monitoring. *Remote Sensing* 11, 161. doi:10.3390/rs11020161
- Mwale, D., Gan, T. Y., Devito, K., Mendoza, C., Silins, U., and Petrone, R. 2009. Precipitation variability and its relationship to hydrologic variability in Alberta. *Hydrological Processes*, 23(21), 3040-3056. <https://doi.org/10.1002/hyp.7415>
- Natural Resources Canada. 2017. The State of Canada's Forests. Annual Report 2017. Canadian Forest Service, Ottawa. 92. Retrieved May 30, 2020 from <https://cfs.nrcan.gc.ca/publications/download-pdf/38871>
- Nelson, K., Thompson, D., Hopkinson, C., Petrone, R., and Chasmer, L. 2021. Peatland-fire interactions: A review of wildland fire feedbacks and interactions in Canadian boreal peatlands. *Sci Total Environ*, 769, 145212. <https://doi.org/10.1016/j.scitotenv.2021.145212>
- Nunez, S., Arets, E., Alkemade, R., Verwer, C., and Leemans, R. 2019. Assessing the impacts of climate change on biodiversity: is below 2 °C enough? *Climatic Change*, 154(3-4), 351-365. <https://doi.org/10.1007/s10584-019-02420-x>
- Nwaishi, F., Petrone, R. M., Macrae, M. L., Price, J. S., Strack, M., and Andersen, R. 2016. Preliminary assessment of greenhouse gas emissions from a constructed fen on post-mining landscape in the Athabasca oil sands region, Alberta, Canada. *Ecological Engineering*, 95, 119-128.



- Ørka, H. O., Næsset, E., and Bollandsås, O. M. 2010. Effects of different sensors and leaf-on and leaf-off canopy conditions on echo distributions and individual tree properties derived from airborne laser scanning. *Remote Sensing of Environment*, 114(7), 1445-1461. <https://doi.org/10.1016/j.rse.2010.01.024>
- Paul Dana, L., Brent Anderson, R., and Meis-Mason, A. 2009. A study of the impact of oil and gas development on the dene first nations of the sahtu (great bear lake) region of the canadian northwest territories (NWT). *Journal of Enterprising Communities.*, 3(1), 94-117. <https://doi.org/10.1108/17506200910943706>
- Price, D. T., Alfaro, R. I., Brown, K. J., Flannigan, M. D., Fleming, R. A., Hogg, E. H., Girardin, M. P., Lakusta, T., Johnston, M., McKenney, D. W., Pedlar, J. H., Stratton, T., Sturrock, R. N., Thompson, I. D., Trofymow, J. A., and Venier, L. A. 2013. Anticipating the consequences of climate change for Canada's boreal forest ecosystems. *Environmental Reviews*, 21(4), 322-365. <https://doi.org/10.1139/er-2013-0042>
- Prévost, M., and Raymond, P. 2012. Effect of gap size, aspect and slope on available light and soil temperature after patch-selection cutting in yellow birch–conifer stands, Quebec, Canada. *Forest Ecology and Management*, 274, 210-221. <https://doi.org/10.1016/j.foreco.2012.02.020>
- Revel, R.D., Dougherty, T.D., and Downing, D.J. 1984. *Forest Growth & Revegetation Along Seismic Lines*. University of Calgary Press, Calgary, Alberta, United States. Available from <https://www.osti.gov/servlets/purl/6109132>.
- Rooney, R. C., Bayley, S. E., and Schindler, D. W. 2012. Oil sands mining and reclamation cause massive loss of peatland and stored carbon. *Proc Natl Acad Sci U S A*, 109(13), 4933-4937.
- San-Miguel, I., Coops, N. C., Chavardès, R. D., Andison, D. W., and Pickell, P. D. 2020. What controls fire spatial patterns? Predictability of fire characteristics in the Canadian boreal plains ecozone. *Ecosphere (Washington, D.C)*, 11(1), n/a. <https://doi.org/10.1002/ecs2.2985>
- Saraswati, S., Bhusal, Y., Trant, A. J., and Strack, M. 2020. Roads Impact Tree and Shrub Productivity in Adjacent Boreal Peatlands. *Forests*, 11(5), 594. <https://doi.org/10.3390/f11050594>
- Schiks, T. J., Wotton, B. M., Turetsky, M. R., and Benscoter, B. W. 2016. Variation in fuel structure of boreal fens. *Canadian Journal of Forest Research*, 46(5), 683–695.
- Schmidt, M., Davidson, S. J., and Strack., M. 2021. CO<sub>2</sub> uptake decreased and CH<sub>4</sub> emissions increased in first two years of peatland seismic line restoration. *Research Square*, DOI: 10.21203/rs.3.rs-759056/v1. [in press]

- Schmidt, K. and Skidmore, A. 2003. Spectral discrimination of vegetation types in a coastal wetland. *Remote Sensing of the Environment*, 85(1), 92–108.
- Schneider, R. R., Devito, K., Kettridge, N., and Bayne, E. 2016. Moving beyond bioclimatic envelope models: integrating upland forest and peatland processes to predict ecosystem transitions under climate change in the western Canadian boreal plain. *Ecohydrology*, 9(6), 899-908. <https://doi.org/10.1002/eco.1707>
- Sheriff, R., and Geldart, L. 1995. *Exploration Seismology* (2nd ed.). Cambridge: Cambridge University Press. doi:10.1017/CBO9781139168359
- Sherwood, J. H., Kettridge, N., Thompson, D. K., Morris, P. J., Silins, U., and Waddington, J. M. 2013. Effect of drainage and wildfire on peat hydrophysical properties. *Hydrological Processes*, 27(13), 1866-1874. <https://doi.org/10.1002/hyp.9820>
- Sniderhan, A. E., and Baltzer, J. L. 2016. Growth dynamics of black spruce (*Picea mariana*) in a rapidly thawing discontinuous permafrost peatland. *Journal of geophysical research. Biogeosciences*, 121(12), 2988-3000. <https://doi.org/10.1002/2016JG003528>
- Strack, M., Hayne, S., Lovitt, J., McDermid, G. J., Rahman, M. M., Saraswati, S., and Xu, B. 2019. Petroleum exploration increases methane emissions from northern peatlands. *Nature communications*, 10(1), 2804-2808. <https://doi.org/10.1038/s41467-019-10762-4>
- Stralberg, D., Wang, X., Parisien, M. A., Robinne, F. N., Sólymos, P., Mahon, C. L., Nielsen, S. E., and Bayne, E. M. 2018. Wildfire-mediated vegetation change in boreal forests of Alberta, Canada. *Ecosphere (Washington, D.C)*, 9(3), e02156-n/a. <https://doi.org/10.1002/ecs2.2156>
- Stern, E., Riva, F., and Nielsen, S. 2018. Effects of narrow linear disturbances on light and wind patterns in fragmented boreal forests in northeastern alberta. *Forests*, 9(8), 486. <https://doi.org/10.3390/f9080486>
- Stevenson, C., Filicetti, A., and Nielsen, S. 2019. High precision altimeter demonstrates simplification and depression of microtopography on seismic lines in treed peatlands. *Forests*, 10(4), 295. <https://doi.org/10.3390/f10040295>
- St-Onge, B., Audet, F., and Bégin, J. 2015. Characterizing the height structure and composition of a boreal forest using an individual tree crown approach applied to photogrammetric point clouds. *Forests*, 6(12), 3899-3922. <https://doi.org/10.3390/f6113899>
- Tarnocai, C. 2009. The Impact of Climate Change on Canadian Peatlands. *Canadian Water Resources Journal / Revue canadienne des ressources hydriques*, 34(4), 453-466. <https://doi.org/10.4296/cwrj3404453>



- Tarnocai, C., and Stolbovoy, V. 2006. Chapter 2 Northern Peatlands: their characteristics, development and sensitivity to climate change. In (Vol. 9, pp. 17-51). Elsevier Science & Technology. [https://doi.org/10.1016/S0928-2025\(06\)09002-X](https://doi.org/10.1016/S0928-2025(06)09002-X)
- Thompson, D. K., Baisley, A. S., and Waddington, J. M. 2015. Seasonal variation in albedo and radiation exchange between a burned and unburned forested peatland: implications for peatland evaporation. *Hydrological Processes*, 29(14), 3227-3235. <https://doi.org/10.1002/hyp.10436>
- Thompson, D. K., Benscoter, B. W., and Waddington, J. M. 2014. Water balance of a burned and unburned forested boreal peatland. *Hydrological Processes*, 28(24), 5954-5964. <https://doi.org/10.1002/hyp.10074>
- Thompson, D. K., Parisien, M. A., Morin, J., Millard, K., Larsen, C. P. S., and Simpson, B. N. 2017. Fuel accumulation in a high-frequency boreal wildfire regime: from wetland to upland. *Canadian Journal of Forest Research*, 47(7), 957-964. <https://doi.org/10.1139/cjfr-2016-0475>
- Thompson, D. K., Simpson, B., N., Whitman, E., Barber, Q., E., and Parisien, M., A. 2019. Peatland hydrological dynamics as a driver of landscape connectivity and fire activity in the boreal plain of Canada. *Forests*, 10(7). <https://doi.org/10.3390/f10070534>
- Tiner, R. W., Lang, M. W., and Klemas, V. 2015. In Tiner R. W., Lang M. W. and Klemas V. V.(Eds.), *Remote sensing of wetlands: Applications and advances*. CRC Press, Taylor & Francis Group. <https://doi.org/10.1201/b18210>
- Töyrä, J., Pietroniro, A., Hopkinson, C., and Kalbfleisch, W. 2003. Assessment of airborne scanning laser altimetry (lidar) in a deltaic wetland environment. *Canadian Journal of Remote Sensing*, 29(6), 718-728. doi:10.5589/m03-040.
- Töyrä, J., Pietroniro A., Martz, L.W., and Prowse, T.D. 2002. A multi-sensor approach to wetland flood monitoring. *Hydrological Processes* 16(8):1569–1581
- Turetsky, M., Wieder, K., Halsey, L., and Vitt, D. 2002. Current disturbance and the diminishing peatland carbon sink. *Geophysical Research Letters*, 29, 1526.
- Vanderhoof, M. K., Hawbaker, T. J., Ku, A., Merriam, K., Berryman, E., and Cattau, M. 2021. Tracking rates of postfire conifer regeneration vs. deciduous vegetation recovery across the western united states. *Ecological Applications*, 31(2), e02237-n/a. <https://doi.org/10.1002/eap.2237>
- van der Werf, G. R., Randerson, J. T., Giglio, L., Collatz, G. J., Mu, M., Kasibhatla, P. S., Morton, D. C., DeFries, R. S., Jin, Y., and van Leeuwen, T. T. 2010. Global fire emissions and the contribution of deforestation, savanna, forest, agricultural, and peat fires (1997-2009). *Atmospheric Chemistry and Physics*, 10(23), 11707-11735. <https://doi.org/10.5194/acp-10-11707-2010>

- van Rensen, C. K., Nielsen, S. E., White, B., Vinge, T., and Lieffers, V. J. 2015. Natural regeneration of forest vegetation on legacy seismic lines in boreal habitats in Alberta's oil sands region. *Biological Conservation*, 184, 127-135. <https://doi.org/10.1016/j.biocon.2015.01.020>
- Vitt, D. H. 1994. An overview of factors that influence the development of Canadian peatlands. *Memoirs of the Entomological Society of Canada*, 126(S169), 7-20. <https://doi.org/10.4039/entm126169007-1>
- Vitt, D. H., Halsey, L. A., and Zoltai, S. C. 1994. The bog landforms of continental western Canada in relation to climate and permafrost patterns. *Arctic and Alpine Research*, 26(1), 1-13. <https://doi.org/10.2307/1551870>
- Vitt, D. H. (2019). Peatlands. In (Second ed., pp. 557-566). Elsevier B.V. <https://doi.org/10.1016/B978-0-12-409548-9.00741-7>
- Waddington, J. M., Morris, P. J., Kettridge, N., Granath, G., Thompson, D. K., and Moore, P. A. 2015. Hydrological feedbacks in northern peatlands. *Ecohydrology*, 8(1), 113-127. <https://doi.org/10.1002/eco.1493>
- Walker, X. J., Baltzer, J. L., Bourgeau-Chavez, L., Day, N. J., Dieleman, C. M., Johnstone, J.F., Kane, E.S., Rogers, B.M., Turetsky, M.R., Veraverbeke, S., and Mack, M. C. 2020. Patterns of ecosystem structure and wildfire carbon combustion across six ecoregions of the North American boreal forest. *Front. For. Glob. Change* 3:87. doi: 10.3389/ffgc.2020.00087
- Walker, L. R., Wardle, D. A., Bardgett, R. D., Clarkson, B. D., and Sveriges lantbruksuniversitet. 2010. The use of chronosequences in studies of ecological succession and soil development. *The Journal of Ecology*, 98(4), 725-736. <https://doi.org/10.1111/j.1365-2745.2010.01664.x>
- Wang, G. 2002. Fire severity in relation to canopy composition within burned boreal mixedwood stands. *Forest Ecology and Management*, 163(1-3), 85-92.
- Wang, J. A., Sulla-Menashe, D., Woodcock, C. E., Sonnentag, O., Keeling, R. F., and Friedl, M. A. 2019. Extensive land cover change across Arctic–Boreal Northwestern North America from disturbance and climate forcing. *Global Change Biology*, 26(2), 807-822. <https://doi.org/10.1111/gcb.14804>
- Warner, B. G., and Asada, T. 2006. Biological diversity of peatlands in Canada. *Aquatic Sciences*, 68(3), 240-253. <https://doi.org/10.1007/s00027-006-0853-2>
- Weber, M. G., and Flannigan, M. D. J. E. R. 1997. Canadian boreal forest ecosystem structure and function in a changing climate: impact on fire regimes. 5(3-4), 145-166.

- Wehr, A., and Lohr, U. 1999. Airborne laser scanning—an introduction and overview. *ISPRS Journal of Photogrammetry and Remote Sensing*, 54(2), 68-82. [https://doi.org/10.1016/S0924-2716\(99\)00011-8](https://doi.org/10.1016/S0924-2716(99)00011-8)
- Weltzin, J. F., C. Harth, S. D. Bridgman, J. Pastor, and J. Chen. 2003. Potential effects of warming and drying on peatland plant community composition, *Global Change Biol.*, 9(2), 141–151.
- White, L., Brisco, B., Daboor, M., Schmitt, A., and Pratt, A. 2015. A Collection of SAR Methodologies for Monitoring Wetlands. *Remote sensing (Basel, Switzerland)*, 7(6), 7615-7645. <https://doi.org/10.3390/rs70607615>
- White, L., Brisco, B., Pregitzer, M., Tedford, B., & Boychuk, L. (2014). RADARSAT-2 beam mode selection for surface water and flooded vegetation mapping. *Canadian Journal of Remote Sensing*, 40(2), 135-151. <https://doi.org/10.1080/07038992.2014.943393>
- Witte, T. H., and Wilson, A. M. (2005). Accuracy of WAAS-enabled GPS for the determination of position and speed over ground. *J. Biomech.*, 38, 1717-1722
- Whitman, E., Batllori, E., Parisien, M.-A., Miller, C., Coop, J. D., Krawchuk, M. A., Chong, G. W., and Haire, S. L. 2015. The climate space of fire regimes in north-western North America. *Journal of Biogeography*, 42(9), 1736-1749. <https://doi.org/10.1111/jbi.12533>
- Whitman, E., Parisien, M.-A., Thompson, D. K., and Flannigan, M. D. 2019. Short-interval wildfire and drought overwhelm boreal forest resilience. *Scientific Reports*, 9(1), 1-12.
- Wieder, R. K., Scott, K. D., Kamminga, K., Vile, M. A., Vitt, D. H., Bone, T., Xu, B., Benschoter, B. W., and Bhatti, J. S. 2009. Postfire Carbon Balance In Boreal Bogs Of Alberta, Canada. *Global Change Biology*, 15(1), 63-81. <https://doi.org/10.1111/J.1365-2486.2008.01756.X>
- Wilkinson, S. L., Moore, P. A., Flannigan, M. D., Wotton, B. M., and Waddington, J. M. 2018. Did enhanced afforestation cause high severity peat burn in the Fort McMurray Horse River wildfire? *Environmental Research Letters*, 13(1). <https://doi.org/10.1088/1748-9326/aaa136>
- Zahidi, I., Yusuf, B., Hamedianfar, A., Shafri, H. Z. M., and Mohamed, T. A. 2015. Object-based classification of QuickBird image and low point density LIDAR for tropical trees and shrubs mapping. *European Journal of Remote Sensing*, 48(1), 423-446. <https://doi.org/10.5721/EuJRS20154824>
- Zhuang, W., and Giorgos Mountrakis, G. 2015. Ground peak identification in dense shrub areas using large footprint waveform LiDAR and Landsat images. *International Journal of Digital Earth*, 8(10), 805-824, DOI: 10.1080/17538947.2014.942716

Zhang, X., Wan, H., Zwiers, F. W., Hegerl, G. C., and Min, S.-K. 2013. Attributing intensification of precipitation extremes to human influence. *Geophysical Research Letters*, 40(19), 5252-5257. <https://doi.org/10.1002/grl.5101>.

## APPENDIX 1: GLOSSARY

**Anthropogenic disturbance:** change in environment caused or produced by humans.

**Bog:** ombrogenous peatland that receive water inputs mostly from precipitation with poor nutrient availability.

**Conifers:** evergreen cone-bearing trees or shrubs that have needle like leaves; includes black spruce, white spruce, tamarack, and jack pine.

**Deciduous:** broadleaf trees or shrubs that shed their leaves annually; includes paper birch, balsam poplar, trembling aspen, and willow species.

**Environment:** surrounding biotic and abiotic conditions that influence growth, survival, and functioning of an organism.

**Evapotranspiration:** water loss from surface (evaporation) and transpiration from plants.

**Fen:** minerogenous peatland that receive water input from variety of sources and are nutrient rich.

**Hollow:** flatter open spaces between hummocks that are closer to the water table.

**Hummock:** elevated mounds that can be few cm to m above the water table usually composed of Sphagnum moss.

**Lidar:** sensors that use laser pulse emission and reflection from object to determine distance to object.

**Net Ecosystem Production (NEP):** net primary production minus carbon lost via heterotrophic respiration; net change in carbon storage in the ecosystem.

**Peat:** partially decomposed plant material, primarily composed of mosses and sedges with a Von Post of  $\leq 5$  that accumulates under saturated conditions.

**Peatland:** a wetland with more than 40 cm of accumulated peat and organic matter; includes bogs, fens and some swamps.

**Remote sensing:** collecting data remotely without touching or measuring directly, typically done using sensors.

**Seismic lines:** linear forest clearings used to map oil reserves.

**Shrub:** woody plant that is less than 3 m in height usually having multiple permanent stems.

**Tree:** woody, single-stemmed plant that is taller than 3 m in height; can be deciduous or coniferous.

**Water table:** the water level below which the ground is saturated.

**Wildland fire:** non-structured fire other than prescribed burn that occurs in a vegetated area.